KTH Industrial Engineering
and Management

Phase Change Phenomena During Fluid Flow in Micro channels

Doctoral Thesis

By

Rashid Ali

Division of Applied Thermodynamics and Refrigeration
Department of Energy Technology
Royal Institute of Technology

Stockholm, Sweden 2010

TRITA REFR Report No. 10/03
ISSN 1102-0245
ISRN KTH/REFR/10/03-SE
ISBN 978-91-7415-829-8

Abstract

Phase change phenomena of a fluid flowing in a micro channel may be exploited to make the heat exchangers more compact and energy efficient. Compact heat exchangers offer several advantages such as light weight, low cost, energy efficiency, capability of removing high heat fluxes and charge reduction are a few to mention. Phase change phenomena in macro or conventional channels have been investigated since long but in case of micro channels, fewer studies of phase change have been conducted and underlying phenomena during two-phase flow in micro channels are not yet fully understood. It is clear from the literature that the two-phase flow models developed for conventional channels do not perform well when extrapolated to micro scale.

In the current thesis, the experimental flow boiling results for micro channels are reported. Experiments were conducted in circular, stainless steel and quartz tubes in both horizontal and vertical orientations. The internal diameters of steel tubes tested were 1.70 mm, 1.224 mm and the diameter of quartz tube tested was 0.781 mm. The quartz tube was coated with a thin, electrically conductive, transparent layer of Indium-Tin-Oxide (ITO) making simultaneous heating and visualization possible. Test tubes were heated electrically using DC power supply. Two refrigerants R134a and R245fa were used as working fluids during the tests. Experiments were conducted at a wide variety of operating conditions.

Flow visualization results obtained with quartz tube clearly showed the presence of confinement effects and consequently an early transition to annular flow for micro channels. Several flow pattern images were captured during flow boiling of R134a in quartz tube. Flow patterns recorded during the experiments were presented in the form of Reynolds number versus vapour quality and superficial liquid velocity versus superficial gas velocity plots. Experimental flow pattern maps so obtained were also compared with the other flow pattern maps available in the literature showing a poor agreement. Flow boiling heat transfer results for quartz and steel tubes indicate that the heat transfer coefficient increases with heat flux and system pressure but is independent on mass flux and vapour quality. Experimental flow boiling heat transfer coefficient results were compared with those obtained using different correlations from the

literature. Heat transfer experiments with steel tubes were continued up to dryout condition and it was observed that dryout conditions always started close to the exit of the tube. The dryout heat flux increased with mass flux and decreased with exit vapour quality. The dryout data were compared with some well known CHF correlations available in the literature. Two-phase frictional pressure drop for the quartz tube was also obtained under different operating conditions. As expected, two-phase frictional pressure drop increased with mass flux and exit vapour quality.

Keywords: Micro channels, Mini channels, Phase change, Boiling, Two-phase, Heat Transfer, Pressure Drop, Dry out, Critical Heat Flux, Visualization, Flow patterns.

Acknowledgements

I feel highly indebted to many people on personal and professional level who have helped and supported me during my graduation period.

First and foremost, I greatly acknowledge the unparalleled support, guidance, appreciation from my supervisor professor Björn Palm without which this thesis would not exist. Thank you, Björn for your belief in me and accepting me as a PhD student. I learnt a lot from your knowledge, discussions, and ideas. I really appreciate your care during my whole stay in the division. Indeed, you have always been a great source of inspiration in whole journey towards my graduation, not only as a supervisor but as a wonderful person in my life.

Many thanks, to Rahmat for not only reading this manuscript but support and guidance during the whole period of my graduation.

Special thanks to Claudi Martin-Callizo for helping me to grow from infancy to this stage of research. Without your valuable discussions and help this manuscript would not have been possible. Thank you for your help, support and friendship and all the care you have taken during my whole stay in Sweden. Thanks also to Hamayun for all his help, care and friendship.

I greatly acknowledge the help of Roberta Concilio Hansson from the division of Nuclear Power Safety, KTH in visualization experiments and also valuable discussions, in the initial phase of designing the visualization test section, with Professor Tim Ameel from the University of Utah are acknowledged. Jens Fridh from Heat and Power division of this department is acknowledged for helping in the pressure calibrations.

For help and support in the lab and in the department, I am very thankful to Peter Hill, Inga Du Rietz, Benny Sjöberg, and Benny Andersson, Emma Hedrenius, Lilian Pirashi. Whithout their help, it would not have been possible to accomplish all this. Thanks also, to Tony and Birger for helping in computer and support matters.

I am really grateful to all my colleagues for making it such a wonderful stay in the division. Thanks to Samer Sawalha, Hatef Madani Larijani, Yang Chen, Jose Acuna, Monika Ignatowiz, Jörgen Wallin, Alex Kotial-

sko, Ehsan Betaraf Haghighi, Qingming Liu, Erik Björk, Richard Furberg, Oxana Samoteeva, Alla Kullab, Justin Chew. Many thanks to Prof. Per Lundqvist, Prof. Erik Granryd, Jan-Erik Nowaiki, Hans Havtun, Nabil Kassem, Åke Melinder, Joachim Claesson, Jaime Arias. Special thanks to my friends with whom I played table football, thank you again Samer, Hatef, Alla, Getachew, Marino, Claudi for playing such nice games, I won actually a lot of games isn't it!

Thanks to my colleagues who are not any more in the division but we spent really a good time, Primal Fernando, Getachew Bekele, Wahib Owhaib, Raul Anton.

On personal level, I will like to thank my friends Shabbir Hussain, Waseem Hyder, Waseem Siddique, Waqar ul Hassan, Rizwan Raza, and Mohammad Shoaib. I will also like to greatly thank my friend Mohammad Mursaleen for taking care of my problems in my home country.

I am very thankful to my whole family for their unconditional love and support. I remember my grandfather who died during my PhD with a wish to see me but he couldn't! I have really unforgettable memories of my grandfather. I am really indebted to my parents as I reached this far due to their love and support; especial thanks to my father who despite of very limited resources never said no to my education at any point. I really appreciate and am greatly thankful to my wife Tabassum for her love, patience, care, sacrifice and understanding during whole period of my graduation, I really understand that this whole period of my graduation has not been easy for you. I can't forget the patience of my pretty and lovely daughter Zainab who always wanted to see me, play with me and go out, I know you will miss Sweden! To my son Mohammad who was born in Sweden during my graduation; you are really lovely as I always say you when I see you at home! I thank to all my brothers and sisters I remember all the moments spent with you at our home. To you all my family, I dedicate this thesis!

Rashid Ali

Stockholm, December 2010

Publications

This thesis is based on the following Journal and Conference publications

Journal Papers

Rashid Ali., Björn Palm, Mohammad Hamayun Maqbool., *2010*, Flow Boiling Heat Transfer Characteristics During Flow Boiling of R134a in a minichannel up to Dryout Condition*, Revised version Submitted to ASME Journal of Heat Transfer.*

Rashid Ali., Björn Palm., *2010*, Dryout Characteristics During Flow Boiling of R134a in Vertical Circular Minichannels*, Accepted for publication in International Journal of Heat and Mass Transfer.*

Rashid Ali., Björn Palm. Mohammad Hamayun Maqbool, *2009*, Experimental Investigation of Two-phase Pressure Drop in a Microchannel*, Accepted for publication in Heat Transfer Engineering.*

Conference Papers

Rashid Ali, Björn Palm, Muhammad H. Maqbool, *2009*, Flow Boiling Heat Transfer of Refrigerants R134a and R245fa in a Horizontal Microchannel, *In the Proceedings of 2nd European Conference on Microfluidics, December 8-10, Toulouse, France.*

Rashid Ali, Björn Palm, Claudi Martin-Callizo, Muhammad H. Maqbool, *2010*, Flow Patterns and Flow Pattern Maps for Microchannels, To appear *In the Proceedings of 3rd International Conference on Thermal Issues in Emerging Technologies, December 19-22, Cairo, Egypt.*

Rashid Ali, Björn Palm, Muhammad H. Maqbool, *2010*, A Visualization Study During Flow Boiling of R134a In A Horizontal Microchannel, *In the proceedings of, ASME 2010 3rd Joint US-European Fluids Engineering Summer Meeting and 8th International Conference on Nanochannels, Microchannels, and Minichannels, FEDSM2010-ICNMM2010, August 2-4, Montreal, Canada.*

Other publications not included in this thesis

Martin-Callizo C, Ali R., Palm B., *2010*, Saturated flow boiling Heat Transfer of Refrigerants in a Vertical Microchannel of 640μm*, Submitted to Intenational Journal of Heat and Mass Transfer.*

Martín-Callizo C., Palm B., Owhaib W., Ali R, *2010*, Flow boiling visualization of R-134a in a vertical channel of small diameter, *ASME Journal of Heat Transfer*, 132: 031503-8.

Ali R, Palm B, Maqbool M. H, *2009*, Flow Boiling Heat Transfer Characteristics of A Minichannel Up To Dryout Condition, *In Proceedings of MNHMT09, ASME 2009 2nd Micro/Nanoscale Heat & Mass Transfer International Conference, December 18-22, Shanghai, China.*

Ali R, Palm B, Maqbool M. H, *2009*, Experimental Investigation of Two-phase Pressure Drop in a Microchannel, *In Proceedings of 2nd Micro & Nano flows Conference, September 1-2,* Brunel University, West London, UK.

Martin-Callizo C, Ali R., Palm B., *2008*, Dryout Incipience and Critical Heat Flux in Saturated Flow Boiling of R-134a in a Vertical Microchannel, *In the Proceedings of 6th Int. Conference on Nanochannels, Microchannels and Minichannels, ICNMM08, Darmstadt, Germany*

Martin-Callizo C, Ali R., Palm B., *2007*, New Experimental Results on Flow Boiling of R-134a in a Vertical Microchannel, *In the Proceedings of 10th UK Heat Transfer Conference, Edinburgh, UK*

Martín-Callizo C., Ali R., Palm B, *2007*, Flow Boiling Heat Transfer and Visualization of R-134a in Vertical Tubes of Small Diameter, *IEA Heat Pump Annex 33 Meeting, Stockholm, Sweden*, May 23-24.

Martín-Callizo C., Palm B., Owhaib W., Ali R, *2007*, Flow boiling visualization of R-134a in a vertical channel of small diameter, *ASME-JSME Thermal Engineering Summer Heat Transfer Conference, Vancouver, BC, Canada*, July 8-12.

Maqbool M. H, Palm B, Khodabandeh R and Ali R, *2010*, Two-phase Pressure Drop of Ammonia in a Mini/Micro channel, *In the proceedings of, ASME 2010 3rd Joint US-European Fluids Engineering Summer Meeting and 8th International Conference on Nanochannels, Microchannels, and Minichannels, FEDSM2010-ICNMM2010, August 2-4, Montreal, Canada.*

Maqbool M. H, Palm B, Khodabandeh R and Ali R, *2010*, Two-phase Heat Transfer of Ammonia in a Mini/Micro channel, *In the proceedings of, ASME 2010 3rd Joint US-European Fluids Engineering Summer Meeting and 8th International Conference on Nanochannels, Microchannels, and Minichannels, FEDSM2010-ICNMM2010, August 2-4, Montreal, Canada.*

Table of Contents

1 Introduction

1.1 Background and motivation

Miniaturization in the field of electronics has led to dense packaging and integration of more components on an electronic circuit. Integration of components in an electronic circuit has been driven by Moore's law Moore (1965; Moore (2003) according to which the number of transistors incorporated on a chip roughly doubles every 24 months. Today more than 2 billion transistors are integrated on a chip Moore (2003; Intel (2010) as compared to around 10000 transistors in 1967 as seen in Figure1.1. Apparent consequences of Moore's law are the reduced size and increased performance of a microprocessor and at the same time a decrease in production cost of transistors. Production cost of transistors in the recent years has decreased surprisingly as shown in Figure 1.2, mainly due to advanced and novel micro manufacturing technologies available, providing further impetus to integration and dense packaging of electronic components. Miniaturization of electronics, motivated by new and exciting application areas and modern fabrication techniques, has made it possible to obtain faster chip speeds but at the same time the chip power densities have increased dramatically. Consequently, recent developments in the field of microelectronics due to miniaturization have resulted in dissipation of much higher heat fluxes than ever before which has exceeded the fan cooling limits. Heat fluxes generated in microelectronics have reached about 100 W/cm^2 today and this number keeps rising and might reach 200 W/cm^2 to 300 W/cm^2 in near future. The surface temperature of high heat dissipating microchips has to be maintained below 80 to 85 °C in order to ensure the effective and reliable operation of the electronic circuitry. Practically, the ineffective cooling of high heat flux devices is a major constraint in dense packaging of microelectronics and has to be resolved in order to nurture the miniaturization process. Smaller and light weight design of spacecrafts also needs miniaturization of different electronics and avionics components including integration of single components in a small space/volume and the resulting dense packaging of components poses serious thermal management problems. Therefore, novel technologies for thermal management need to be developed in order to promote the miniaturization process.

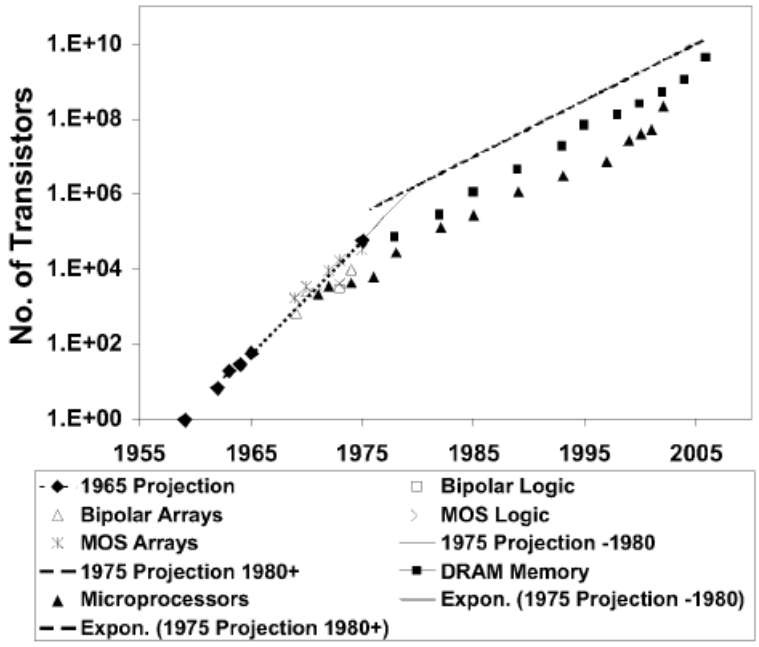

Figure1.1.Increase of number of transistors with time, taken from Moore (2003)

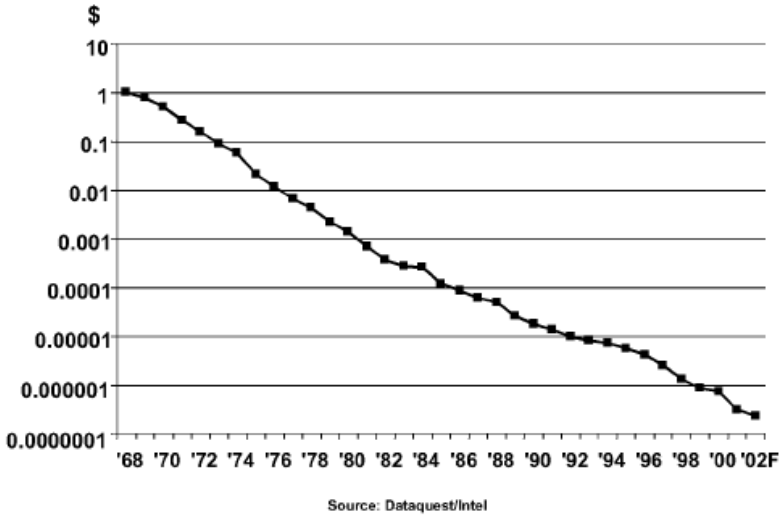

Figure 1.2 Transistor price decreasing with time Moore (2003)

Since, the pioneering work done by Tuckerman and Pease (1981) in early 1980s, the micro channel heat sinks have received much attention from scientific and industrial community due to their very promising and effective cooling potential. Microchannels have comparatively larger heat transfer surface area and higher surface-area-to-volume ratio, therefore, the use of microchannels in heat exchangers makes them compact, light weight and thermally more efficient as compared to their conventional counterparts. Latent heat associated with phase change of the fluids can be exploited to maintain the required temperature of the micro electronics devices, as during the phase change process, the temperature of the fluid is dictated by the saturation temperature. Also the use of boiling of a fluid will allow the design of compact heat exchange devices using the less fluid inventory, for the same heat transfer performance, in comparison to the cases when single phase liquid is used as a coolant.

Although the impetus for microchannel work comes from miniaturization of microelectronics, the application of micro channels is not only limited to microelectronics industry, instead, there are several other application areas which can benefit from the numerous advantages offered by the micro channels. Micro channel heat exchangers may be used in automotive industry to reduce the refrigerant charge significantly as compared to conventional sized heat exchangers for the same effectiveness and heat transfer performance, great design flexibility may be achieved and space constraints can be overcome due to compactness of the heat exchanger. The overall weight and cost of the heat exchange system may be reduced due to the less material required for manufacturing and less requirements of fluid inventory. Manufacturing of multiport aluminium compact heat exchangers have already started in automotive industry.

Domestic Refrigeration, heat pump and air-conditioning industry is potential application area for compact heat exchangers employing micro channels. The compact and efficient evaporators and condensers will increase the performance of the refrigeration and air-conditioning system at the same time reducing the charge of refrigerant. One such example of a typical mini/micro channel heat exchanger which could be used for heat pump, refrigeration and air-conditioning applications is shown in Figure 1.3. Few other application areas of micro channels which may be mentioned here are: fuel cells, chemical processing industry, microfluidics devices, separation and modification of cells in bio applications etc.

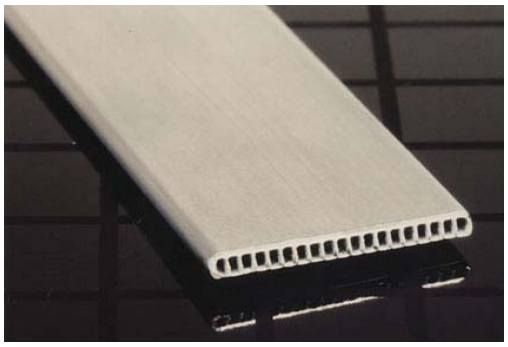

Figure 1.3 A multiport mini channel heat exchanger

Global warming and depletion of ozone layer are most challenging problems of today's fast developing era. The release of different refrigerants in to the atmosphere causes serious damage to ozone layer and promotes global warming. The ever increasing environmental concerns may be addressed by using the micro channels, as the compact heat exchangers employing the micro channels may help in reducing the charge of the refrigerant and increasing the efficiency of the heat exchange system.

Enhanced heat transfer capability of micro channels have been demonstrated in the literature in both single and two-phase flow. Several experiments in the literature show the higher and effective heat transfer in case of compact heat exchangers employing micro channels as compared to their macro counter parts. Higher and effective heat transfer offered by compact heat exchangers can help promote sustainability and at the same time effective use of natural resources may be achieved. Advantages of micro channels common to all the application areas mentioned above may be listed as under:

- Enhanced heat transfer
- Large surface area to volume ratio
- Compactness
- Reduction in the inventory of fluid being used for cooling
- Less material required for manufacture of heat exchange device
- Light weight
- Low cost due to less material and fluid inventory required
- Helpful in addressing environmental issues

Despite the attractive and motivating advantages of the micro channels, the understanding of the fundamental hydrodynamic and thermal transport mechanisms especially during two-phase flow is far from satisfactory. Therefore, more studies are essential focusing on the understanding of governing phenomena in order to be able to use the micro channel heat sinks in appropriate fields of application.

1.2 Structure of the thesis

The current thesis is divided into several chapters. The second chapter presents a thorough literature survey in the field of two-phase flow and heat transfer in microchannels including visualization studies and flow pattern maps. The third chapter explains the objectives of the current research work included in this thesis.

The fourth chapter is devoted to the experimental set up and instrumentation details. This chapter gives the general information regarding the instrumentation such as range, systematic errors. The data reduction methods and uncertainty procedure have also been explained. Other experimental details are also covered thoroughly in this chapter.

Chapters five through nine present the experimental results, main findings and discussion on the results. Chapters five and six contain the visualization results and flow pattern maps respectively. Chapter seven discusses and elaborates on the flow boiling heat transfer results in stainless steel and quartz microchannels and chapter eight discusses the dryout trends during flow boiling in microchannels and presents experimental results on dryout. Chapter nine is devoted to two-phase pressure drop of refrigerants and the results are also compared with different models and correlations available in the literature.

Chapter ten concludes the current work and some recommendations for the continuation of microchannel research are given.

2 Micro Channel Two-Phase Flow Literature Review

2.1 Definition of a micro channel

It is interesting to note that there exists no well-established criterion to define a threshold for transition from macro to a micro scale channel. However, the term "small diameter" has been used as early as 1962 by Bergles (1962) who performed his doctoral research work using small diameter tubes of 0.584 to 4.584 mm. The word micro in fluid flow and heat transfer does not necessarily mean the channels of micron size.

A micro channel could be one that exhibits different hydrodynamic or thermal behaviour as compared to conventional channels and the physical phenomena dominant in conventional channels are no more important in micro channels. It is noted from the literature that single-phase classical theory is applicable in the case of micro channels. Conventional theory for two-phase flow is, however, not appropriate for micro channels due to the reasons that will follow. The terms mini and micro channel have been used in the literature without any particular criterion, although there have been some attempts to define the two terms. Some researchers define the same transition criterion between macro and micro for both single and two-phase flow in a channel while others distinguish between the two depending upon whether single or two-phase flow is prevalent in the channel.

One of the several criteria proposed in the literature is an easy-to-use criterion suggested by Kandlikar and Grande (2003) which the authors suggested for single phase gas, liquid flows and two-phase flows as well and is given as follows.

Conventional Channels: $D_h > 3mm$
Mini channels: $3mm \geq D_h > 200\ \mu m$
Micro channels: $200\ \mu m \geq D_h > 10\ \mu m$
Transitional Channels: $10\ \mu m \geq D_h > 0.1\ \mu m$
Transitional Micro Channels: $10\ \mu m \geq D_h > 1\ \mu m$

Transitional Nano Channels: 1 μm ≥ D_h >0.1 μm
Molecular Nano Channels: 0.1 μm ≥ D_h

The criteria above is not based on any physical laws but was supported by testing it with different studies present in the literature and was found to be applicable for gas and liquid single-phase flows. A similar criteria was suggested by Mehendale et al. (2000). They suggested the channels having hydraulic diameters above 6mm as conventional channels, from 1mm to 6mm as compact heat exchangers, 100 μm to 1mm as mesoscale channels and 1μm to 100 μm as micro channels.

It is known that the surface tension becomes important and the effects of gravity diminish as the channel size is reduced. Based on this observation, Kew and Cornwell (1997) recommended using the confinement number as a basis for defining the channels as macro or micro scale. Confinement number is defined as:

$$Co = \frac{\left[\sigma / g(\rho_l - \rho_v)\right]^{1/2}}{D_h} \qquad (1)$$

According to Kew and Cornwell, for a channel having certain hydraulic diameter if the confinement number is greater than 0.5, the channel can be termed as micro scale channel otherwise it is to be called a conventional channel. The basic idea behind this recommendation is that the confinement effects become dominant beyond certain value of hydraulic diameter where surface tension plays a key role in defining the channel as a macro or micro. Thome et al. (2004) also suggested the confined bubble as the threshold to define the transition from macro to micro scale channel. However, there are indications based on the studies in literature that the confinement effects are dependent upon operating conditions as well.

Laplace constant λ and Eötvös number *Eo* (also known as Bond number Bo) defined as below were also suggested and used for defining the relative importance of gravity and surface tension by Suo and Griffith (1964; Serizawa et al. (2002) Brauner and Maron (1992). Suo and Griffith (1964) defined the criterion as $\lambda/D \geq 3.3$ while Brauner and Maron (1992) proposed a criterion in terms of Eötvös number *Eo* for the significance of surface tension in determining the departure from stratified flow to various bounded flow patterns. They proposed the criterion given as $Eo \leq (2\pi)^2$.

$$\lambda = \sqrt{\frac{\sigma}{g\Delta\rho}} \qquad (2)$$

$$Eo = \frac{g\Delta\rho D^2}{\sigma} \qquad (3)$$

Harirchian and Garimella (2010) suggested another criterion based on a convective confinement number. The authors defined the convective confinement number as $Bo^{0.5} \times Re$ and suggested a critical value of 160 for convective confinement number below which the channel is to be classified as micro channel. This in fact was an attempt to capture the effects of mass flux and viscosity on confinement of flow in a micro channel together with surface tension, gravity and density.

The literature review, however, clearly suggests a lack in any unanimous approach towards defining a macro or micro scale channel. Therefore, there is a need of comprehensively well defined and universal criteria, based on thermo physical properties of a fluid and operating parameters, to know the threshold boundaries between macro and micro scale, where the expected deviation of macro scale models starts appearing. However, in the absence of concrete criteria, the test tubes used for two-phase flow in this thesis are termed as micro channels as it has been observed in the literature that the confinement effects are already present in this range.

2.2 Flow Visualization

Formation of bubbles is termed as the nucleation process and the combined formation, growth and departure of a bubble is termed as ebullition cycle. Nucleation may be heterogeneous or homogeneous. In the former type of nucleation, the bubble formation takes place at the gas entrapped cavities present on a solid surface and in the latter the nucleation occurs in the liquid. In the case of homogenous nucleation, the bubbles are formed in the bulk liquid and relatively higher degree of superheat is required. Heterogeneous nucleate boiling phenomenon is the most commonly encountered phenomenon characterized by the formation of vapor bubbles on a solid surface. Therefore, the bubble nucleation and surface properties of the heater surface are closely related with each other. The smoother the surface, the higher will be the superheat required to initiate the bubble nucleation. However, technical surfaces are never perfectly smooth instead there are always imperfections in the form of cavities present on the surfaces. The presence of the cavities is usually accompanied with some entrapped gases which greatly help to lower the superheat required to initiate the bubble nucleation. As the superheat increases, more cavities or nucleation sites become active. It will

also be expected that the wetting properties of the liquid may have some influence on bubble nucleation as the entrainment of the gas in a cavity is also dependent on how well wetted is the solid surface. The less wetted the solid surface is, the higher are the chances that the gas will be trapped in the cavities.

A fairly good prediction of nucleate boiling heat transfer is possible by knowing the ebullition cycle (number of nucleation sites, bubble growth and departure size) and the bubble frequency. The bubble growth at the solid surface is controlled by different forces such as surface tension (acting along the contact line) which tends to keep the shape of the bubble and holds the bubble on the surface while the other forces such as buoyancy force, drag force and inertia forces resulting from the motion of nearby liquid tend to pull the bubble out of the surface. The bubble is released as the surface tension loses hold on the bubble and other forces become stronger. The diameter of the bubble at the time of departure then shall be dictated by the force balance between theses forces. Other factors affecting the bubble growth could be the thermo-physical properties of the fluid and the contact angle. Several correlations for determining the bubble departure diameter can be found in the literature such as one by Fritz (1935) based on the surface properties, fluid properties, operating conditions and balance between different forces such as buoyancy and surface tension forces.

The bubble frequency is also related to the bubble departure diameter and growth rate. The relations between bubble departure diameter and bubble frequency have long been established for pool boiling such as one suggested by Zuber (1963; Ivey (1967) thereby gaining some insight into boiling of fluids and its relation to heat transfer. Some relations connecting the heat flux and the wall superheat have also been formulated and discussed Gaertner and Westwater (1960; Kurihara and Myers (1960; Nishikawa and Yamagata (1960). From the flow boiling studies conducted for conventional channels it has been shown that nucleate boiling is characterized with formation of vapor bubbles at the active nucleation sites present on the heater surface (with the help of visualization studies) and heat transfer coefficient in this region has been shown to be dependent on heat flux and system pressure and independent of vapor quality and mass flux in macro scale channels. Flow visualization studies in micro channels focusing on bubble behavior and it's relation to boiling heat transfer are very limited in literature.

Lee et al. (2004) performed experiments to study the bubble dynamics in a trapezoidal microchannel of 41.3 μm. The mass fluxes tested were 170, 341 and 477 kg/m^2 s and heat flux was in the range 2 to 449 kW/m^2. They observed a decrease in bubble departure radius with increase in

heat flux but mass flux had a mixed effect. For low heat fluxes, the bubble departure radius was highest while bubble departure radius at G=341 kg/m^2 s was smaller than that at G=477 kg/m^2 s. Bubble frequency increased with heat flux at relatively low heat fluxes, but at higher heat fluxes, the bubble frequency decreased while for highest mass flux the bubble frequency was higher than the two lower mass fluxes.

Experimental investigation was carried out by Lie and Lin (2005; Lie and Lin (2006) to study the saturated and sub cooled flow boiling heat transfer and bubble characteristics of R134a in narrow annular ducts having gap sizes of 1 mm and 2 mm (hydraulic diameters of 2 mm and 4 mm). The results indicated that the heat transfer coefficient increased with decrease in duct size while it decreased with increasing inlet sub cooling degree. The bubble size was observed to decrease with increasing the mass flux and inlet sub cooling degree. The confinement effects were also observed due to limited gap size which according to the authors squeezed and deformed the bubbles. The increase in heat flux caused an increased bubble frequency, coalescence rate and bubble population. The bubble frequency also increased with decreasing the duct gap size due to increased effect of shear force at small hydraulic diameter.

Owhaib et al. (2007) used a high speed camera to investigate bubble behavior in a micro channel of 1.33 mm inner diameter using R134a as working fluid. Mass flux was in the range 29 to 202 kg/m^2 s, heat flux ranged from 5 to 20 kW/m^2 and system pressure was 6.425 bar. Experimental results indicated that as the mass flux increased, the bubble frequency increased and bubble departure diameter decreased. At higher heat fluxes, bubbles merged to form larger bubbles.

Huh et al. (2007) investigated the effects of elongated bubble behavior during flow boiling, both experimentally and numerically. Experiments were conducted in a rectangular, horizontal microchannel of 0.1 mm hydraulic diameter during flow boiling of water. The elongated bubbles grown from single bubbles dominated the major flow regimes and heat transfer mechanism. The growth of the elongated bubble was governed by thin film evaporation. The bubble frequency could be calculated with Zuber (1963) relationship of bubble frequency and diameter.

Hsieh et al. (2008) experimentally investigated the flow boiling heat transfer and associated bubble characteristics of R407 in narrow annuli of 1mm and 2 mm gap size. Experimental conditions were: heat flux from 0 to 45 kW/m^2, system pressure 776 to 899 kPa and mass flux from 300 to 600 kg/m^2 s. Experimental results showed that the mean bubble departure diameter decreased with increase in mass flux and the bubble departure frequency increased with decrease in diameter. At

higher heat fluxes, the bubbles departing from cavities increased and merged with each other to form larger bubbles.

Elongated bubble length and velocity were experimentally investigated by Revellin et al. (2008) for R134a flowing in a 0.5 mm micro channel. Measurements were carried out at the exit of the micro evaporator. Velocity of the bubbles increased linearly with the length of the bubbles up to a point where a plateau was observed which was explained as the merging point for the bubbles. Lower saturation temperature resulted in higher bubble length and bubble velocity.

A detailed study of thin liquid film formed between vapor and the channel wall was carried out by Han and Shikazono (2009). They used five different tubes of diameters 0.3 to 1.3 mm and air, ethanol, water and FC-40 were used as working fluids. The authors concluded that at small capillary numbers, the liquid film thickness is determined by capillary number but as the capillary number increases the inertial effects cannot be neglected.

A study of bubbly laminar two-phase flow in an open capillary channel was conducted by Salim et al. (2010) under micro gravity conditions. The channel consisted of two parallel plates of width b=25 mm and a distance of 10 mm between them. The bubbles were injected at the nozzle of capillary channel via six capillary tubes of 100 μm inner diameter. The mean bubble velocities were measured by processing the images obtained and the mean velocities were found to be directly proportional to the mixture velocity. The bubble size was also observed to increase along the channel due to coalescence.

The literature survey conducted for micro tubes focusing on the studies of bubble dynamics shows that a very limited data bank is available as compared to conventional channels. Looking at the importance of visualization studies in understanding the phase changing process in channel flows, more visualization studies in microchannels are certainly required to enrich the knowledge of two-phase flow.

2.3 Flow Patterns and Flow Pattern Maps

Gas-liquid two-phase flow in a system can exhibit different patterns depending upon the system (or geometric) boundaries. Different geometric configurations and orientations have been studied for flow patterns in conventional channels and most common of those being vertical and horizontal tubes. Discrepancies exist among the researchers in identification of flow patterns and about 100 different flow pattern names have been used in the literature Whalley (1987) and most of which are merely alternative names for the similar flow patterns. According to Whalley (1987) the minimum number of flow patterns in a gas-liquid two-phase flow which can 'sensibly' be defined in vertical up flow and horizontal orientations are shown in Figure 2.1 and Figure 2.2 respectively. Flow patterns usually depend upon several factors such as channel orientation, operating parameters, fluid thermo-physical properties and surface properties. In the case of vaporization and condensation, the vapor quality along the channel changes and so do the flow patterns. These changing flow patterns are usually presented on two-dimensional graphs called the flow pattern maps. The flow pattern maps can be plots between mass flux and vapor quality or plots between superficial liquid and vapor velocities or any other suitable dimensional or non-dimensional numbers. Superficial liquid and vapor velocities which are more often used in flow pattern maps are defined by the following equations:

$$J_g = \frac{Gx}{\rho_g} \qquad (4)$$

$$J_l = \frac{G(1-x)}{\rho_l} \qquad (5)$$

One of the most widely believed causes of deviation of gas-liquid two-phase flow behavior in micro channels from that of conventional scale channels is due to the confinement of vapor bubbles which consequently results in difference of flow patterns occurring during the flow. Flow pattern studies will greatly help in understanding the complex interaction of liquid and vapor phases occurring in two-phase macro and micro channels.

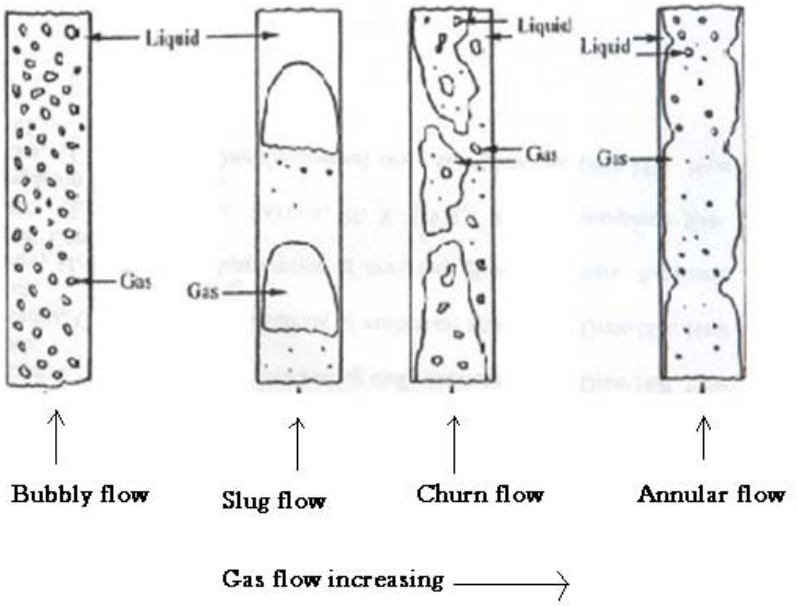

Figure 2.1 Flow patterns in a conventional vertical tube for upward flow Whalley (1987)

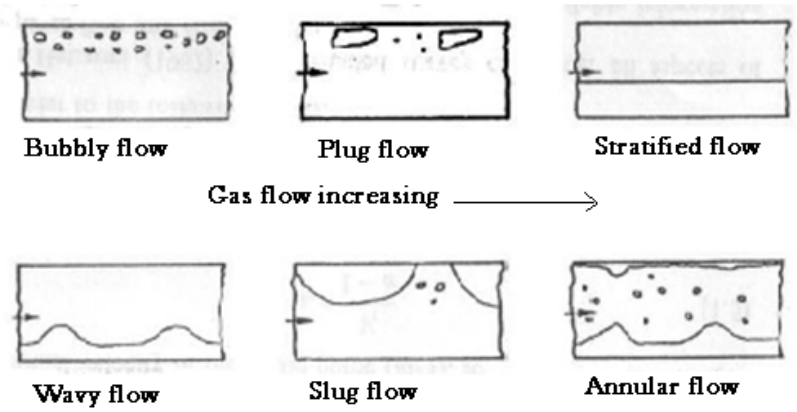

Figure 2.2 Flow patterns in a conventional Horizontal tube flow Whalley (1987)

One of the earliest studies was conducted by Suo (1963) to investigate the flow patterns in capillary tubes of 0.5 to 0.7 mm. Different combinations of liquid-vapor were used during the experiments with water, n-heptane and n-octane as liquids and helium, air and nitrogen as gases. The photographs were taken with a Polaroid camera. The author presented transition from bubbly to slug and from slug to annular flows by using the method of dimensional analysis and based on some physical reasoning. The authors concluded that the surface tension was an important parameter controlling the flow patterns evolved.

A flow pattern study was conducted with air-water two-phase flow by Damianides and Westwater (1988) in which they used horizontal tubes of hydraulic diameter 1 mm to 5 mm. The flow patterns observed during the experiments were: bubbly, slug, dispersed droplet and annular. They obtained a flow regime map and also suggested the surface tension as an important parameter for lower diameters than 5 mm. The bubbly-slug transition in their flow map was predicted by the Taitel and Dukler (1976) while the other transition boundaries were not predicted.

Triplett et al. (1999) experimentally investigated the flow patterns of air-water flow in circular channels with diameters of 1.1 mm and 1.45 mm and semi triangular channels with diameters of 1.09 mm and 1.49 mm. The liquid superficial velocity was in the range 0.02-8 m/s and the gas superficial velocity was in the range 0.02-80 m/s. Five distinct flow patterns were recorded for both the microchannel diameters which were: bubbly, slug, slug-annular, churn and annular. The experimental data was observed to be matching with similar studies performed by Damianides and Westwater (1988) and Fukano and Kariyasaki (1993), with slight discrepancies mainly attributable to difficulties in identification of flow patterns. The flow pattern map was compared with the models and correlations available in the literature with generally poor agreement.

Air-water two-phase flow pattern visualization experiments were conducted by Fukano and Kariyasaki (1993), Mishima and Hibiki (1996), Xu et al. (1999), Chung and Kawaji (2004). Bubbly, slug and annular flows were observed in the experiments as major flow patterns among other sub categories and channel size was concluded to have significant effect on transition boundaries of different flow patterns. Surface tension was noted to be important e.g. in Fukano and Kariyasaki (1993; Coleman and Garimella (1999). Chung and Kawaji (2004) observed different behaviour for smaller channels from 50 to 100 μm.

Huo et al. (2004) performed experiments to study flow patterns and flow boiling heat transfer of R134a in small diameter tubes of 2 mm and 4.26 mm. The experimental operating conditions were: G=100 kg/m^2 s to

G=500 kg/m² s, system pressure 8-12 bar, heat flux from 13 to 150 kW/m² and vapor quality up to 0.9. The flow patterns were also recorded using high speed digital camera and it was found that the flow patterns were the same for the two diameters but the transition boundaries of slug to churn and churn to annular flow patterns shifted to higher gas velocities as the diameter reduced. They presented the flow maps for the 4.26 mm diameter and the 2.01 mm. The transition lines for the 4.26 mm diameter tube were compared with Taitel (1990) model and Mishima and Ishii (1984) model with poor match between the experimental and predicted transition lines.

In Fu et al. (2008) flow patterns were studied during flow boiling of liquid nitrogen in a vertical mini channel of 1.93 mm inner diameter. The test conditions were: mass flux G=26- 906 kg/m² s, vapor quality x=0.001-0.91 and pressure p=1.12-2.96 bar. Bubbly, slug, churn and annular flow patterns were observed during the tests together with some interesting phenomena of liquid entrainment and deposition. Flow reversal, usually found in parallel microchannels was also observed in their single channel study. The authors observed that the bubbly flow was not stable and did not prevail long and was converted to elongated bubble and slug flow patterns. The annular flow pattern was the dominant and was the only flow pattern observed above a vapor quality of 0.15 for all the mass fluxes tested. Flow maps were presented in different coordinates such as mass flux and vapor quality, Weber number and superficial liquid and gas velocities.

More recently, flow visualization studies were conducted by Martin-Callizo et al. (2010) in a vertical circular channel having internal diameter of 1.33 mm and R134a was used as working fluid. The experimental operating conditions were: System pressure 7.70 and 8.87 bar, heat flux 5-45 kW/m², mass flux 100-500 kg/m² s, inlet sub cooling degree 3 to 8 °C and vapor quality -0.05 to 0.97. Seven distinct low patterns were identified as: bubbly, elongated bubble, slug, churn, slug-annular, annular and mist flow. Experimental flow pattern maps were presented in the form of mass flux versus vapor quality and superficial gas and liquid velocities. The effect of system pressure and inlet sub cooling on flow pattern transition were discussed. Higher saturation pressure shifted the transition boundaries to higher vapor qualities. Experimentally obtained flow pattern maps were compared with existing macro and micro scale methods, such as Taitel et al. (1980) and Triplett et al. (1999), with poor agreement. However, the transition lines of intermittent and non intermittent flow patterns were predicted surprisingly well with flow map of Garimella et al. (2002), basically developed for condensation process.

A literature review concerning the flow patterns and flow pattern maps has been presented in this section and some studies are also presented in Table 2-1. The following observations can be made based on the literature review:

The relative importance of surface tension increases and that of gravity decreases as the channel size is reduced.

Definitions for flow patterns do not fully agree. Most common and agreed flow patterns are bubbly, slug and annular. Sub categories of these flow patterns also exist.

Most of the studies employ air-water as working medium and are for adiabatic conditions. Therefore, a lack of flow pattern studies with other fluids of interest such as refrigerants is clearly felt.

Flow pattern transition lines in microchannels are not predicted well by existing models and flow pattern maps developed for conventional channels.

Table 2-1 Previous flow pattern studies in micro channels

Author(s) & Ref	Fluid	Dh [mm]	q" [kW/m²]	G [kg/m²s]	T_{sat} [°C]	Adiabatic/Diabetic	Remarks
Cornwell and Kew (1992)	R113	Two multiport channels of 1.2×0.9mm and 3.25×1.1mm	3-33	124-627	-	Diabatic	Flow patterns observed included isolated bubble, confined bubble and slug-annular. Isolated bubble regime was nucleate boiling dominant, heat flux was less important in confined bubble and slug-annular regime was convection dominant. Also reported that flow was unstable at low flow rate conditions.
Coleman and Garimella (1999)	Air-water	1.3 to 5 mm round and rectangular	-	0.1-100m/s gas velocity and 0.01-10m/s liquid velocity	-	Adiabatic	The flow patterns observed during experiments included the bubble, elongated bubble, slug, stratified wavy, wavy annular, dispersed and annular. The smooth stratified was not observed for any of the diameters tested while stratified wavy was not observed for diameters less than 5.50 mm.
Yang and Shieh (2001)	Air-water & R-134a	1 to 3	-	300 to 1600 for R134a	30 for R134a	Adiabatic	Air-water results agreed with previous work but with R134a transition from slug to annular boundary shifts to lower values of gas velocity. They concluded that surface tension is important parameter for flow pattern transition with decreasing diameter. No model predicts flow pattern transitions.
Kawahara et al. (2002)	Nitrogen-water	0.1	-	-	-	Adiabatic	Flow patterns observed were intermittent and semi-annular. Bubbly and churn flow were not observed. A serpentine-like gas core with deformed liquid film was observed. Differences were observed with existing flow maps but not discussed.
Hetsroni et al. (2003)	Air-water and Steam-water	15×15, triangular Multi-channels	51-500	-	Atmospheric	Adiabatic and Diabatic	For air-water, bubbly, slug and annular flow patterns were observed. Flow reversal was observed in case of steam-water flow. Different behaviour of steam-water flow was observed in comparison to air-water flow.
Nino et al. (2003)	R134a	1.5, Multichannel	-	50-300	-	Adiabatic	Flow visualizations revealed that different flow configurations may exist at maintained flow and quality conditions in parallel microchannels. Stratified, dispersed flow and annular mist flow pattern were not observed.
Chen et al. (2005)	R-134a	1.10 to 4.26	-	-	21, 39 and 52	Diabetic	Flow patterns were observed from the Pyrex glass tube located at the exit of the steel test tube. Flow patterns observed were: bubbly, dispersed bubble, confined bubble, slug, churn, annular and mist. Slug-churn and churn-annular transition boundaries are diameter and pressure dependent. Poor agreement was found with existing flow maps.
Revellin et al. (2006)	R-134a	0.5	3.7-129.7	350-2000	30	Diabetic	Flow patterns observed were bubbly, slug, semi-annular and annular at the exit of the test tube. Flow patterns did not compare well with macro and

							micro scale flow maps.
Ide et al. (2007)	Air-water	1, 2.4 and 4.9	-	-	-	Adiabatic	Flow separation was not found and hence flow direction was observed to have small effect on flow patterns. Flow patterns become axisymmetric and liquid film becomes uniform. Rectangular channels were also tested.
Megahed and Hassan (2009)	FC-72	0.276×0.225 rectangular Multichannels	60.4-130.6	341-531		Diabatic	Flow patterns observed were: bubbly, slug and annular. Flow maps were not presented and compared.
Ong and Thome (2009)	R-134a, R236a, R245fa	1.030	2.3-250	100-2000	29,31and 33	Adiabatic	Flow patterns observed were: Bubbly, elongated bubble, slug, churn annular and mist flow. The flow pattern agreed with Revellin and Thome obtained for same fluid and tube diameters of 0.5 and 0.79 mm.
Arcanjo et al. (2010)	R134a, R245fa	2.32	-	50-600	22,31 and 41		Flow patterns were recorded through a glass tube placed at the exit of the test section. Flow patterns observed were: bubbly, elongated bubble, slug, churn and annular. Ong and Thome (2009) and Felcar et al. (2007) flow maps predict their data reasonably well.
Saisorn and Wongwises (2010)	Air-water	0.15, 0.22 and 0.53	-	-	-	Adiabatic	Flow pattern observed are slug, throat-annular, churn, annular-rivulet, annular. Additionally for 0.15 mm tube, the serpentine-like gas core flow and liquid-alone flow were observed. Transition criteria by Garimella et al. (2002) predicts the transion boundary of intermittent and non-intermittent regimes. Partial agreement was also found with Revellin and Thome (2007) flow pattern map.

2.4 Flow Boiling Heat Transfer

Flow boiling has been investigated since long, as early as 1950s, to understand the basic phenomena involved in the boiling process. The boiling of a fluid is associated with the formation of bubbles and is characterized by higher heat transfer rates at relatively uniform temperatures and small temperature differences as compared to single-phase liquid flows. Boiling may take place in a situation when the fluid is still i.e. not moved with external means, or it may occur when the fluid is set to motion by external means such as circulation of a fluid by a pump. The former type is called pool boiling and the latter flow boiling and may exist in the form of sub cooled or saturated boiling. In the case of sub cooled flow boiling the bulk of the liquid is below saturation and bubbles formed at the solid surface collapse in the sub cooled liquid thereby transferring their latent heat to the liquid. In saturated flow boiling, the bulk liquid is maintained at saturation state. The wall is at a higher temperature than saturation in both types of processes. The surface properties such as surface roughness play an important role in both pool boiling as well as in flow boiling. The basic knowledge of boiling has been augmented with the understanding obtained from pool boiling. Pool boiling helped in understanding different mechanisms during phase change and based on this knowledge, different boiling mechanisms such as nucleate boiling, transitional boiling and film boiling have been identified. These different regimes can be seen in a pool boiling curve produced in many heat transfer books such as in Holman (1992).

Based on the knowledge gained from flow boiling in conventional channels, it is generally believed that there are two contributions in boiling process, one is from nucleate boiling characterized by the nucleation of bubbles and the other is convective boiling where a thin liquid film exists between the wall and the vapor and the evaporation takes place at the liquid-vapor interface. Different flow boiling heat transfer prediction correlations and models for conventional channels are based on the generally agreed idea of relative importance of the two mechanisms; nucleate boiling and convective boiling. The heat transfer models for predicting the local heat transfer coefficient can be classified into three main groups as enhancement models, superposition models and asymptotic models. Correlations for predicting the average heat transfer coefficient also exist. Many models and correlations for predicting local and average heat transfer coefficients in macro and micro channels can be found in Watel (2003; Owhaib (2007).

The two-phase flow in micro channels has not been investigated extensively and is relatively a developing filed. The investigations performed thus far reveal that the two-phase flow is affected by confinement effects present mainly due to reduction in channel size. Therefore, the two-phase studies in micro channels were initiated to investigate the underlying phenomena responsible for deviations from macro scale models. A brief overview of flow boiling heat transfer in micro channels is presented below.

One of the early studies concerning two-phase flow in small diameter tubes was conducted by Lazarek and Black (1982). They used a vertical circular tube of 3.1 mm internal diameter and two heated lengths of 126 mm and 246 mm to measure the two-phase heat transfer, pressure drop and critical heat flux. The refrigerant used in the experiments was R113. The experimental conditions included: a mass flux range of 125 kg/m² s to 750 kg/m² s, heat flux from 14-380 kW/m² and inlet sub cooling from 3 to 73 ºC. The experimental results indicated that the saturated boiling heat transfer coefficient increased with heat flux and was independent upon vapour quality. The authors concluded from the results that the nucleate boiling mechanism was dominant during the tests and convective heat transfer mechanism was not found to be important in the experimental range covered. The authors used their 728 saturated flow boiling data points to obtain a curve fit and suggested the following correlation for predicting the flow boiling heat transfer coefficient.

$$\alpha_{tp} = 30 Re_{lo}^{0.857} Bo^{0.714} \frac{k_l}{D_i} \qquad (6)$$

Wambsganss et al. (1993) reported similar nucleate boiling dominated results as Lazarek and Black (1982) for a 2.92 mm diameter tube. They used the flow pattern map of Damianides and Westwater (1988) obtained for a 3 mm inner diameter tube and identified the slug flow pattern up to vapour qualities of about 0.6 to 0.8 and concluded that the slug flow pattern with thick liquid film and high boiling number cause the nucleate boiling dominant heat transfer mechanism. The authors tested the applicability of several correlations taken from the literature. The flow boiling correlation of Lazarek & Black (1982) and the pool boiling correlation by Stephan and Abdelsalam (1980) predicted their experimental data well. The Liu and Winterton (1988) and the Jung and Radermacher (1991) correlations were next after the Lazarek & Black and Stephan & Abdelsalam correlations.

Kew and Cornwell (1997) experimentally studied the flow boiling heat transfer coefficient in small diameter tubes. They tested different diameter tubes ranging from 1.39 to 3.69 mm having fixed heated length of

500 mm and used R141b as working fluid. Their experimental results indicated that the tubes with diameter of 3.69 and 2.87 mm behaved in a similar fashion as conventional channels and the heat transfer coefficient was a function of heat flux at low vapour qualities and at higher vapour qualities the heat transfer coefficient increased with vapour quality and was essentially independent of heat flux. They observed different behaviour of the small 1.39 mm diameter tube compared to the other tubes. They observed that for a higher mass flux (G=1480 kg/m^2 s) the heat transfer coefficient in this tube decreased rapidly with increase in vapour quality while this behaviour was not found for low mass flux (G=478 kg/m^2 s). They concluded that local dryout occurred for the small diameter tube. The correlations available in the literature performed poorly especially for the smaller diameter tubes having confinement number of 0.5 and above.

Kureta et al. (1998) experimentally investigated the flow boiling heat transfer and pressure drop of water in small diameter tubes and conventional diameter tubes. The diameter ranged from 6 mm down to 2 mm and the heated length from 4 mm to 680 mm. During the experiments, mass flux was varied from 100 to 10170 kg/m^2 s, the inlet sub cooling from 70 to 90 K and the maximum heat flux achieved was 33 MW/m^2. The heat transfer coefficient was observed to increase with local quality in sub cooled region. The dependence on vapour quality diminished at a local vapour quality below zero and slightly higher than zero. A local peak was found in heat transfer after that the heat transfer coefficient increased monotonically with quality which was attributed to vaporization of a thin liquid film and higher vapour velocity. Surprisingly, they found higher heat transfer coefficients for the 6 mm diameter tube than that for the 2 mm diameter tube. This was attributed to the suppression of nucleate boiling heat transfer and the fact that flow was laminar in the smaller diameter tube.

Warrier et al. (2002) studied the flow boiling heat transfer and pressure drop of FC-84 in narrow aluminium rectangular parallel channels having hydraulic diameters of 0.75 mm. The range of heat flux and mass flux was not clearly stated but the results presented in the paper are for a heat flux up to 4.5 W/cm^2 and mass flux of 557 to 603 kg/m^2 s. Their results indicated that the heat transfer coefficient decreased monotonically with increase in vapour quality for all the cases. The deterioration of heat transfer was attributed to a dryout region occurring under the bubble. They examined different correlations taken from literature for predicting their experimental data but with poor agreement and found that most of the correlations were over predicting their experimental data.

Owhaib et al. (2004a) investigated the heat transfer of R134a during flow boiling in vertical channels of diameters 1.70, 1.224 and 0.826 mm and a fixed heating length of 220 mm. The heat flux was in the range 3 to 34kW/m^2, mass flux 50 to 400 kg/m^2 s, system pressures 8.626 and 6,458 bar and vapour qualities up to slightly above 0.6. Their results indicated that heat the transfer coefficient was a strong function of heat flux and was only weakly dependent on mass flux and vapour quality up to vapour qualities of about 0.6 above which the heat transfer coefficient decreased. The authors explained the decrease in heat transfer coefficient by the phenomenon of partial dryout. They obtained higher heat transfer coefficient for a smaller diameter tube.

Sobierska et al. (2006) performed experiments for flow boiling of water in a rectangular vertical micro channel of 1.2 mm hydraulic diameter. Mass flux was varied from 50 to 1000 kg/m^2 s, heat flux up to 100 kW/m^2 and inlet sub cooling from 2 to 20 degrees. Heat transfer coefficient decreased with increase in vapour quality and was influenced with both heat and mass flux. The authors, based on their visualization results, observed no nucleation occurring at comparatively higher vapour qualities.

Harirchian and Garimella (2008) used rectangular micro channels of widths ranging from 100 to 5850 μm and a depth of 400 μm. They used FC-77 as the working fluid and the experiments were performed for a mass flux range of 250 to 1600 kg/m^2 s, the heat flux range is not specifically mentioned but from experimental data maximum limit is approximately 650kW/m^2. They observed that nucleate boiling was present at low heat fluxes and the heat transfer coefficient was dependent upon heat flux. However, at higher heat fluxes the convective mechanism was found to be the dominating contributor to the heat transfer coefficient. At higher heat fluxes a decrease in heat transfer coefficient was also observed and was attributed to partial dryout. The authors observed that heat transfer was independent of channel width for channel widths of 400 μm and higher. For 250 μm channel the heat transfer coefficients were lower than larger channels. They compared the experimental results with predictions from several correlations, including pool boiling and flow boiling correlations, from literature and found that the pool boiling correlation by Cooper (1984) best predicted their data among all the correlations considered.

A literature survey for flow boiling heat transfer in micro channels has been conducted and a few of these studies are also listed in Table 2-2. For several tube diameters, many working fluids and a wide range of operating parameters the results can be summarized as follows:

Different mechanisms have been found to be controlling the heat, for example it has been shown by Lazarek and Black (1982; Wambsganss et al. (1993; Tran et al. (1996; Bao et al. (2000; Huh and Kim (2007) that the nucleate boiling heat transfer mechanism dominated for most of the experimental conditions. Contrarily, other studies Kureta et al. (1998; Oh et al. (1998; Lee and Lee (2001; Sumith et al. (2003; Kuznetsov and Shamirzaev (2007; Madrid et al. (2007) show that the heat transfer was mainly due to forced convective evaporation of thin liquid film between the wall and the vapor core. In some studies Owhaib et al. (2004a; Saitoh et al. (2005; Bertsch et al. (2009) the nucleate boiling dominated for a certain vapor quality range and beyond that the heat transfer coefficient decreased with increase in vapor quality. Interestingly, studies by Ravigururajan (1998; Warrier et al. (2002; Yen et al. (2003; Steinke and Kandlikar (2004; Yen et al. (2006) show that the heat transfer coefficient decreased with increase in vapor quality even from the beginning of the boiling process i.e. decrement in the heat transfer coefficient starts from very low vapor qualities. Kew & Cornwell also observed that the heat transfer coefficient decreased rapidly with increasing quality and was essentially independent of heat flux for a tube diameter of 1.39 mm and a mass flux of 1489 kg/m^2 s. The effect of channel dimensions has also been checked in a few studies and an increase in heat transfer coefficient is observed with decrease in hydraulic diameter in Owhaib et al. (2004a; Saitoh et al. (2005; Hsieh et al. (2008) and a reverse trend is found in Kureta et al. (1998; Harirchian and Garimella (2008). Partial dryout has also been found to exist in microchannels e.g. in Kew and Cornwell (1997; Warrier et al. (2002; Owhaib et al. (2004a; Saitoh et al. (2005; Harirchian and Garimella (2008). Interestingly, the study by Saitoh et al. (2005) clearly indicated that the dryout occurred at lower vapor qualities when the channel diameter was reduced. Notably, results from an experimental study by Sobierska et al. (2006) showed a mechanism similar to nucleate boiling but no nucleation was seen to occur from visual observations.

Based on the literature review conducted, it is clear that the experimental results for flow boiling heat transfer coefficient in microchannels are inconclusive and are found to have different trends. Therefore, more experiments and investigations in this area are certainly needed to clarify further the behavior of boiling fluids in small diameter channels.

Table 2-2 Previous flow boiling heat transfer studies for micro channels

Author(s) & Ref	Fluid	Dimensions/Dh [mm]	q" [kW/m²]	G [kg/m²s]/other	P_{sat}/T_{sat} [°C]	Geometry/Orientation	Remarks
Tran et al. (1996)	R12, R113	2.46, 2.40 and 2.92	3.6-129	44-832	-	Circular and Rectangular	The heat transfer coefficient was observed to be only dependent on heat flux and fairly independent of vapour quality and mass flux. This made authors conclude that the nucleate boiling was the controlling mechanism during the heat transfer process. A correlation was also recommended by the authors for calculating heat transfer coefficient.
Oh et al. (1998)	R134a	2, 1 and 0.75	10 to 20	240-720	4 bar	Circular, Horizontal	Heat transfer coefficient for 0.75 mm tube increased linearly with vapour quality from very low vapour qualities up to 0.6. For larger tube diameters the heat transfer coefficient increment was small at low vapour qualities up to 0.3 and then increased up to vapour qualities of about 0.9 and then decreased which was attributed to dryout.
Bao et al. (2000)	R11, R123	1.95	5-200	50-1800	200-500 kPa	Circular, Horizontal	The dominant heat transfer mechanism was concluded to be nucleate boiling where mass flux and vapour quality had relatively low impact on heat transfer coefficient. The correlations tested did not predict the whole range of their data.
Lee and Lee (2001)	R113	0.4 to 2 mm gap size	Up to 15	50-200	-	Rectangular, Horizontal	The heat transfer coefficient and pressure drop were measured. The heat transfer coefficient increased with mass flux and vapour quality and heat flux was of minor important. For the smallest tube the thin film evaporation was concluded to be the dominant heat transfer mechanism. For higher flow rate conditions, the Kandlikar correlation predicts the data with a mean deviation of 10.7%.
Sumith et al. (2003)	Water	1.45	10-715	23.4-152.7	Atmoshpheric pressure	Circular, vertical	Slug-annular and annular were the dominant flow patterns during the tests. The correlations from literature under predicted their data. Vapour Reynolds number dependence of heat transfer coefficient was found for Re_g> 2000 while below this value Re_g had negligible effect on heat transfer coefficient.
Sumith et al. (2003)	Water	1.45	10-715	23.4-152.7	Atmoshpheric pressure	Circular, vertical	Slug-annular and annular were the dominant flow patterns during the tests. The correlations from literature under predicted their data. Vapour Reynolds number dependence of heat transfer coefficient was found for Re_g> 2000 while below this value Re_g had negligible effect on heat transfer coefficient.
Yen et al. (2003)	R123, FC-72	0.19, 0.3 and 0.51	7-27	50-300	Atmospheric pressure at exit	Circular	Mass and heat fluxes are not specifically mentioned but have been deduced from the data in the paper. In saturated boiling regime, the heat transfer coefficient decreased with increase in vapour quality but was independent of mass flux.

Steinke and Kandlikar (2004)	Water	0.207	5-930	157-1782	Atmospheric pressure at exit		Heat transfer coefficient decreased with increase in vapour quality and heat flux dependency was also found for lowest mass flux tested. Flow patterns were recorded; flow reversal and dryout were also visualized.
Kuznetsov and Shamirzaev (2007)	R21	1.6×6	Up to 40	50 and 215	1.5 to 2.4 bar	Rectangular/Vertical	Convective boiling dominated for G=215 kg/m2 s and for this mass flux and q"=6 kW/m2, the degradation in heat transfer coefficient was not observed up to vapour quality of 0.97. The data was not predicted by correlations in general except from modified form of Cooper correlation and Kandlikar & Balasubramanian correlation which predicted values up to vapour quality of 0.5.
Huh and Kim (2007)	Water	0.1	200-500	90-267	-	Rectangular	Flow patterns were also observed. Nucleate boiling was the dominant heat transfer mechanism; however, the flow pattern observed was very long slug and semi-annular flow. Correlations by Chen, Shah, Kandlikar, Gungor-Winterton and Liu-Winterton were tested for predictions with mostly over prediction and poor agreement.
Madrid et al. (2007)	HFE-7100	0.840	1.0490-6.156	69-194	61 ºC	Rectangular/Vertical Multichannels	Heat flux was observed to have no effect on heat transfer coefficient hence; the authors concluded the convective boiling to be the dominant heat transfer mechanism. Heat transfer coefficient deteriorated at higher vapour quality which was attributed to dryout. Dryout was said to be dependent on superficial velocity of two-phase fluid in the experiments.
Bertsch et al. (2009)	R134a, R245fa	1.09 and 0.54	0-220	20-350	8 to 30 ºC	Rectangular	Nucleate boiling was concluded to be the dominant mechanism. At higher vapour qualities the heat transfer coefficient decrease with increase in vapour quality. Flow boiling heat transfer coefficient for R134a was higher than R145fa. Heat transfer increased with decrease in hydraulic diameter.
Tibiriçá and Ribatski (2010)	R134a, R245fa	2.3	5-55	50-700	22,31 and 41 ºC	Circular/Horizontal	Heat transfer coefficient was found to be a function of heat flux, mass flux and vapour quality. Ten correlations from literature were used to compare with experimental data. Liu-Winterton, Saitoh et al. and Zhang et al. worked best for their data for all data.

2.5 Dryout

Critical heat flux (CHF) during the boiling process represents the situation when liquid deficiency occurs at the heater surface. Usually this is a consequence of either vapor blanketing on the heater surface or complete dryout of the liquid film at the channel wall. The situations where CHF occurs, pose a serious challenge for the designers of heat exchange devices as the CHF has to be avoided for the safe and effective operation of the heat exchange device and the device being cooled. Two different mechanisms usually lead to CHF condition, termed as departure from nucleate boiling (DNB) and dryout. At relatively higher inlet sub cooling and low vapor quality conditions where normally the nucleate boiling is the dominant heat transfer mechanism; the CHF is reached at high heat flux through DNB and is characterized by wall temperature excursion and burn out of the heater surface. Dryout occurs at comparatively higher vapor fractions when the annular flow is usually prevalent in the channel and a liquid film is formed between the vapor core and heater surface and convective boiling is the dominant heat transfer mechanism. Dryout of the liquid film usually occurs due to complete evaporation of the liquid film but may also be prompted due to the effects of liquid entrainment and deposition. Dryout can also be reached also at low heat flux and is characterized by wall temperature fluctuations and deterioration of heat transfer.

Dryout type CHF is the focus of the current thesis. Dryout or CHF defines an upper or critical limit for the safe and efficient operation of the heat exchange devices. Practically, the heat exchange devices are operated below this critical limit as serious temperature excursions result due to deterioration of heat transfer. In case of micro channels, the heat transfer is deteriorated at the onset of dryout i.e. below dryout point, where the fluctuations in wall temperature start appearing. In applications where the uniformity of wall temperature is a key issue such as in cooling of electronics, the onset of dryout is very important to be known which otherwise can give rise to what is called the local hot spots and might cause failure of the electronic components. Dryout during flow boiling in micro channels is, therefore, a critical issue to be understood before the utilization of micro heat exchange devices starts in demanding situations such as in high heat flux cooling applications as also suggested in many reviews and critical studies on CHF in micro channels.

Bergles (1962) was probably among first few researchers to conduct forced convective and burn out experiments in small diameter tubes ranging from less than a mm to approximately 4.5 mm diameter tubes

using water as working fluid. Direct heating of the test section was adopted for all the tests. The burn out was observed to start always at the exit of the test tube. The author observed an increase in burn out heat flux with decrease in diameter. It was further observed that at high sub cooling conditions, the burn out heat flux decreased with decrease in sub cooling degree. Due to system limitations, the effect of pressure was not studied and the exit pressure was fixed at 15.5 psi for all the tests. Burn out flux was observed to be inversely related to L/D ratio.

Lazarek and Black (1982) investigated CHF in a 3.1 mm diameter tube, the experimental details for which have already been given in section 2.4. They presented a temperature profile obtained close to the exit of the test section where oscillations due to intermittent rewetting of the tube wall were observed. The dryout type CHF conditions were observed to occur always from the exit of the tube. The authors proposed a correlation to predict the critical quality at which CHF conditions would be reached.

Bowers and Mudawar (1994) measured CHF and two-phase pressure drop in mini and micro channels of diameters 2.54 mm and 0.510 mm respectively using R113 as working fluid. The experiments were performed at a pressure of 1.38 bar, at inlet sub cooling from 10 to 32 ºC and mass flow rate from 19 to 95 ml/min. For the low flow rates tested, the authors did not find any dependency on inlet sub cooling. Interestingly, superheated exit conditions were observed for the lowest mass flow rate tested. Higher CHF values were achieved when using a micro channel. Later, Qu and Mudawar (2004) investigated CHF in parallel microchannels and found that CHF increased with mass velocity. Based on their data and data from Bowers and Mudawar (1994) they presented a CHF correlation for micro channels.

Inasaka and Nariai (1992) and Celata et al. (1995) carried out sub cooled CHF experiments mainly for fusion reactor component cooling. They found an increasing trend of CHF with mass velocity, as expected and found that CHF also increased with inlet sub cooling. However, the effect of pressure on CHF was negligible at least compared to the effect of inlet sub cooling and mass velocity.

Sumith et al. (2003) performed experiments to measure the flow boiling heat transfer and CHF in a vertical channel of 1.45 mm inner diameter and further experimental details are given in Table 2-2. They observed that near the CHF conditions the wall temperature close to the exit oscillated with a period of 10 second or longer. The authors attributed these fluctuations in wall temperature to the intermittent rewetting of the tube wall. The dryout vapor quality varied from 0.5 to 0.7 depending on the

mass flux. Moreover, they observed that the CHF conditions always was initiated close to the exit of the tube. The Katto (1980) captured the trend but over predicted the data by 20%.

Kosar and Peles (2007) presented experimentally obtained CHF characteristics of R123 in parallel rectangular microchannels, 0.2 mm wide and 0.264 mm deep. Experimental conditions were: mass flux 291-1118 kg/m^2 s, system pressure 227-520 kPa, heat flux 53-196 W/cm^2. Flow patterns obtained during their experiments revealed that CHF was reached through dryout of the liquid film during the annular flow of the refrigerant. Increased heat flux caused complete evaporation of the liquid film which was thicker at relatively lower heat fluxes. CHF increased with mass flux and decreased with exit quality at which CHF occurred. The effect of system pressure was complex and CHF first increased to a maximum with increase in system pressure and then decreased. Correlations by Katto and Ohno (1984) and Shah (1987) provided better predictions of the experimental data as compared to micro channel correlations by Kosar et al. (2005), Bowers and Mudawar (1994) and Qu and Mudawar (2004). However, none of the correlations predicted the variation in CHF with pressure. Therefore, a new CHF correlation was proposed accounting for the system pressure increment.

CHF studies just reviewed and some studies presented in Table 2-3 show almost a similar trend with respect to variation of mass flux but the effects of tube diameter, inlet sub cooling, vapor quality and system pressure on CHF are not clear and different trends are found in different studies. For example, the dryout/CHF increases almost linearly with mass flux as found in the studies by Inasaka and Nariai (1992; Celata et al. (1995; Kuan and Kandlikar (2006; Wojtan et al. (2006; Kosar and Peles (2007; Martin-Callizo et al. (2008). The quality at dryout decreased with increase in heat flux Bowers and Mudawar (1994; Kuan and Kandlikar (2006; Kosar and Peles (2007) but a more complex relationship of CHF and vapour quality was obtained by Roday and Jensen (2009) where CHF first decrease with vapour quality in sub cooled region and increased with increase in vapour quality in saturated condition. The experiments by Lazarek and Black (1982; Sumith et al. (2003; Chen and Garimella (2007) show that critical conditions started at the exit. Similarly discrepancies exist for the trends of CHF dependence on diameter, pressure and inlet sub cooling, as observed in studies reviewed in this section.

It can easily be observed from the literature survey presented that most of the CHF/dryout experiments conducted are for water. The CHF data for refrigerants and other fluids is scarce. To the author's best knowledge, quantitative dryout incipience results have not been reported ex-

cept by Martin-Callizo et al. (2008). Therefore, a clear need is felt for more CHF/dryout tests in mini and micro channels using fluids other than water such as refrigerants for refrigeration and heat pumping technologies and dielectric fluids which are of interest in electronics cooling.

Table 2-3 Previous CHF and dryout studies conducted for micro channels

Author(s) & Ref	Fluid	Dimensions/Dh [mm]	q" [kW/m²]	G [kg/m²s] /other	P_{sat}/T_{sat} [°C]	Geometry/Orientation	Remarks
Mishima and Nishihara (1985)	Water	2.4 mm gap size and 40 mm width	Up to 1300	7 to 610	Atmospheric exit pressure	Rectangular/Vertical	Experiments in both upward and downward direction were performed. Increasing trend was found for CHF with increase in mass flux. Effect of inlet sub cooling was not obvious in up flow while in case of down flow the CHF increased with increase in sub cooling.
Oh and Englert (1993)	Water	1.98 mm gap size	-	20 to 80	20 to 85 kPa exit pressure	Rectangular/Vertical	Temperature fluctuations were observed close to CHF condition. Effect of inlet sub cooling was negligible while with increase in mass flux the CHF increased. For their low rates tested, the CHF increased with pressure.
Celata et al. (1995)	Water	2.5 to 8	-	2 to 40 m/s liquid velocity	Exit pressures from atmospheric to 5MPa	Circular/Horizontal and Vertical	Sub cooled flow boiling CHF was presented. CHF increased almost linearly with mass flux and inlet sub cooling. Pressure effect was negligible on CHF as compared to the effect of inlet sub cooling and mass flux but slightly increasing effect of CHF was concluded. For velocities 2 to 8 m/s, the influence of channel orientation was negligible while CHF increased with decrease in inner tube diameter.
Roach et al. (1999)	Water	1.17, 1.45 and 1.131	-	250-1000	344-1043 kPa exit pressure	Circular and triangular	Dryout type CHF was concluded to be the mechanism due to high qualities achieved in the tests. CHF increased with mass flux however unlike high mass flux tests, the CHF decreased with decreasing channel diameter. Bowring correlation predicted their CHF data reasonably among many correlations tested.
Yu et al. (2002)	Water	2.98	-	50-200	200 kPa	Circular/Horizontal	Flow boiling heat transfer, pressure drop and CHF were obtained from experimental data. CHF increased with mass flux and occurred at comparatively higher vapour qualities as compared to conventional channels.
Kuan and Kandlikar (2006)	Water	1.054×0.157	203.6-538.9	50.4-231.7	34.1-91.5 kPa		CHF increased with mass flux and decreased with vapour quality.
Wojtan et al. (2006)	R134a, R245fa	0.8 and 0.5	3.2 to 600	400-1600	30 ºC and 35 ºC	Circular/Horizontal	CHF increased with mass flux and CHF for larger diameter tube was higher. For mass flux up to 1000 the effect of saturation temperature was not obvious but at higher mass flux CHF was higher for Tsat=35 ºC. Inlet sub cooling had negligible effect on CHF. With increase in heated length, the CHF dropped. Existing correlations did not predict the experimental results.

Chen and Garimella (2007)	FC-77	0.839	-	30 to 50 ml/min	-	Horizontal	Temperature fluctuations were observed close to CHF condition and CHF condition was identified with abrupt rise in wall temperature. Based on wall temperature measurements, it was observed that CHF first occurred near the exit of micro channels. CHF increased with mass flow rate.
Martin-Callizo et al. (2008)	R134a, R245fa, R22	0.64	5 to 69	185 to 535	26.6 to 35 ºC	Circular/Vertical	Temperature fluctuations were observed close to CHF condition. Dry-out incipience heat flux was also determined which increased with mass flux. CHF increased with mass flux. Dryout incipience occurred earlier for R245fa than other two refrigerants. Katto-Ohno correlation gave reasonable predictions. Pressure showed negligible effect for the narrow band of pressures tested.
Roday and Jensen (2009)	Water and R123	0.700, 0.427and 0.286		320-1570	26 to 225 kPa exit pressure	Circular/Horizontal	CHF increased with mass flux. CHF increased with decrease in diameter from 0.427 to 0.286 but increment in CHF also occurred when increasing diameter from 0.427 to 0.700 so the effect of diameter on CHF was rather complex. CHF decreased with exit quality first in sub cooled region but in saturated region after vapour quality CHF increased with increase in exit vapour quality.
Mauro et al. (2010)	R134a, R236fa, R245fa	0.199 mm width and 0.756 mm deep	-	250 to 1500	20 to 50 ºC		Experiments were performed by employing a split flow system with one inlet at the middle of the channels and two outlets at either end which resulted in enhanced CHF as compared to single inlet and single outlet system. CHF base values increased with all fluids with increase in flow rate. Saturation temperature increment gave a slightly decreased CHF for R134a and R236fa but for R245fa there was no change in CHF.
Park and Thome (2010)	R134a, R236fa, R245fa	0.467mm wide,4.052mm deep and 0.199 mm wide,0.756 mm deep	37 to 342 W/cm²	1000 to 4000	10 to 50 ºC	2 types of multi port microchannels	CHF increased with mass flux, as expected. When channel size decreased, the inlet sub cooling was less important. CHF showed reverse tendency with increasing saturation temperature. Experimental data was in good agreement with Katto-Ohno, Wojtan et al. and Tevellin & Thome models.

2.6 Two-Phase Pressure Drop

In general, a decrease in channel diameter will cause an increased pressure drop; therefore, use of micro channels may result in a penalty in the form of increased pressure drop in the heat exchange system. However, to mitigate the problem and optimize the overall efficiency of the heat exchange system it will be expected to have more parallel micro channels. The two-phase pressure drop is more complicated than single phase flow due to complex interaction of liquid and vapor phases during the flow. The increased pressure drop in a two-phase flow is a consequence of increased vapor velocity and resulting higher vapor shear. Diabatic two-phase pressure drop in a horizontal channel will generally comprise of two components one of which is contributed by frictional pressures drop and the other is due to change in momentum of the vapor along the channel (acceleration pressure drop). If the channel orientation is other than horizontal then an additional part caused by gravity will have to be added to get the total two-phase pressure drop. The acceleration and gravitational parts can be calculated by the relations found in the literature such as in Collier and Thome (1994). The most challenging and most frequently investigated part of the two-phase pressure drop is the frictional part.

The two-phase pressure drop is of great importance in a wide variety of industrial applications such as in refrigeration evaporators and condensers, process industry applications, petroleum and gas industry and has been investigated extensively in conventional channels. There are models available to estimate the two-phase pressure drop reasonably well in conventional channels. Two widely used models are the homogeneous model and the separated flow model. The homogeneous model considers the two phases flowing with same velocity as a single phase with mixture averaged properties while the separated flow model considers the two phases flowing as two separated streams with constant velocity but not necessarily the same velocity. Other correlations for two-phase frictional pressure drop include Pierre (1969; Friedel (1979). However, in micro channels there have been comparatively fewer studies of two-phase pressure drop and the models developed for macro channels do not seem to work well as can be seen in several studies found in the literature.

Bergles and Dormer (1969) investigated the sub cooled flow boiling pressure drop of water in small diameter tubes ranging from 0.062 inch (1.57 mm) to 0.198 inch (5.029 mm). Other experimental conditions were: exit pressure 30-80 psia (2.06-5.51 bar), liquid velocity 5-60 ft/s (1.52-18.28 m/s) and heat flux 0-5500000 Btu/hft^2 (0-17.5 MW/m^2). The data were obtained by setting the flow and inlet conditions and in-

creasing the heat flux in steps up to just below CHF or up to a point where exit saturated conditions were reached. There was a general increase in pressure drop once the boiling initiated, as expected.

Lin et al. (1991) investigated local frictional pressure drop during vaporization of R12 in capillary tubes of 0.66 mm and 1.17 mm internal diameter. Experimental conditions included: mass flux from 1440 to 5090 kg/m^2 s, inlet pressure from 6.3 to 13.2 bar and inlet sub cooling from 0 to 17 degrees. The two-phase flow multiplier increased with vapor quality. It was noted that in adiabatic capillaries the variation of quality was non-linear. Acceleration and frictional pressure drops both increased more rapidly in the part of the tube where equilibrium two-phase flow was established.

Cavallini et al. (2005) obtained adiabatic pressure drop data in a rectangular multiport micro channel with a hydraulic diameter of 1.4 mm using three refrigerants. The refrigerants tested were R236ea, R134a and R410A at a saturation temperature of 40 ºC. Tests were performed for a mass flux range from 200 to 1400 kg/m^2 s. The frictional pressure gradient was obtained from saturation temperature drop measurement. The Lockhart and Martinelli (1949) worked partially for R236ea but not for the other refrigerants. The Friedel (1979) worked better for R134a and R236ea but R410A data was over predicted by this correlation. The Muller-Steinhagen and Heck (1986) correlation worked well for R134a and R236ea while data for R410A was over predicted. R134a data was also well predicted with correlations by Mishima and Hibiki (1996; Zhang and Webb (2001).

An experimental study was conducted by Pehlivan et al. (2006) for air-water two-phase flow and pressure drop in micro channels having diameters of 3, 1 and 0.8 mm. The homogenous model gave reasonable predictions but the model validity decreased as the diameter was reduced. The Friedel (1979) over predicted the experimental data. In general it was concluded that the available conventional two-phase pressure drop models are not valid when reducing the channel size to micro level.

Two-phase pressure drop was studied experimentally by Lie et al. (2008) in small diameter horizontal tubes of 0.83 mm and 2.0 mm inner diameter. Other experimental conditions were: mass flux from 200 to 1500 kg/m^2 s, heat flux from 5 to 15 kW/m^2, saturation temperature from 5 to 15 ºC and inlet vapor quality from 0.2 to 0.8. Pressure drop increased with mass flux and decreased with increase in T_{sat}. Smaller diameter tube

resulted in a higher pressure drop penalty, as expected. A correlation was proposed based on their data.

In Quan et al. (2008), the two-phase pressure drop was measured for condensation of water in trapezoidal micro channels of hydraulic diameter 0.109 mm, 0.142 mm, 0.151 mm and 0.259 mm. Increased mass flux and vapor quality resulted in higher two-phase frictional pressure drop. Decreased hydraulic diameter resulted in higher pressure drop. The Friedel (1979) correlation, the homogeneous model, the Lockhart and Martinelli (1949) model and Mishima and Hibiki (1996) correlation, all over predicted their experimental data. It was observed that the Lockhart-Martinelli model even with a minimum C parameter value of 5 over predicted their data.

The literature review presented in this section and in Table 2-4 for two-phase pressure drop shows that most of the studies conducted are for two-phase air-water and for adiabatic conditions. Other than air-water, many studies focus on boiling of water in micro channels. Therefore, a clear lack of two-phase data for fluids other than water is observed. Another important point to note is the partial success of Lockhart-Martinelli in predicting the experimental data with a modified value of Chisholm parameter C. This might be interpreted as, most of the studies found in the micro channels fall in laminar-laminar region. The value of parameter C in the Lockhart-Martinelli parameter is solely dependent on flow conditions and the value has since then been modified to incorporate the effects of different parameters such as channels size. A modified C value in many cases has proven to give reasonable predictions of the individual experimental data bases. As a conclusion, there is a need of more two-phase pressure drop experiments for micro channels focusing on refrigerants and diabatic test conditions and to develop new models for predicting the two-phase pressure drop.

Table 2-4 Previous two-phase pressure drop studies in micro channels

Author(s) & Ref	Fluid	Dimensions/Dh [mm]	q" [kW/m²]	G [kg/m²s]/other	P_{sat}/T_{sat} [°C]	Geometry/Orientation	Remarks
Mishima and Hibiki (1996)	Air-water	1 to 4mm	-	-	-	Circular	They considered the effect of tube diameter on parameter c and redefined it. Lockhart-Martinelli with modified c parameter was suggested to be used in small diameter tubes for the prediction of pressure drop.
Tran et al. (2000)	R12, R113 and R134a	2.46 to 2.92mm circular and 4.06×1.7mm rectangular	2.2 to 90.8	0.03-2.39m/s liquid 0.05-18.7m/s gas superficial velocities	138 to 856 kPa	Circular and Rectangular	Pressure drop increased with increase in mass flux and vapour quality. Five large tube correlations worked poorly. A new correlation based on β-coefficient method of Chisholm was proposed.
Lee and Lee (2001)	Air-water	0.4 to 4mm gap size and fixed width of 20mm	-	0.03-2.39m/s liquid 0.05-18.7m/s gas superficial velocities	Atmospheric pressure	Adiabatic	Lockhart-Martinelli model was suggested with a new definition of parameter c. Effects of mass flux and channel gap size were considered in the modified definition of C.
Kawahara et al. (2002)	Air-water	0.10 mm	-	-	-	Circular	Two-phase pressure drop increased with increase in superficial liquid and gas velocities. Homogeneous model with Dukler's definition of viscosity was reasonably good to predict the experimental data. Lockhrt-Martinelli with even C=5, over predicted the data however, with a c value of about 0.24, the model worked well. Mishima-Hibiki correlation over predicted the experimental data by about 10%.
Yu et al. (2002)	Water	2.98mm	-	50 to 200	200 kPa	Circular/Horizontal	Two-phase multiplier increased with increase in mass flux and exit vapour quality. A modification of Chisholm correlation was given which predicted their data well.
Qu and Mudawar (2003)	Water	0.231×0.713mm	-	134.9 to 400.1	1.17 bar exit pressure	21 Parallel micro channels	Better accuracy is achieved by using micro and mini channel correlations. Correlations based on tubulent-tubulent flow condition over predict the data which is the case in many macro scale correlations. A new correlation was proposed taking into account the effects of channel dimensions and mass velocity.
Wen and Kenning (2004)	water	2×1mm² cross section	25-105	57 to 211	-	Rectangular/Vertical	Lockhart-Martinrlli model with a modified value of parameter c predicted the data with an uncertainty of ±35% while other models were poor.
Sobierska et al. (2006)	water	1.2	Up to 100	50 to 1000	-	Rectangular/Vertical	Pressure drop increased with mass flux and vapour quality.
Chen et al.	Air-	3 to 9mm width and	-	100-700		Rectangular/Horizontal	It was observed that none of the few correlations tested could

(2007)	Water	3mm fixed gap					predict the two-phase pressure drop data. Therefore, a modified form of c parameter in Chisholm method was proposed.
Revellin and Thome (2007)	R-134a, R245fa	0.509 and 0.79	-	210-2094	26, 30 and 35	Circular/Horizontal	Increased pressure drop was obtained with increase in mass flux and vapour quality. However, a change of slope was observed at a mass flux corresponding to flow pattern change to annular flow. At higher saturation temperature, lower pressure drop was observed. decreased diameter resulted inhigher pressure drop and also pressure drop for R245fa was higher than R134a.
Saisorn and Wongwises (2008)	Air-Water	0.51	-	Superficial gas velocity 0.37-16, superficial liquid velocity 0.005-3.04 m/s	-	Circular/Horizontal	Two-phase pressure drop increased with increase in superficial liquid and gas velocities. Homogeneous model predictions were not in agreement while the Lockhart-Martinelli model predictions were in better agreement using a value of 5 for parameter c.
Lee and Lee (2008)	Air-water	1.62 to 2.16 mm	-	-	-	Adiabatic	In wet wall condition the two-phase pressure drop was correlated well by homogeneous model, Mishima-Hibiki and Chisholm methods. In dry wall conditions these models did not work well and a modified Lockhart-Martinelli type correlation was proposed by taking in to account the moving contact line.
Lee and Garimella (2008)	Water	0.102 to 0.997mm width and fixed depth 0.400mm	10-340 W/cm^2	46-126 ml/min	-	Multichannel	Mishima-Hibiki, Lee & Lee, Tran and Lockhart-Martinelli models were used for comparing the experimental data with a poor agreement with all. A new correlation was suggested based on Mishima-Hibiki model.
Dutkowski (2009)	Air-Water	1.05 to 2.3 mm		139-8582	-	Circular	Eight different channel diameters were checked. Results indicated that models developed for conventional channels are not applicable to small diameter tubes.
Megahed and Hassan (2009)	FC-72	0.276×0.225 rectangular Multichannels	60.4-130.6	341-531		Rectangular	Two-phase frictional pressure drop increased with increased in exit vapour quality and mass flux. Mishima-Hibiki, Lee & Lee and Qu & Mudawar were in agreement with data but Qu & Mudawar was best among the three followed by Mishima-Hibiki.

3 Objectives and Scope of the current study

3.1 Objectives of the study

It has now been well established that the classical single-phase theory for friction factor and heat transfer used in conventional channels, is also applicable in micro scale channels Lelea et al. (2004; Owhaib and Palm (2004b; Owhaib and Palm (2004c; Hrnjak and Tu (2007), with some minor deviations perhaps due to difficulties and uncertainties in experimentation and measurements at such a small scale Palm (2001) and some unnoticed parameters which did not prove to be important in macro scale or conventional channels. However, in the case of two-phase flow in micro channels, the underlying phenomena are not well understood and consequently the models are not fully established for design purposes. It has been shown in the previous chapter listing the previous micro channel studies that several discrepancies still exist among the researchers in almost all the aspects of micro channel two-phase flow pressure drop and heat transfer. Not surprisingly, based on the literature survey presented, the models and correlations developed for macro or conventional channels are not suitable for the design of micro heat exchange devices in case of two-phase flow. The fundamental reason behind the inapplicability of macro scale models in case of micro scale is the decreased importance of the governing phenomena which otherwise play important role during two-phase flow in macro channels.

Two-phase flow in micro channels is not straight forward and several different trends of boiling heat transfer, pressure drop, flow patterns and dryout are found in the literature. The relative importance of different hydrodynamic and thermal transport mechanisms in case of micro channels has not yet been investigated comprehensively. For this purpose an experimental study to investigate the two-phase flow phenomena in micro channels has been conducted. The objectives of the present study, based on the discussion in the first chapter on background and motivation and the conclusions drawn from the previous chapter on literature survey, are summarised below:

A fundamental requirement from a design point of view of micro heat exchange devices is that it should be possible to accurately predict the heat transfer and pressure drop. Open literature clearly suggests a lack of such models and correlations for the prediction of flow boiling heat transfer and two-phase pressure drop. Therefore, the basic purpose of the current work is to study the heat transfer and pressure drop characteristics of micro channels to provide accurate data for developing models and correlations for the design of mini channel heat exchangers.

During flow boiling, the most important requirement will be to define the upper limit of heat flux for a micro heat exchange device for a given set of other operating parameters and channel geometry. One of the important features of the current study is to investigate the critical heat flux (CHF) focusing on the dryout type of CHF. Also, the CHF data has mostly been obtained for water at highly sub cooled conditions. Therefore, more CHF/dryout data for refrigerant flow in micro channels and at saturated and at low sub cooling conditions is needed which is also one of the objectives of the current study.

The relative importance of different forces, such as inertial, viscous, gravitational and surface tension, changes and deviations from conventional two-phase theory start when a transition to mini and micro scale takes place. It is widely believed that two-phase flow and heat transfer show different behaviour with changing flow regimes. A key objective of the current study is to conduct visualization based flow boiling experiments in order to better understand the fundamental transport mechanisms responsible for the deviating trends during two-phase flow in micro channels.

The purpose of the present study is also:

- To investigate the effects of channel diameter and orientation on bubble behaviour and flow patterns.
- Explore and elucidate the effects of operating parameters and fluid properties on micro channel two-phase flow pressure drop, boiling heat transfer, dryout, flow patterns and bubble behaviour by using different channel diameters and different fluids.
- To assess further the applicability of macro scale models and correlations to micro scale channels in case of single phase flow.
- Contribute in the research and development of reliable and optimum design tools for compact heat exchangers.

3.2 Scope of the study

At the beginning of this study, single phase tests were already carried out on the same experimental set up using the same test sections, except the quartz test section which will be described later. The scope of this thesis is, therefore, to study the phase change phenomena in micro channels. However, some single phase tests were performed with the quartz test section to validate the experimental set up and assess further the applicability of conventional single phase theory in micro scale channels. The flow boiling experiments have been performed during the phase change of refrigerants including flow boiling heat transfer, two-phase pressure drop, dryout during flow boiling and flow boiling visualization experiments to record the flow patterns evolved and to study the associated bubble dynamics. The visualization results have been compared to previous results from the same test rig for a vertical micro channel to study the effects of channel orientation and diameter.

4 Experimental Schemes and Instrumentation

Experiments preformed during this study can be divided into two schemes. The first scheme involves the experimentation with steel tubes and the second one involves the experiments with a quartz tube. The major motive behind using the quartz tube was to visualize the two-phase flow. The main flow loop however, was the same for both the schemes of experiments with some changes in measurement instrumentation to improve the accuracy of measurements. A general description of the experimental set up is first given followed by specific descriptions of the two types of tests.

4.1 Experimental set up

The flow boiling experiments with steel tubes were conducted in vertical up flow configuration. The schematic diagram of the set up for experiments with vertical test tubes is given in Figure 4.1 and a photograph of the test rig is shown in Figure 4.2. The refrigerant, which was provided in sub cooled condition from the condenser to the suction side of the pump, was driven by a gear pump, type ISMATEC MCP-Z standard, to the pre heater section of the flow loop. Two Coriolis Effect mass flow meters were installed after the pump and one of the two flow meters was used to measure the refrigerant flow rate before entering the pre heater section. As can be seen in Figure 4.1, the pre heater is located before the test sections; therefore, the required inlet sub cooling degree was achieved by passing the fluid through the pre heater. The pre heater section was basically a section of the main tubing with an electric heater wound around it. The electric power to the pre heater was controlled by using a PID controller. Just before the inlet of the test sections and after the pre heater, there was an absolute pressure transducer to measure the system pressure. The refrigerant in the required inlet state entered either of the test sections, absorbed the heat and finally returned to the condenser thereby completing the flow loop. The boiling incipience in the test section depended on the heat flux and the mass flow rate. The test sections were heated by joule effect utilizing a DC power supply. The temperature along the outer wall of the test tube was measured by thermocouples attached on the surface of the tubes with a thermally conduc-

tive epoxy. The tip of each thermocouple was insulated electrically before being glued onto the tube surface. The pressure of the system was adjusted by controlling the water flow rate to the condenser and further fine control of the system pressure was achieved by regulating the liquid level in the condenser by adjusting the heat to a refrigerant tank connected after the condenser. Heat input to the refrigerant tank was controlled by a PID controller to set the liquid level in the condenser and consequently the system pressure. The role of the refrigerant tank in the whole system may be visualized as a shock absorber in a mechanical system where in the current system the refrigerant tank absorbed pressure fluctuations and maintained the system pressure to a very fine level. At the inlet and outlet of the test tubes, glass tubes of the same inner diameter were placed just to isolate the test sections electrically and thermally from the rest of the experimental set up. The whole set up was thermally insulated with special attention given to the test sections.

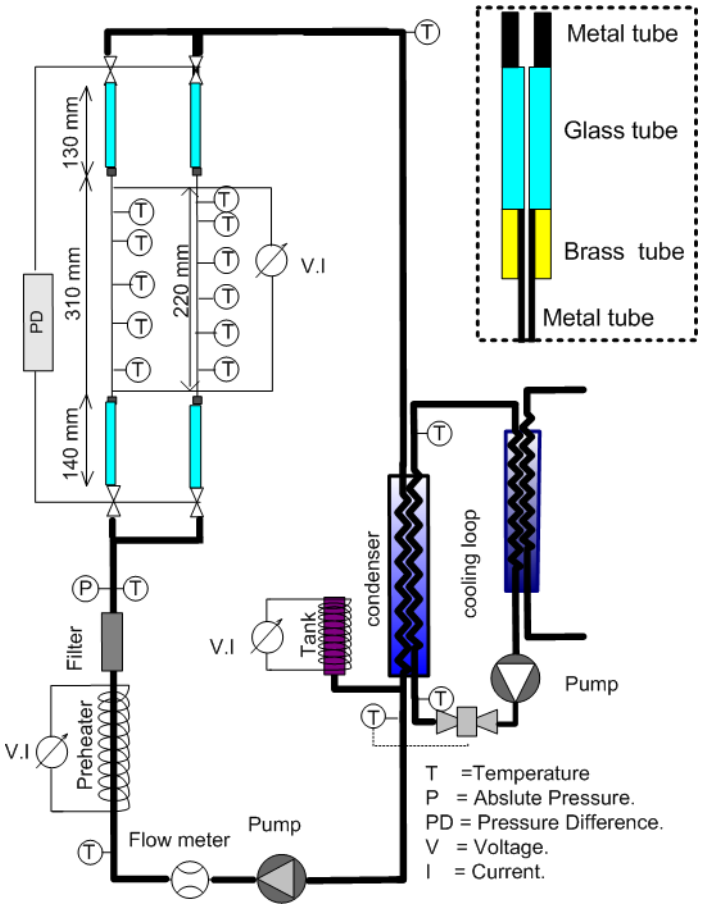

Figure 4.1 Schematic representation of experimental set up used for vertical steel test sections

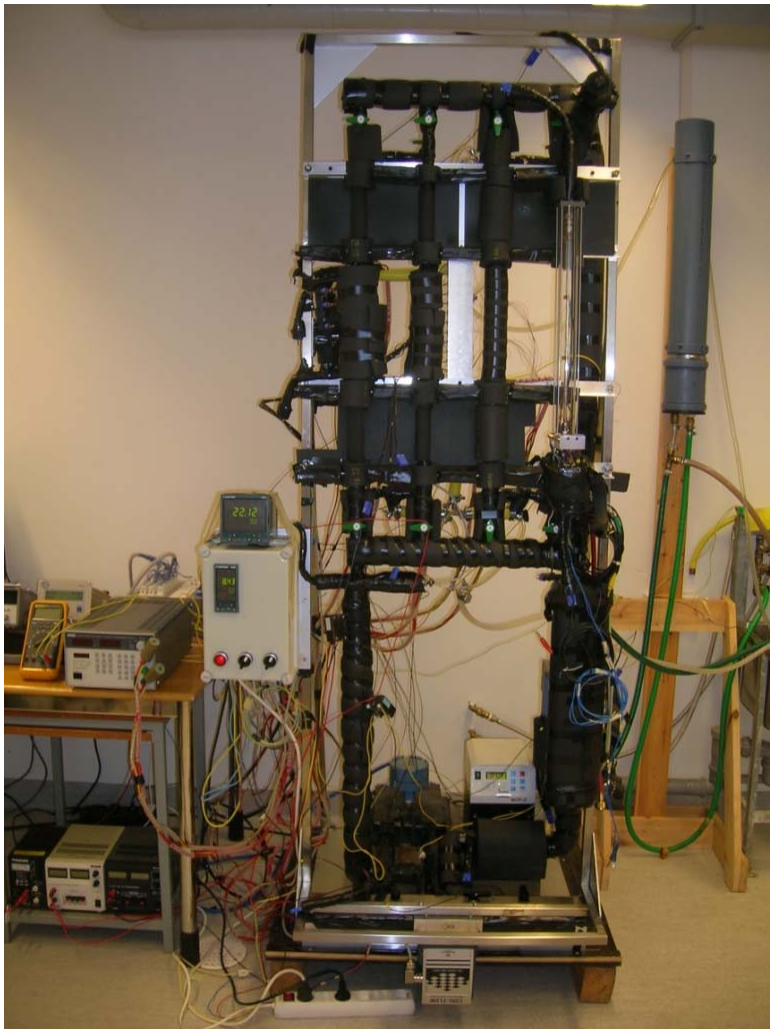

Figure 4.2 Picture of micro channel test facility

The test runs with the quartz tube were conducted using the same flow loop except that the orientation in this case was horizontal. A separate water line was provided for heating or cooling of the tubes connecting the differential pressure transducer to the system, for ensuring single phase liquid or vapour in these tubes.

4.1.1 Dimensions of steel test sections

Two steel test tubes were used with inner diameters of 1.700 mm and 1.224 mm and the heated length of both the test tubes was fixed at 220

mm. The inner tube diameter was measured by taking the mass difference of the test tube when empty and filled with a fluid of known density (in this case with distilled water), for a given length of the test tube. In this way the inner volume was obtained and assuming the inner space of the tube as a cylinder, the inner tube diameter was calculated. The measurements were repeated several times and an average value of the tube diameter obtained was used. A highly accurate balance (Mettler Toledo AX205) was used for carrying out the measurements. The uncertainty in the inner diameter was estimated to be ±0.0035 mm for 1.700 mm test tube and ±0.0047 mm for 1.224 mm test tube. Scanning electron microscope (SEM) images obtained for the two test tubes can be viewed in Figure 4.3.

(a)D=1.700 mm (b)D=1.224 mm

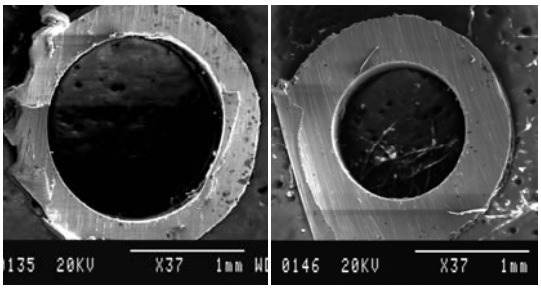

Figure 4.3 SEM images of the two test tubes of 1.700 mm and 1.224 mm inner diameter

Inner tube surface characterization was also performed to obtain the surface roughness information of the test tubes to be employed later in the calculations of boiling heat transfer. The method of stylus profilometry was used to characterize the inner surface of the tubes with 5 independent profiles obtained for a fixed sampling length of each measurement. The average values were obtained for different surface roughness parameters from the measurements carried out. The arithmetic mean roughness Ra value and maximum valley depth R_v for test tube of 1.70 mm were calculated to be 0.21 μm and -0.73 μm respectively and the same dimensions for test tube of 1.224 mm were calculated as 2.55 μm and -5.08 μm respectively. The scanning images obtained from surface characterization can be viewed in Figure 4.4 for 1.700 mm tube and in Figure 4.5 for 1.224 mm inner diameter tube.

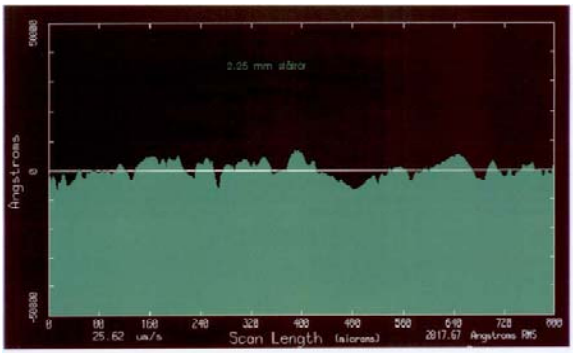

Figure 4.4 Inner surface roughness, image obtained for D=1.700 mm

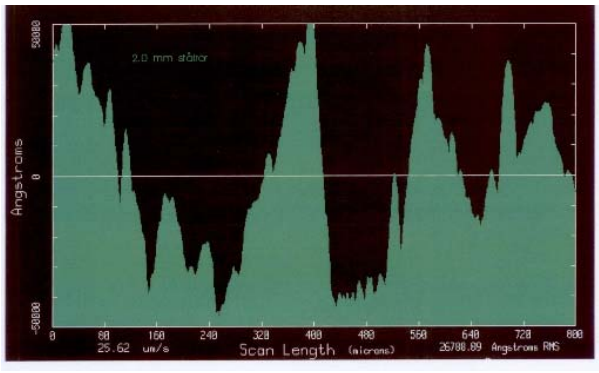

Figure 4.5 Inner surface roughness, image obtained for D=1.224 mm

4.2 Experiments with quartz tube

The quartz tube made of fused silica was unique in two aspects. Firstly, it was coated with a thin electrically conductive layer of Indium-Tin-Oxide (ITO) to allow simultaneous heating and visualization of the boiling process. Secondly, two holes were drilled for pressure taps just at the inlet and outlet of the test section, contrary to many studies in the literature where pressure taps are located away from the inlet and outlet and compensation has to be made for the two-phase pressure drop measured in the unheated length of the section. The compensated two-phase frictional pressure drop at the outlet is usually calculated by using models present in the literature. Since, there is no well agreed model for two-phase frictional pressure drop calculations in micro channels; the result-

ing frictional pressure drop calculations after compensation are then questionable with regard to accuracy.

The main flow loop employed during the experiments with quartz test section was the same as shown in Figure 4.1 in the previous section for the steel test tube experiments except that the glass test section was designed to have horizontal orientation mainly for two reasons. Firstly, to investigate the differences in flow patterns and heat transfer characteristics of a horizontally and vertically oriented test section. Secondly, to eliminate the gravitational part of pressure drop from over all pressure drop. It is worthwhile to mention here that two phase flow visualization tests in a vertical quartz test section of 1.33 mm inner diameter were carried out by (Owhaib 2007) and (Martin-Callizo 2010) using the same experimental set up and flow loop.

The test section was connected to the rest of the flow loop with Swagelock connections at both ends. Brass cylinders having approximately same inner diameter (0.90 mm) was inserted into the Swagelock connections and brazed so that the cylinders meet in line with the two ends of the test section. For improved pressure drop measurements, two holes on the Swagelock connection, normal to the flow direction and just at the inlet and the outlet of the test section (approximately 3 to 4 mm from the inlet and exit of the test section) were drilled for pressure taps as shown in Figure 4.6. Having two pressure ports just at the inlet and outlet of the test section allowed to avoid the unheated two phase pressure drop length which would otherwise introduce an unwanted contribution in the two-phase frictional pressure drop calculations. The inner diameter of the connecting brass cylinder within the Swagelock was chosen to be the same as that of the test tube in order to eliminate the sudden contraction and expansion pressure losses which will otherwise contribute to the total pressured drop.

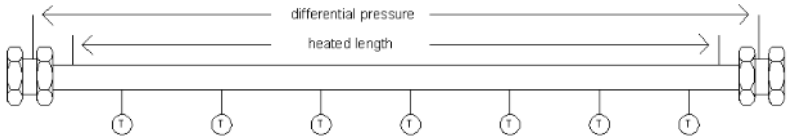

Figure 4.6 Test section with pressure drop measurement points just at the inlet and outlet of the quartz tube

4.2.1 Dimensions of quartz test section

The quartz test section used for visualization of the flow had an inner diameter of 0.781 mm. The inner diameter was measured employing the same procedure as discussed in the previous section for the steel tubes. To check the homogeneity of the inner tube diameter along the whole length of the test section, different measurements were done by varying the length of water column in the tube. It was found that the diameter changed slightly along the tube but was within ±5% of the average from one end to the other end of the tube. The estimated uncertainty in the diameter for the quartz tube was ±0.004 mm. The inner surface characterization of the glass tube was done with the same procedure as described for the steel test tubes to obtain the surface roughness information. The arithmetic mean roughness Ra value determined was 0.015 μm and the maximum valley depth was -0.036 μm. The image obtained for the inner surface characterization is shown in Figure 4.7. As expected, the inner tube surface of the quartz tube is quite smooth as compared to the steel tubes.

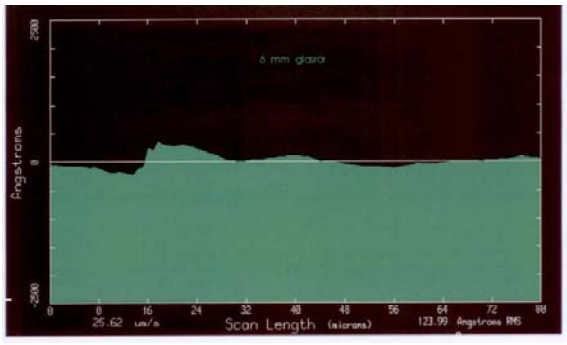

Figure 4.7 Inner surface roughness, image obtained for D=0.781 mm quartz tube

4.3 Instrumentation and Systematic Uncertainties

Most of the instrumentation used in the experiments is same as described in Owhaib (2007) and Martin-Callizo (2010). Therefore, when the same instruments have been used, these will not be explained in detail. Instead the reader is referred to the reference mentioned.

4.3.1 Absolute pressure transducer

The system pressure was measured at the inlet of the test sections as shown in Figure1.1 using a highly accurate and calibrated absolute pressure transducer PDCR 4060 having a range of 0 to 20 bar with an output range of 0-100 mV. A calibration of the sensor was performed before the experiments to check the compliance of the calibration curve provided by the manufacturer. In both schemes of experiments with vertical and horizontal test sections, the system pressure was measured with the same pressure transducer. The accuracy of the transducer, as provided by the manufacturer, was 0.04% of full scale including the non-linearity and hysteresis effects. The transducer was calibrated routinely using a certified pressure calibrator (DRUCK DPI 603) to check any offset during the time of the measurements. Therefore, as a conservative approach, the systematic uncertainty in the pressure measurements was estimated to be $\pm$10 mbar.

4.3.2 Differential pressure transducer

Pressure difference was measured using a differential pressure transducer, PDCR 2160, having a range of 0 to 350 mbar differential with an output voltage range of 0-50 mV. The accuracy of the sensor, as provided by the manufacturer, was 0.06% of full scale. The sensor was calibrated regularly using a pressure calibrator (DRUCK DPI 603) to check the reliability and accuracy of the sensor during the time. A separate water line was provided for heating or cooling to ensure single phase liquid or vapour in the lines connecting the differential pressure transducer to the flow loop as shown in Figure 4.1. In the case of single phase heat transfer and pressure drop tests, the connecting line was filled with refrigerant liquid by cooling the line with the secondary water line and in the case of two phase tests the connecting line was heated to have vapour in the line.

4.3.3 Temperature Measurement Sensors

Wall temperatures were measured with T-type thermocouples using a method employed by Palm (1991). The idea with this method is to have the same reference temperature for all the thermocouples in order to eliminate the offset in temperature difference measurements. A Pt100 was used as a reference temperature sensor in this method. The thermocouples for the test section wall temperature measurements were ob-

tained from the same lot and were calibrated in an ice-water homogenous mixture. All the thermocouples were found to be fluctuating within ±0.1 °C for a time of 6 to 8 hours. The systematic error associated with data logger was due to two components. First component was due to the voltage resolution of the data logger which according to the manufacturer (Agilent Technologies) was 0.004 mV for a range of 100 mV signal which translates to 0.024 ºC. Second error was due to conversion from voltage to temperature which was less than 0.001 ºC. Therefore, the overall uncertainty in the temperature measurements was estimated to be within ±0.1 °C (i.e. error due to calibration).

Apart from the wall temperature measurements, stainless steel sheathed thermocouples were used to measure the fluid temperatures at the inlet and outlet of the tests sections and at different locations in the flow loop as shown in Figure 4.1. These thermocouples were also calibrated in an ice bath before using them in the measurements. These thermocouples during the calibration fluctuated within ±0.05 ºC and considering the other contributions in systematic error due to data logger as stated before, the overall systematic uncertainty for these thermocouples was estimated to be ±0.06 ºC. More details concerning the temperature measurements can also be found in Owhaib (2007) and Martin-Callizo (2010).

4.3.4 Power measurements

The steel tubes were electrically heated using high current switching mode power supply, Manson SPS-9600, with remote sensing and control,. The power supply was controlled remotely using a remote control data cable connected to an Agilent data logger. The accuracy of the power supply was, as stated by the manufacturer to be ±(1%+1) of the reading. To improve the accuracy in power measurements, the voltage was measured separately with a *FLUKE 45 Dual display multimeter* measuring instrument having uncertainty of ±(0.025%+2) of reading.

The horizontal glass test section was provided with a low current high voltage power supply *TTi EX752M* and the power measurements were carried out using an accurate *YOKOGAWA WT130* power measurement instrument. The accuracy of the power measuring instrument was (0.15% of reading+0.1% of range).

4.3.5 Flow rate measurements

Two highly accurate coriolis effect flow meters were installed in the flow loop to measure the low flow rates associated with the micro channel flow. One of the two flow meters was used depending on the diameter of the test section. Flow rates of about 0.3 g/s and higher were measured

using a Micro-motion DS006 flow meter and for flow rates smaller than 0.3 g/s, a *Bronkhorst Cori-Tech BV,* was used. The accuracy of *micro-motion DS006* flow meter was ±2.29% of flow rate at 1% of nominal flow and less than ±0.58% of flow rate for a nominal flow of 5% and accuracy improved as the flow rate increased as shown in Figure 4.8; therefore, the Micro-motion flow meter was never used for flow rates below 4% of nominal flow (i.e. 0.3 g/s). The accuracy of Cori-Flow meter was ±0.5% of reading and was used during the experiments for the flow rates below 0.28 g/s. The systematic uncertainty in the measurements range of the current experiments was from ±1 to 1.25% for both the flow meters and including the error associated with the data logger.

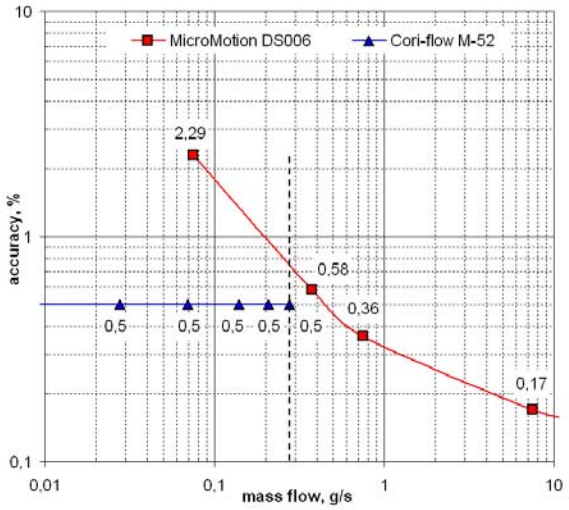

Figure 4.8 Accuracy in % of Corioli-flow meters with flow rate

4.3.6 High speed camera

A high-speed CMOS digital camera (Redlake HG50LE) with a maximum frame rate of 100000 together with tungsten lights was used for the visualization of flow boiling along the test section. Close up lens was used with the camera to get the required magnification and obtain good spatial and temporal resolution for studying the bubble dynamics. Flow patterns were recorded at 1000 to 5000 fps at different positions along the test section. Images were taken at the thermocouple positions or just at the middle of any of the two thermocouple positions. Appropriate lighting intensity and conditions were first set to obtain good quality images.

4.3.7 Data acquisition

All the signals from the related instrumentation were acquired using an Agilent data logger (34970A) with multiplexers (34901A). The data logger supplied the converted analogue signal in a digital mode to a personal computer. The computer was connected with the data acquisition system using HP-VEE interface software. HP-VEE program was also used to acquire the real time data such as system pressure, temperatures, flow rates etc. The system was run for a long enough time to ensure the steady state before recording any data. In routine measurements, the data was recorded with a frequency of 0.3 Hz for about 5 minutes and more than 100 data points were recorded for each parameter. The average value and standard deviation of these recorded parameters were then used for calculating the derived parameters and corresponding uncertainties. In case of dryout tests, a continuous data recording was made to see the behavior of wall temperatures along the test section and other parameters such as system pressure, flow rates. All the fluid properties were calculated using REFPROP 7, developed by National Institute of Standards (NIST).

4.4 Data reduction procedures

The data reduction methods for both single and two-phase are described in this section. The experimental single phase friction factor was calculated from the pressure drop measured during the experiments using Darcy-Weisbach equation as

$$f = \Delta P \times \frac{2\rho}{G^2}\frac{D_i}{L} \qquad (7)$$

The Darcy friction factor obtained from the above equation was compared with the friction factor calculated with the Hagen-Poiseuille equation for laminar flow and the Blasius (1913) equation for turbulent flow.

$$f = \frac{64}{Re} \qquad (8)$$

$$f = 0.3164 \times Re^{-0.25} \qquad (9)$$

The test sections were heated electrically using DC power supply. The power in watt applied to the test section was calculated using the voltage and current across the test section.

$$q = I \times V \qquad (10)$$

The heat flux added to the test section was then determined as

$$q" = \frac{q}{A} \qquad (11)$$

Where *q"* is the heat flux, *q* is the power and A is the heat transfer area defined as, $A = \pi D_i L_{hs}$

The single phase heat transfer coefficient was expressed in terms of dimensionless Nusselt number defined as

$$Nu = \frac{\alpha D_i}{k_l} \qquad (12)$$

The heat transfer coefficient α was calculated using the heat flux added to the section as

$$\alpha = \frac{q"}{T_w - T_f} \qquad (13)$$

Where α is the heat transfer coefficient, T_w is the inner wall temperature and T_f is the fluid temperature. The inner wall temperatures for steel tubes were calculated using steady state one dimensional heat conduction equation for cylinders with heat generation as given by the following equation

$$T_w = T_o + \frac{q}{4\pi kL}\left[\frac{\varphi(1-\varphi)-1}{\varphi - 1}\right] \qquad (14)$$

$$\varphi = \left(\frac{D_o}{D_i}\right)^2 \qquad (15)$$

The inner wall temperature for the glass tube was calculated using one dimensional heat conduction equation for cylinders.

The fluid temperature used for calculations in case of boiling was the local saturation temperature of the fluid where drop in saturation temperature due to pressure drop (assuming linear variation of pressure drop along the test section) was taken into account while in case of single phase it was calculated from the heat added to the fluid as

$$T_f = T_{in} + \frac{q"\pi z D_i}{\dot{m} C_p} \qquad (16)$$

The thermodynamic vapor quality in two phase flow was calculated using the following equation:

$$x_{th}(z) = \frac{q"\pi D_i(z - z_{sat})}{A_c G h_{fg}} \qquad (17)$$

z_{sat} is the axial position along the channel where saturated conditions are reached and was calculated as

$$z_{sat} = \frac{\dot{m} C_p (T_{sat} - T_{in)}}{q"\pi D_i} \qquad (18)$$

The thermo-physical properties were evaluated at the mean temperature between inlet and outlet for single phase tests and for boiling tests the properties were evaluated at the saturation temperature.

4.5 Experimental set up Validation

As part of the experimental system and instrumentation validation, single phase heat transfer and pressure drop experiments were performed prior to the boiling tests. The single phase results for steel tubes can be seen in Owhaib and Palm (2004b; Owhaib and Palm (2004c) and will not be repeated here. A general conclusion from those tests was that the single phase classical correlations were able to predict the friction factor and Nusselt number for steel tubes reasonably well. It is emphasized that the heat losses to ambient were less than 2% and were therefore neglected in the calculations.

4.5.1 Single phase pressure drop results for quartz test section

For the quartz test section the single phase friction factors and Nusselt numbers are reported in this thesis. As can be seen in Figure 4.9, Figure 4.10 and Figure 4.11, the single phase friction factor for R134a and for R245fa is in reasonably good agreement with Hagen-Poiseuille (f=64/Re) equation in the laminar regime and with Blasius (1913) equation in the turbulent regime. The experiments for pressure drop measurements were repeated several times for both diabatic and adiabatic conditions and an excellent repeatability was observed in the results as viewed in Figure 4.9 for adiabatic tests with R245fa and in Figure 4.10 for diabatic tests with R245fa.

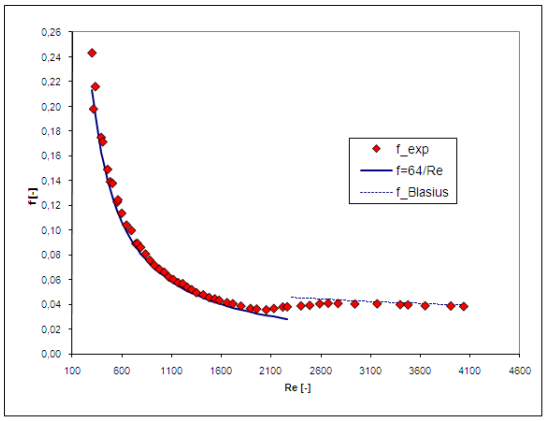

Figure 4.9 Single phase friction factor for R245fa, for adiabatic condition

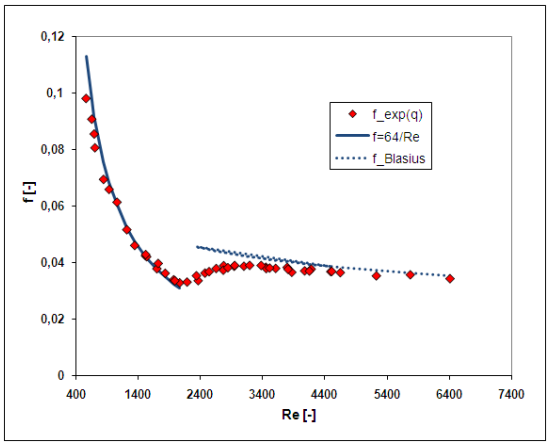

Figure 4.10 Single phase friction factor for R245fa, under heated conditions

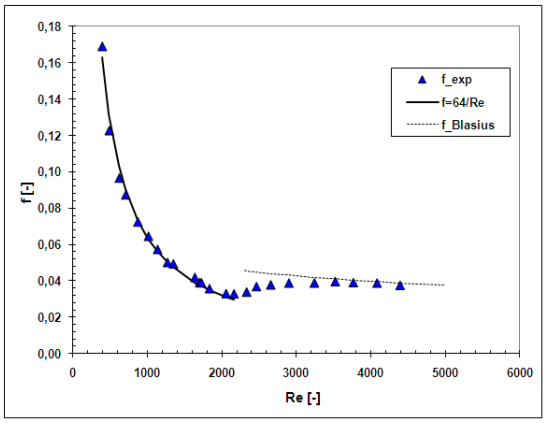

Figure 4.11 Single phase friction factor for R134a

4.5.2 Heat losses for glass test section

The test section was enclosed in another glass tube having outer diameter of about 40 mm and a low pressure was provided in the annulus in an effort to reduce the heat losses. However, it was found that this system was not effective enough to allow neglecting the heat losses. Therefore, the convective heat losses to the ambient were estimated by correlating the applied power with temperature difference between the tube wall and the ambient without refrigerant flow. The power was applied in small steps and the temperature was noted when the wall temperatures became stable. The ambient temperature was controlled in the room and was the same in all the cases. The heat losses so correlated were also compared with predictions from different correlations for natural convection taken from literature.

Natural convection losses were estimated using single cylinder correlations Churchill and Chu (1975); Kast and Klan (19929); Incropera and Dewitt (2006) and also correlations for cylindrical annuli Itoh et al. (1970) and for constant heat flux and constant wall temperature conditions. Heat losses due to radiation heat exchange were also estimated and results obtained for combined convection and radiation heat exchange are in close agreement with our experimental heat losses obtained by correlating the wall temperature and applied power. Convective heat losses obtained with single cylinder correlations are 30 to 40% lower than the experimentally obtained heat losses and if heat losses due to radiation are added then the results are very close to the experimental heat losses. Convective heat losses obtained with natural convection correlations for horizontal cylindrical annuli are in good agreement with the ex-

perimental heat losses and if heat losses due to radiation are added then depending upon the temperature difference, the total heat losses are 10 to 20% higher than the experimentally determined heat losses.

Moreover, for lower power levels encountered during flow boiling, the experimentally estimated heat losses are at most 10% of the actual power levels and for higher power levels the heat losses are less than 10%. Therefore, 10 to 20% difference in heat losses will give 1 to 2% difference in the actual power used for flow boiling experiments.
In order to estimate the influence of any axial conduction heat losses, the conduction number as defined by Chiou (1980); Maranzana et al. (2004) was calculated. This number gives the relative importance of wall conduction and convection in the fluid. Maranzana et al. (2004) used a numerical model to develop the criteria that if the conduction number M is less than 10^{-2} then the conduction losses may be neglected. The criterion for relative importance of conduction in wall and convection in fluid in terms of the conduction number M for a circular tube is given by the following equation

$$M = \left(\frac{k_t}{k_f}\right)\left(\frac{D_o^2 - D_i^2}{D_i L}\right)\left(\frac{1}{RePr}\right) > 10^{-2} \qquad (19)$$

The same above equation was also proposed by Chiou (1980). The experimental conduction number based on the above equation for different Reynolds numbers was calculated for all the single phase data points and it was found that M ranged from 0.000202 to 0.001226 which is very small as compared to the above criterion. Therefore, the axial conduction losses were assumed to be negligible.

Single phase heat transfer measurement provides a reasonable estimate of the heat losses and thereby a way to evaluate the estimated losses. We can determine the heat transferred to the fluid by the flow rate of the fluid, specific heat and the temperature difference between the inlet and the outlet as given by the following equation

$$q_f(W) = \dot{m} C_p (T_{out} - T_{in}) \qquad (20)$$

where q_f is the heat transferred to the fluid. This value can be compared to the *effectively* applied electrical power, calculated by deducting the heat losses to the ambient from the applied electrical power, by defining a ratio of heat transferred to the fluid to the effective applied electrical power as

$$\eta = \frac{q_f}{q_{eff}} \qquad (21)$$

The resulting values of the ratio η for single phase tests of R134a are plotted in the Figure 4.12 against the effective electrical power applied.

.

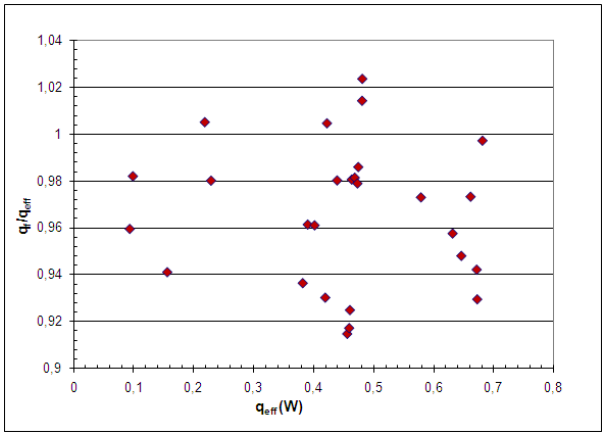

Figure 4.12 Electrical power plotted against the ratio η_{th} during single phase tests for R134a

4.5.3 Single phase heat transfer results for quartz test section

The experimentally determined single phase heat transfer coefficients, expressed in the form of dimensionless Nusselt numbers, were compared with the Gneilinski (1976) correlation and the Dittus-Boelter (1930) correlation for turbulent flow conditions. The uncertainty in single phase heat transfer coefficient with a 95% confidence level was from 10 to 30% depending up on the temperature difference i.e. the uncertainty was higher for a smaller temperature difference. For laminar flow, the heat transfer coefficient expressed in dimensionless form was compared to the constant value of Nu=4.36 as determined by analytical solutions. Experimental results for single phase heat transfer of R245fa and R134a can be seen in Figure 4.13 and Figure 4.14 respectively. As seen in these figures, the agreement between experimental and predicted values is reasonable and within the uncertainty of the experimental values. Experiments for both the refrigerants were repeated with very good repeatability of results.

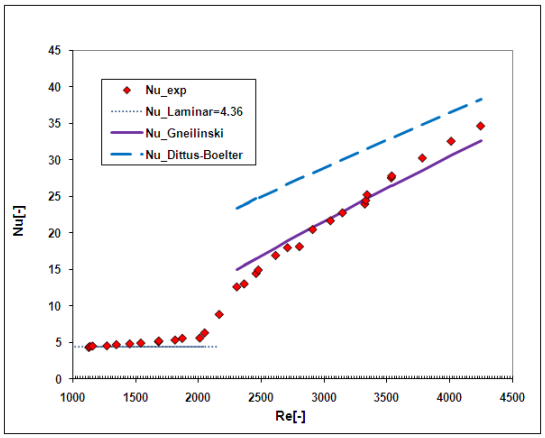

Figure 4.13 Single phase Nusselt number for R245fa, experimental values and predicted values using Gneilinski (1976) and Dittus-Boelter (1930) correlations for turbulent conditions and for Laminar Nu=4.36 for a circular tube

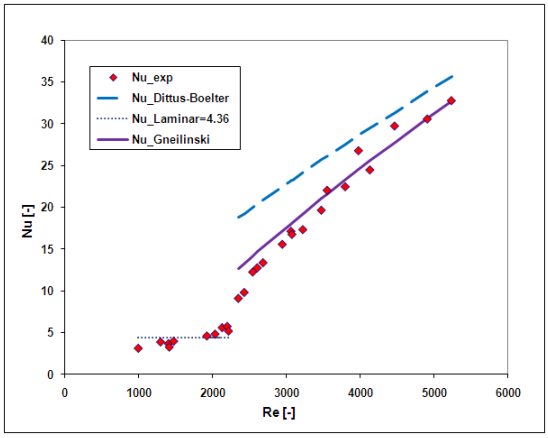

Figure 4.14 Single phase Nusselt number for R134a, experimental values and predicted values using Gneilinski (1976) and Dittus-Boelter (1930) correlations for turbulent conditions and for Laminar Nu=4.36 for a circular tube

Single phase heat transfer and pressure drop results together with the heat balance (Figure 4.12) of the micro evaporator thus confirm the accuracy of the measuring instruments and show that the single phase classical theory is applicable for the range of channel sizes tested.

4.6 Uncertainty Analysis

4.6.1 Introduction to uncertainty

There is no need to estimate uncertainty if one can find the true value of a measurement quantity. Unfortunately, the correct value of a measured or a derived quantity cannot be calculated although it exists. Best practice is to estimate the uncertainty of a quantity and define the quantitative limits of the uncertainty of a calculated quantity. Uncertainty of a measured or a derived quantity defines a band or range where the actual or correct value is most probable to lie. Experimental results without stating the corresponding uncertainties will of course not be meaningful as one will not know how far a measured and derived parameter is from the correct value. Therefore, the experimental results have to be expressed together with an uncertainty limit.

Uncertainty is defined as a combination of two components called uncertainty of type A $(s_{\bar{x}})$ and uncertainty of type B $(w_{\bar{x}})$. Type A (also called random or precision error) uncertainty is statistical in nature and can be estimated by the standard deviation of the mean value for a quantity which has been measured for a sufficiently large number of times (usually measured for more than 20 times). Type B (also called systematic or bias error) uncertainty is however, not statistical in nature and most of the times is constant and must be estimated Taylor and Kuyatt (1994) from the previous available measurement data, the documents and calibration certificates provided by the manufacturers and personal knowledge of the operator regarding the behavior of the instruments. The various sources of error of type B, just mentioned, are independent and can be combined using the root-sum-square (RSS) method to calculate the total uncertainty due to type B. According to BIPM/ISO standards, the combined or overall uncertainty u of a quantity due to the two types of uncertainties i.e. A and B is thus determined by root-sum-square (RSS) method given as

$$u_{\bar{x}} = \sqrt{(s_{\bar{x}})^2 + (w_{\bar{x}})^2} \qquad (22)$$

The uncertainty obtained with the above relation lies within 68% (1σ) confidence level for a normal distribution of variables. However, many times the uncertainty is indicated in a 20:1 odds meaning that a measured or a derived parameter lies within 95% (2σ) confidence level for a normal distribution of random variables.

4.6.2 Uncertainty of a measured or derived parameter

It is most of the times required to obtain or calculate a result y which can be a function of many independent variables such as heat flux which is a function of voltage, current and heating area. The uncertainty of the result y will therefore, be influenced by a change in independent or individual variables. Consider the final result y which is a function of many independent variables as defined below

$$y = f(x_1, x_2, \dots\dots\dots x_n) \qquad (23)$$

In the above equation, x_1 through x_n are independent variables. One of the methods to calculate the combined or overall uncertainty in the result y is the sequential perturbation method (SPM). In SPM, at a time one independent variable x_i is sequentially perturbed to estimate the influence on the results y and then all the independent variables are sequentially perturbed to estimate the uncertainty due to all the independent variables. The combined uncertainty in the result y is estimated using the root-sum-square (RSS) method. If the uncertainty in an independent variable x_i is u_i then the combined or overall uncertainty in the result y will be given by the following equation

$$u_y = \sqrt{\sum_{i=1}^{n}\left[\left(\frac{\partial f_i}{\partial x_i}\right)u_i\right]^2} \approx \sqrt{\left[\sum_{i=1}^{n}[f(x_i+u_i)-f(x_i)]^2\right]} \quad (24)$$

In the above equation x_i is the independent variable which is perturbed with respective uncertainty u_i composed of both type A and type B uncertainties.

4.6.3 Uncertainty analysis in the current thesis

In this thesis, the uncertainty analysis has been performed by the method recommended by Moffat (1988) and NIST Taylor and Kuyatt (1994). Type A uncertainty has been determined from the standard deviation of the mean of a measured quantity as obtained from the data acquisition system. As described in the section 4.3.7, the data was recorded to obtain more than 100 data points for each measured parameter and the average

and standard deviation were used in the calculation of derived parameters and the respective uncertainties. It is worth mentioning here that the type A uncertainty for system pressure and mass flow rate has been neglected as the standard deviation in the measurements was very small as compared to type B uncertainty. Uncertainty of type B was calculated by using the information provided by the manufacturers which has been described in section 4.1, section 4.2 and section 4.3. The uncertainty in a derived parameter was calculated by the method of propagation of error or SPM as recommended in NIST Taylor and Kuyatt (1994) and the overall uncertainty in a parameter was determined using the RSS method as described in section 4.6.1 and section 4.6.2. Further details of the method are also available in the NIST document Taylor and Kuyatt (1994) and in Owhaib (2007). A program in an Excel sheet was developed for uncertainty analysis in each data point as per recommendations in the citations just listed. For each data point, the uncertainty u_y in result y was calculated by perturbing the i_{th} independent variable x_i by its corresponding uncertainty u_i. This procedure was repeated for n independent variables i.e. i=1 to n for x_i. The overall uncertainty was the RSS of the terms $f(x_i+u_i)-f(x_i)$ as defined in the previous section 4.6.2. To elaborate more on the procedure, the uncertainty in the heat transfer coefficient was calculated by perturbing the heat flux, wall temperature and fluid temperature as given by the following equation:

$$w_h = \sqrt{\begin{aligned} &\left\{\frac{q" + w_{q"}}{T_w - T_f} - \frac{q"}{T_w - T_f}\right\}^2 \\ &+\left\{\frac{q"}{(T_w + w_{Tw}) - T_f} - \frac{q"}{T_w - T_f}\right\}^2 \\ &+\left\{\frac{q"}{T_w - (T_f + w_{Tf})} - \frac{q"}{T_w - T_f}\right\}^2 \end{aligned}} \qquad (25)$$

Uncertainties in all the other derived parameters were calculated using the similar equations and perturbing the individual variables. The maximum quantitative uncertainties calculated at a confidence level of 95% (i.e. 2σ) are given in Table1.

Table 4-1 Uncertainties in experimental parameters

Parameter	Uncertainty	
	R134a	R245fa
Steel Tube diameter	1.70±0.007 mm, 1.224±0.009 mm	
Glass tube diameter	0.781±0.008 mm	0.781±0.008 mm
Wall temperature	±0.1 ºC	±0.1 ºC
Absolute pressure	±10 mbar	±10 mbar
Differential pressure	±1 mbar	±1 mbar
Saturation temperature	±0.15 ºC	±0.2 ºC
Mass flow rate	±2.5%	±2.5%
Mass flux:		
Steel tubes	±3%	
Quartz tube	±3.25%	±3.25%
Single phase friction factor	17%	15%
Heat flux:		
Steel tubes	±4%	
Glass tube	±3%	±3%
Single phase heat transfer coefficient	25%	20%
Vapor quality:		
Steel tubes	±5%	
Glass tube	±5%	±5%
Boiling heat transfer coefficient:		
Steel tube	±14%	
Glass tube	±12%	±15%

5 Flow Boiling Visualization

The objective of the flow boiling visualization experiments was to study the flow patterns and associated two-phase flow characteristics. Different flow regimes show different behaviour which affects the heat transfer, pressure drop and dryout mechanism during two-phase flow in a channel.

5.1 Experimental flow visualization results (Paper #1)

Flow boiling visualization in a horizontal, circular quartz micro channel with an internal diameter of 0.781 mm was carried out. The outer surface of the tube was coated with a thin, electrically conductive layer of ITO, which made simultaneous heating and visualization possible. The results of bubbly and elongated bubble regime for R134a are presented in the following sections. A comparison is also made with a previous flow visualization study conducted on same experimental facility for R134a with a vertical quartz tube of diameter 1.33 mm.

5.1.1 Flow patterns identified during experiments

The following flow patterns were identified in the experiments that are explained below with some major visualization observations and are shown in Figure 5.1.

Isolated bubble: Bubble diameter is smaller than the tube diameter. Bubble growth is not hindered by the tube walls. In addition there is enough space for evaporation at the liquid vapour interface. This flow regime is characterized with distinct and almost spherical bubbles. The bubbly flow regime was observed to prevail for very short lengths. After the onset of boiling, as the heat flux was increased, the nucleation sites shifted to upstream and ultimately at higher heat fluxes for a given mass flux, the bubbly flow was restricted to a region close to the inlet of the test section. For all mass fluxes this flow regime was only observed for very short lengths and in some situations the confined bubble regime was ob-

served immediately after the departure of the bubbles (almost direct transition to confined bubble regime).

Confined bubble: The bubbles soon after the departure from nucleation sites grow to the diameter comparable to the tube diameter and further growth of bubble in radial direction is restricted by channel walls. The confined bubbles are characterized by the non-spherical bubbles due to small diameter of the tube.

Elongated bubble: Due to the restricted growth in radial direction because of the small diameter of the channel, the confined bubbles occupy almost the entire cross-section of the microchannel and start growing in axial direction. In the current study this type of flow pattern is termed as the elongated bubble. This flow pattern is characterized by a very thin liquid film which surrounds the elongated bubble and fills the gap between the vapour bubble and the channel walls. In the current study if the length of the bubble is from slightly larger than the diameter of the channel up to 5 times the diameter, it is termed as the elongated bubble.

Slug flow: As the length of elongated bubbles grows along the tube, the face of the trailing bubble meets the rear of the leading bubble to form large vapour plugs which are very large compared to the elongated bubbles. Liquid slugs are present between the two successive vapour plugs where in some cases smaller bubbles are also present in these liquid slugs. The tail of vapour plugs is wavy and in many cases touching the upper or lower part of the channel as the flow proceeds along the tube. In the current study, the bubbles longer than 5D are considered to be slug flow regime.

Wavy annular/semi annular flow: Slug-annular and churn-annular flow patterns are included in semi annular flow regime. If transition to annular flow occurs through the slug flow (which is mostly true for low and medium mass fluxes in present tests) then the two large plugs meet to form the wavy annular flow and the tail of the plugs which is wavy creates waves in the liquid film which flows along the channel walls. Waves in both top and bottom liquid layers are observed. Occasionally, the annular flow regime is interrupted by liquid plugs.

Wavy annular flow is also reached through churn flow (at high mass fluxes). At increased mass fluxes usually annular flow is disturbed periodically by chaotic waves of liquid originating somewhere upstream of the channel.

Annular flow: annular flow pattern is characterized with a continuous liquid ring surrounding the channel walls. The thickness of the liquid film decreases with increase in vapour fraction along the tube. The thickness of the liquid film also decreases with an increase in heat flux at a given position. The vapour flows in the channel core with very small liquid droplets entrained in the vapour core.

Annular mist flow: this is a transitional flow regime between annular and mist flow where the mist flow is disturbed with flushing liquid coming

from upstream. This liquid which flows at the channel walls is then evaporated and tube walls again become dry while some tiny liquid droplets flow in the centre of the channel.
Mist flow: characterized with tiny liquid drops flowing mainly dispersed in the channel core while tube walls are blanketed with vapour. Heat transfer is mainly due to vapour in contact with tube walls and due to the liquid droplets hitting the wall.

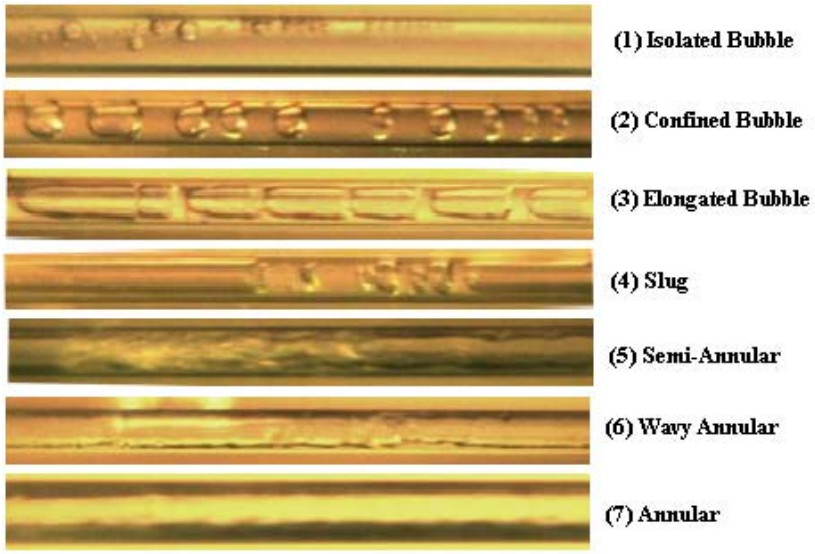

Figure 5.1 Flow patterns captured during the flow boiling of R134a

5.1.2 Bubbly flow regime

Evaluation of the nucleate boiling part of the flow boiling requires information regarding active nucleation sites, bubble size and bubble frequency. The number of active nucleation sites was counted from the videos obtained during the experiments and the results are shown in Figure 5.2 where the number of active nucleation sites is plotted against the heat flux. As the sub cooled liquid entered the test section, the heat was transferred to the fluid and boiling started for a given heat flux condition at a certain axial length from the inlet of the test tube. For a given mass flux condition, further increase in heat flux either increased the number of nucleation sites as can be seen in Figure 5.2 or promoted vigorous boiling. The previously active nucleation sites became inactive when the increment in heat flux shifted the boiling front towards upstream of the tube. The initiation of boiling was observed to require a

higher superheat as compared to a stainless steel tube due to the very smooth inner surface of the current fused silica tube as is also shown in Figure 4.7 which is the image obtained during surface characterization. Slightly higher heat flux was required for a higher mass flux to start the nucleation.

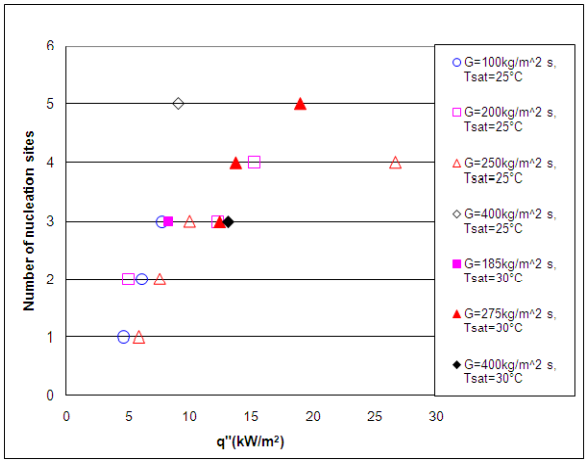

Figure 5.2 Number of active nucleation sites for R134a obtained at two different system pressures corresponding to T_{sat}=25 ˚C and T_{sat}=30 ˚C

The bubble growth after departure is shown in Figure 5.3 for different mass fluxes and at a saturation temperature of 25 ˚C. Due to insufficient image magnification and very quick growth of the vapor bubbles, it was not possible to calculate the bubble size just before the detachment. Therefore, the bubble diameter at time zero is not zero but it is the diameter of the bubble at the detachment. It may be observed from the Figure 5.3 that for a given mass flux the bubble diameter increases with heat flux. Except for G=400 kg/m² s it may be observed that for a higher mass flux the bubble diameter is smaller for a given heat flux condition. This decrease in bubble departure diameter with mass flux is in agreement with our previous flow visualization studies Owhaib et al. (2007) at the same test facility and a tube diameter of 1.33 mm and also with other studies in literature for example Chih-Jung et al. (2006) and the main reason for this trend is the increased drag force experienced by the departing bubbles with increase in mass flux.

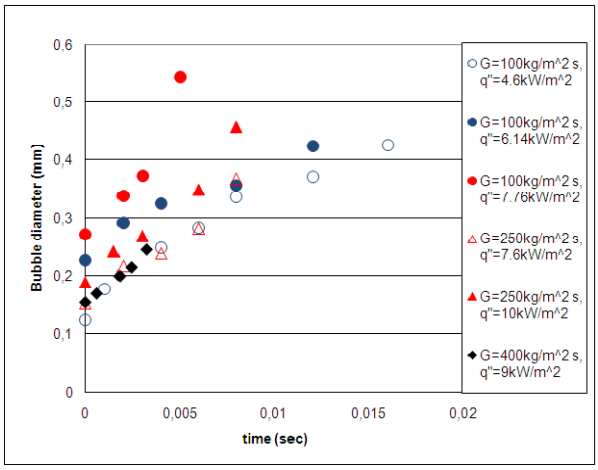

Figure 5.3 Bubble growth after departure for R134a, T_{sat}= 25 ˚C

Bubble frequency is shown in Figure 5.4 plotted versus heat flux for a saturation temperature of 25 ˚C and for several mass flux conditions. The bubble departure frequency was determined by counting the number of frames between bubble departures, and as the frame rate for the particular case was known, the frequency of the departing bubbles could be calculated. It was observed from the videos that for a given nucleation site, the frequency increased with heat flux. More than one value of bubble frequency is due to more than one active nucleation sites at a given heat and mass flux condition. It is noted that the frequency is different for different nucleation sites at a given heat and mass flux condition. A probable reason could be the different size and shape of the cavities present on the tube surface and also the amount of gas entrapped in the cavities. A comparison of the present study with our previous study Owhaib et al. (2007) carried out for a 1.33 mm inner diameter vertical test section shows that bubble frequency is higher for the smaller diameter channel (i.e. current test tube) for the same operating conditions which may mean that the transition from bubble to slug will occur earlier and also the slug to annular transition will be expected to occur earlier for a smaller diameter channel. This intuition is also supported when looking at the major differences in flow pattern transitions between the macro and micro scale channels reported in the literature where it is shown that the annular flow is encountered earlier in micro scale channels than macro scale channels.

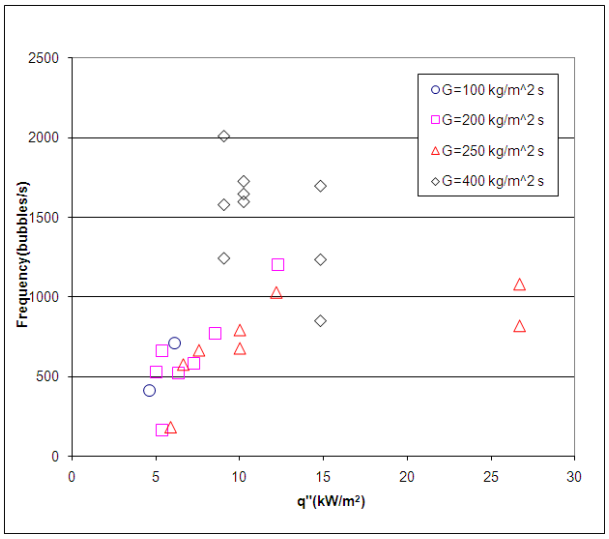

Figure 5.4 Bubble frequency for R134a, T_{sat}=25 ˚C

5.1.3 Elongated bubble flow regime

Elongated bubble flow is a unique flow regime existing in microchannels evolving due to the confinement of flow and is characterized by a thin liquid film trapped between the vapour and the channel wall. The existence of this flow pattern also shows the increased importance of surface tension forces as the channel diameter is decreased. The thin liquid film contributes to heat transfer; therefore, the modelling of flow boiling heat transfer in microchannels will require a good knowledge of under what conditions the elongated bubble flow pattern and associated patterns exist. Experimental values of mean elongated bubble length and velocity were calculated from the images captured during the experiments. The procedure of calculating the length and velocity and the corresponding uncertainty of the elongated bubble is explained in paper no 2 attached with this thesis. Experimental results of mean elongated bubble length and velocity obtained for R134a are shown in Figure 5.5 and Figure 5.6 respectively. As expected, the bubble velocity and bubble length increase with vapour quality which is in agreement with basic physics and with previous studies found in literature. The elongated bubble velocity at zero vapour quality in Figure 5.6 is that for single phase liquid calculated from mass flux and liquid density. Increase in elongated bubble velocity and length facilitate the transition to the annular flow regime because of the merger of the bubbles. It might be possible to propose transition cri-

teria for annular flow regime with quantitative information of bubble velocity and length.

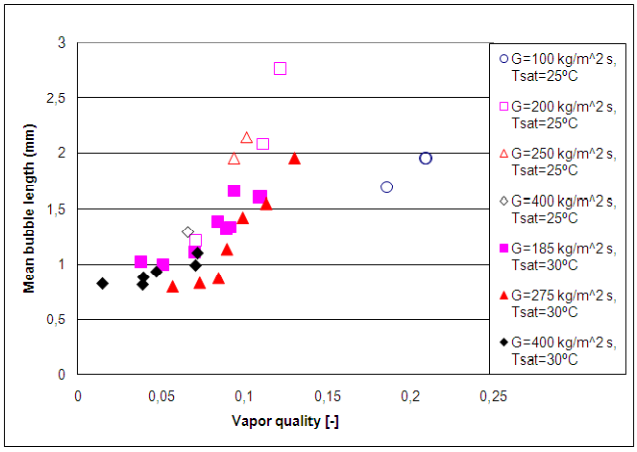

Figure 5.5 Mean length of elongated bubbles for R134a at two system pressures corresponding to T_{sat}=25 ˚C and T_{sat}=30 ˚C

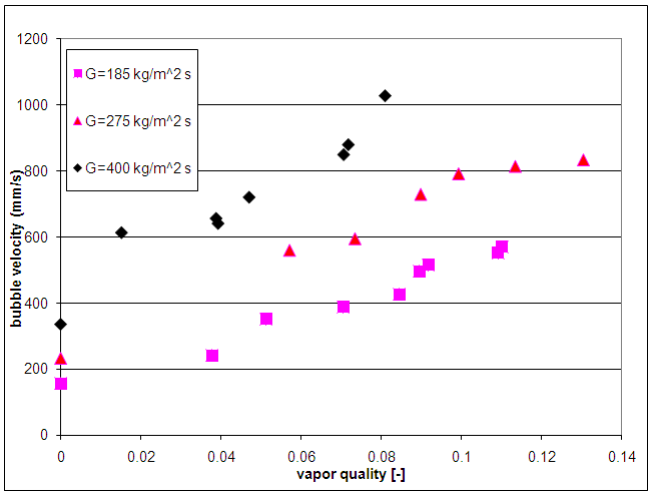

Figure 5.6 Mean elongated bubble velocity of R134a at T_{sat}=30 ˚C

6 Flow Pattern Maps

This chapter presents the experimental flow pattern maps obtained by plotting the data on mass flux versus vapour quality plots, Reynolds number versus vapour quality plots and superficial liquid versus superficial gas velocity plots. The experimental flow pattern transition lines have also been compared with other flow pattern maps present in the literature both for macro and micro scale channels. Paper # 2 attached with this thesis is regarding the flow pattern maps and comparisons with other flow maps and will be referred to in this chapter.

6.1 Experimental flow pattern maps (Paper #2)

The flow patterns defined in the previous chapter were combined into five main flow patterns and were plotted to show different flow regime zones on a graph. The isolated bubble and confined bubble flow patterns were combined to the bubbly flow regime. The elongated bubble and slug flow were combined and named the slug flow regime. The slug-annular, wavy-annular were combined as the semi-annular flow pattern. The flow pattern maps were obtained at two system pressures corresponding to saturation temperatures of 25 ºC and 30 ºC. Other operating conditions were: mass flux 100 to 400 kg/m^2 s, heat flux 5 to 45kW/m^2. The flow patterns were recorded at frame rates of 1000 to 5000 fps. All tests were made with R134a.

The flow pattern maps in terms of superficial gas and liquid velocities at a saturation temperature of 30 ºC and 25 ºC are shown in Figure 6.1 and Figure 6.2 respectively. The flow patterns change with increase in superficial gas velocity. As the nucleation starts, the vapour bubbles are travelling at the velocities close to superficial liquid velocities. With the increase in vapour fraction along the test section, the superficial gas velocity increases and the flow patterns change from slug to semi annular and then to annular. The mist flow was observed for the lowest mass flux at the saturation temperature of 25 ºC only.

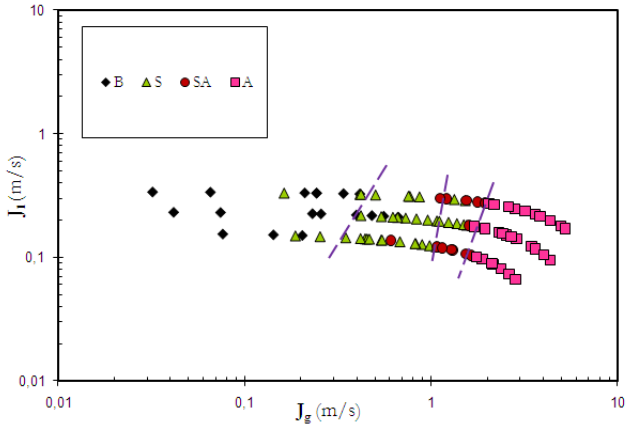

Figure 6.1 Experimental flow pattern map in terms of superficial liquid and gas velocities for D=0.781 mm at T_{sat}=30 ºC,, B=Bubbly, S=Slug, SA=Semi Annular, A=Annular

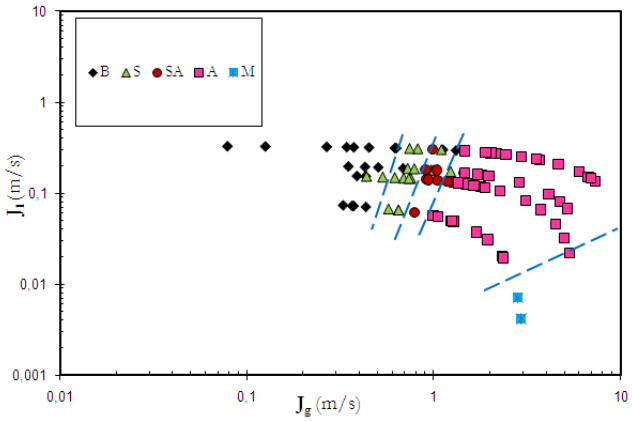

Figure 6.2 Experimental flow pattern map in terms of superficial liquid and gas velocities for D=0.781 mm at T_{sat}=25 ºC,, B=Bubbly, S=Slug, SA=Semi Annular, A=Annular and M=Mist

The flow pattern maps in terms of Reynolds number and vapour quality are shown in Figure 6.3 and Figure 6.4 for T_{sat}=30 °C and T_{sat}=25 °C respectively. The Annular flow is the dominant flow regime in the current tests as can be seen in these figures. The transition for annular flow shifts towards lower vapour qualities as the mass flux increases and this trend is in agreement in a previous study Martin-Callizo et al. (2010) in the same test facility which was conducted for a circular, vertical quartz tube of 1.33 mm inner diameter. It is observed from the figures that for

a given Reynolds number condition, two flow patterns coexist for a certain range of vapour quality.

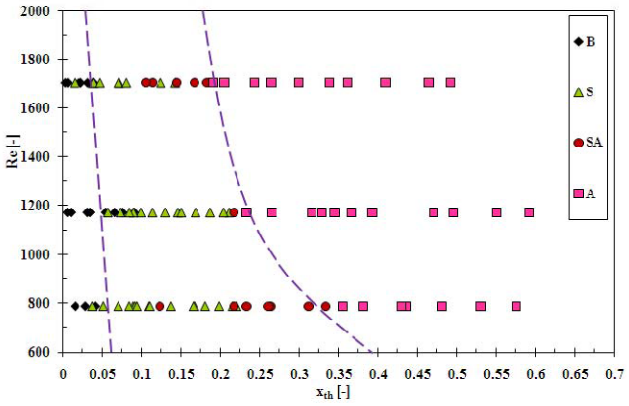

Figure 6.3 Experimental flow pattern map in terms of Reynolds number and vapour quality for D=0.781 mm at T_{sat}=30 ºC,, B=Bubbly, S=Slug, SA=Semi Annular, A=Annular

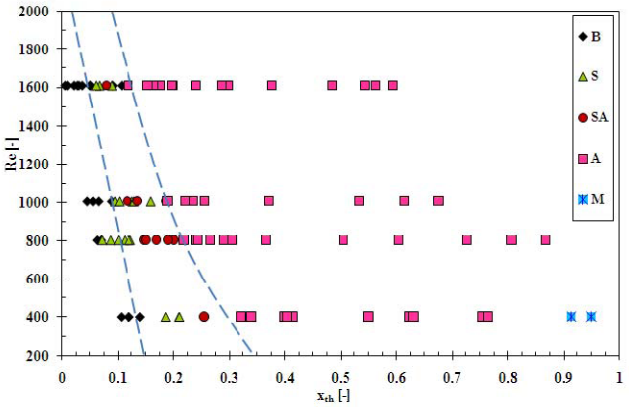

Figure 6.4 Experimental flow pattern map in terms of Reynolds number and vapour quality for D=0.781 mm at T_{sat}=25 ºC, B=Bubbly, S=Slug, SA=Semi Annular, A=Annular and M=Mist

6.1.1 The effect of saturation temperature on flow pattern transition lines

The effect of saturation temperature on flow pattern transition lines is shown in Figure 6.5. Transition line for bubbly to slug flow is shifted to lower superficial gas velocities while the annular flow transition line is shifted to higher superficial gas velocities for T_{sat}=30 ºC as compared to T_{sat}=25 ºC. The effect of saturation temperature on flow patterns transitions can also be seen by comparing the Figure 6.3 and the Figure 6.4 where the transition for annular flow shifts to higher vapour qualities for a higher saturation temperature. The difference in annular flow pattern transition line for the two saturation temperatures can be defined by the difference in liquid to gas density ratio. The lower the system pressure, the lower will be the vapour density (higher ϱ_l/ϱ_g) and consequently lead to higher vapour velocity which may result in a flow pattern change from slug to semi annular and ultimately to annular flow earlier (at lower vapour fractions) than at higher system pressure.

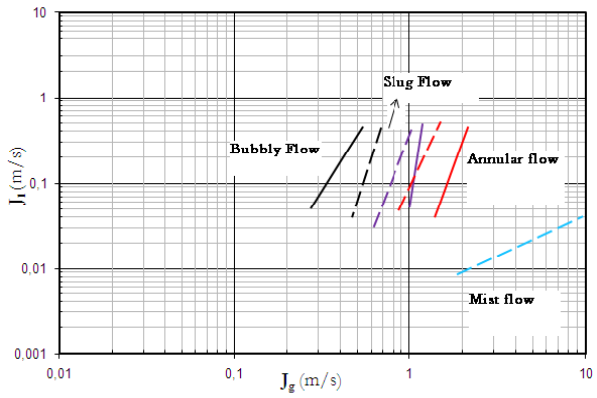

Figure 6.5 Effect of system pressure on experimental flow pattern transition lines for D=0.781 mm, solid lines for T_{sat}=30 ºC and dotted lines for T_{sat}=25 ºC

6.1.2 The effect of channel diameter on flow pattern transition lines

It is believed that as the channel diameter gets smaller, the effect of gravity diminishes and that of surface tension becomes enhanced. Therefore, it may be expected that the channel orientation will not influence so much on the evolving flow patterns in horizontal and vertical microchannels. The effect of channel diameter on flow pattern transition lines

has been assessed by comparing the present study for the horizontal tube of 0.781 mm inner diameter with a previous study using the same experimental set up by Martin-Callizo et al. (2010) for a vertical tube of 1.33 mm inner diameter. The transition lines of 1.33 mm diameter tube taken from the previous study using the same experimental set up by Martin-Callizo et al. (2010) are plotted together with the current experimental flow pattern map in Figure 6.6. The fact that the stratified flow was not observed in the current experiments for a horizontal tube supports the intuition that the effect of gravity is diminished. However, more experiments are necessary to test this assumption. The transition to slug flow occurs at slightly lower vapour fractions for the current study as compared to that of the 1.33 mm diameter tube. The confinement of vapour bubbles due to smaller channel dimensions in the case of current study is believed to be responsible for the earlier transition to confined bubble and consequently to slug flow. Slug to semi-annular transition for the current study is delayed to higher vapour fractions which might be due to increased effect of surface tension as the diameter becomes smaller. Semi-annular to annular transition however seems to be occurring at similar vapour fractions.

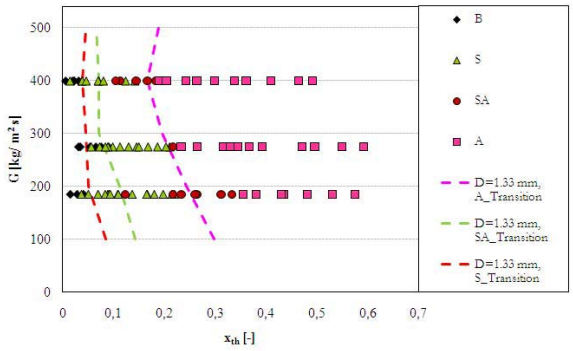

Figure 6.6 Flow pattern transition lines at T_{sat}=30 ºC from Martin-Callizo et al. (2010) plotted on the flow pattern map obtained from the current study at T_{sat}=30 °C

6.1.3 Comparison with some existing flow pattern maps

Comparison with flow pattern maps for conventional channels and for micro scale channels was done in order to assess the generality of flow patterns and flow pattern maps. There is no generally agreed, universal flow pattern map available neither for conventional channels nor for micro scale channels. The Figure 6.7 and Figure 6.8 show the comparison with the Baker (1954) flow pattern map and Figure 6.9 and Figure 6.10

show the comparison with the Mandhane et al. (1974) flow pattern map respectively, both developed for conventional sized channels. Baker's map seems to predict the transition line for slug to annular flow for T_{sat}=30 °C while slug flow to bubbly flow transition is poorly predicted. The data for T_{sat}=25 °C is also poorly predicted by Baker's map. The Mandhane et al. flow pattern map is in poor agreement with experimental data at both the saturation temperatures. The reason for this discrepancy might be the increased importance of surface tension which is not of importance for two-phase flow in conventional channels. Also the flow pattern maps developed for adiabatic conditions may not be expected to predict precisely the transition lines for a flow map obtained for non-adiabatic conditions.

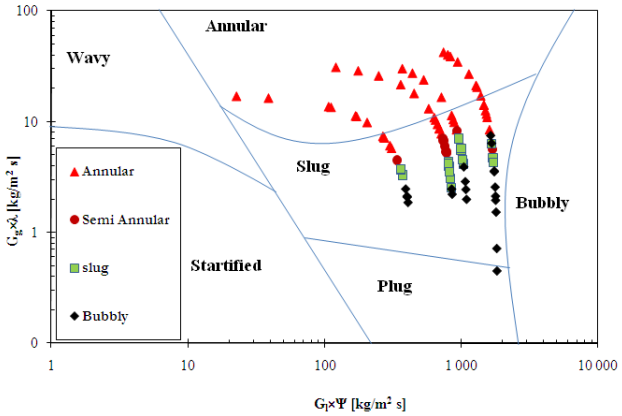

Figure 6.7 Comparison of experimental flow patterns at T_{sat}=25 °C with Baker (1954) flow regime map

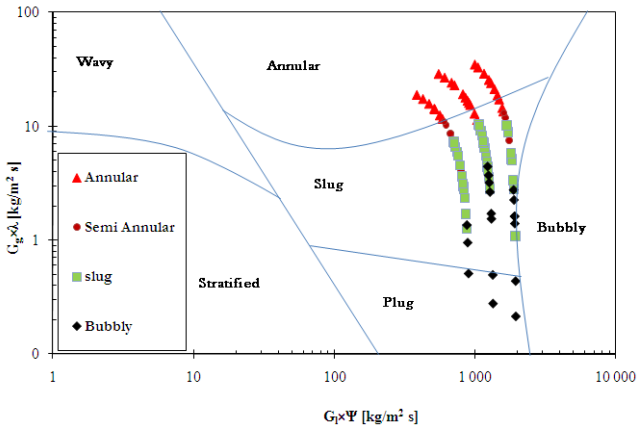

Figure 6.8 Comparison of experimental flow patterns at T_{sat}=30 °C with Baker (1954) flow regime map

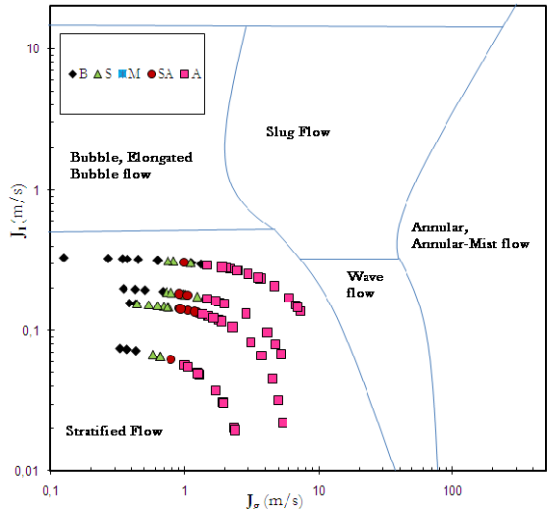

Figure 6.9 Comparison of current experimental data points at T_{sat}=25 ºC with the flow regime map of Mandhane et al. (1974)

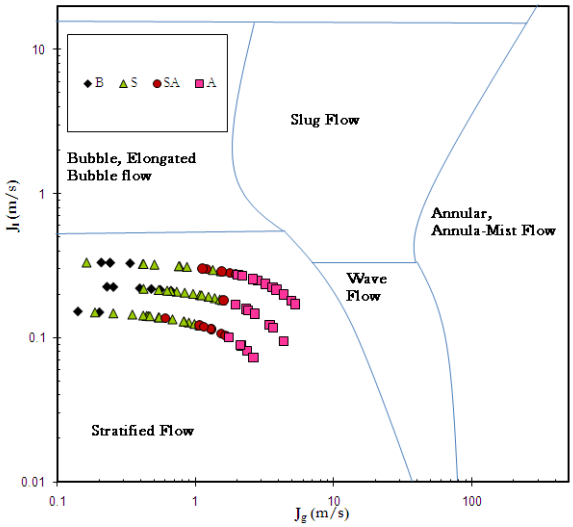

Figure 6.10 Comparison of current experimental data points at T_{sat}=30 ºC with the flow regime map of Mandhane et al. (1974)

The comparison with flow pattern maps developed for small diameter channels did not show a reasonable agreement either, except the correlation of Garimella et al. (2002) which was developed for predicting the intermittent (this flow pattern is characterized by the discontinuity in liquid and vapor phases and includes slug flow and plug flow) and non-

intermittent (this flow pattern includes annular flow) flow pattern transition lines in a condensing flow. Comparisons with the flow pattern maps for small channel diameters are shown in Figure 6.11 to Figure 6.16.

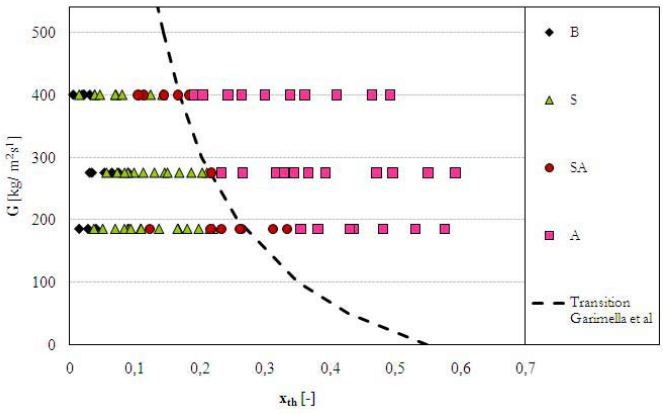

Figure 6.11 Comparison of experimental transition lines for intermittent and non-intermittent flow pattern with the transition line prediction correlation of Garimella et al. (2002), T_{sat}=30 ºC

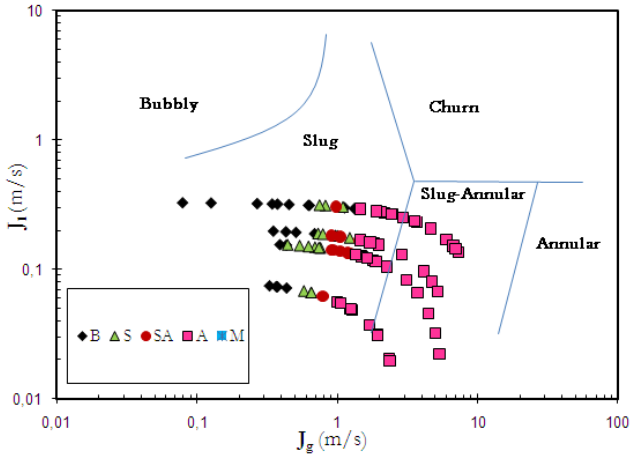

Figure 6.12 Comparison of current experimental data points at T_{sat}=25 ºC with the experimental transition lines of Triplett et al. (1999) for air-water two-phase flow in a circular test section of 1.097 mm

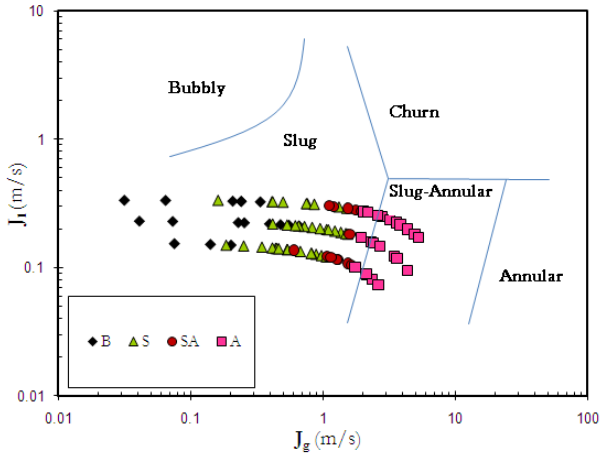

Figure 6.13 Comparison of current experimental data points at T_{sat}=30 ºC with the experimental transition lines of Triplett et al. (1999) for air-water two-phase flow in a circular test section of 1.097 mm

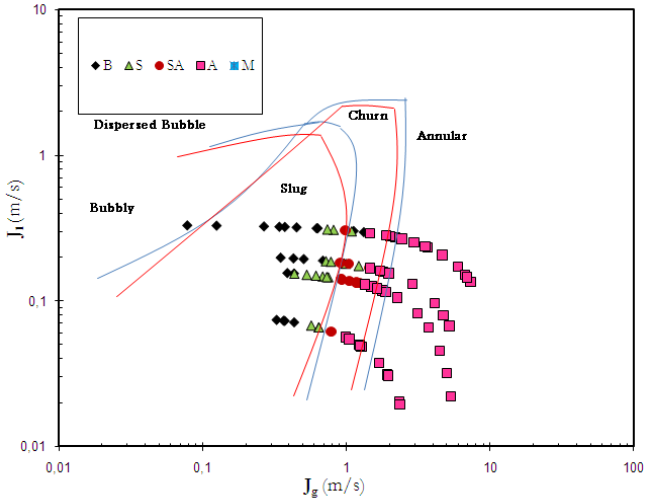

Figure 6.14 Comparison of current experimental data points at T_{sat}=25 ºC with the experimental transition lines of Chen et al. (2005) for R134a in a circular test section of 1.10 mm at system pressures of 6 bar (blue lines) and 10 bar (red lines)

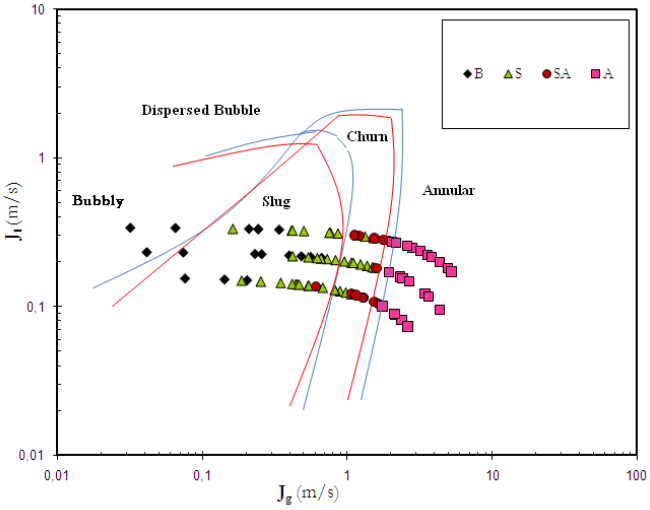

Figure 6.15 Comparison of current experimental data points at T_{sat}=30 ºC with the experimental transition lines of Chen et al. (2005) for R134a in a circular test section of 1.10 mm at system pressures of 6 bar (blue lines) and 10 bar (red lines)

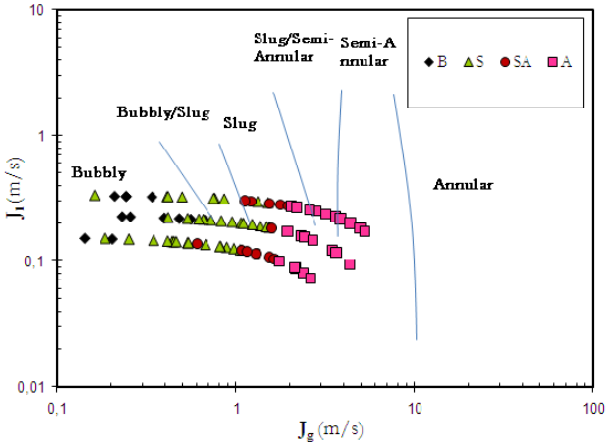

Figure 6.16 Comparison of current experimental data points at T_{sat}=30 ºC with the experimental transition lines of Revellin and Thome (2007) for R134a in a circular test section of 0.5 mm at T_{sat}=30 ºC and ΔT=3 ºC

Generally, none of the flow pattern maps is able to catch the trends in the current experimental points except with partial agreement with transition lines of some of the flow maps.

7 Flow Boiling Heat Transfer

7.1 Objectives of flow boiling heat transfer experiments

The micro channel two-phase flow and heat transfer is a developing field and relatively less data is available for flow boiling in small sized channels. Moreover, discrepancies exist within the available heat transfer data for micro channels. Design tools are required for manufacturing compact heat exchangers in many fields of industrial interest and predicting the heat transfer performance is fundamental for the design and optimization of such devices. The purpose of this study was to understand the flow boiling characteristics of micro channels. The experiments were carried out for a steel tube and a glass tube. Two refrigerants were used during the experiments one of which was a low pressure fluid R245fa and the other fluid was medium pressure R134a. Parametric effects on flow boiling heat transfer were ascertained. Discussion of the steel tube results was also supported by the visualization studies carried out on the same experimental set up for a micro channel glass test section in an attempt to get an insight into the underlying flow boiling phenomena. Macro scale and micro scale correlations were also tested to assess their applicability for design purposes.

7.2 Experimental results of flow boiling heat transfer in a steel tube (Paper # 3)

Flow boiling heat transfer was studied for a micro channel having an internal diameter of 1.70 mm. The experiments were performed using R134a as working fluid for two different system pressures. The experimental operating conditions can also be viewed in paper no 3 attached with the thesis. The following sections report on the experimental results.

7.2.1 Boiling curves

Boiling curves at two different system pressures corresponding to T_{sat}=27°C and T_{sat}=32°C are shown in Figure 7.1. Data points on these curves were taken at steady state conditions and the figure shows the plot of the heat flux versus temperature difference between the outer wall temperature, recorded at the last thermocouple position (down-stream of the channel) and the saturation temperature. As shown, the boiling curves for the different mass fluxes are almost identical up to a certain heat flux. Beyond this point the temperature difference increases considerably with only a minor change in heat flux. This indicates partial dryout of the heated surface. The heat flux at which the partial dryout occur increases with mass flux, as could be expected, as increased mass flux at a given heat flux corresponds to a decrease in vapour fraction. The boiling curves are similar to those obtained for pool boiling. However, the dryout appears at much lower heat fluxes than would be expected for critical heat flux in pool boiling.

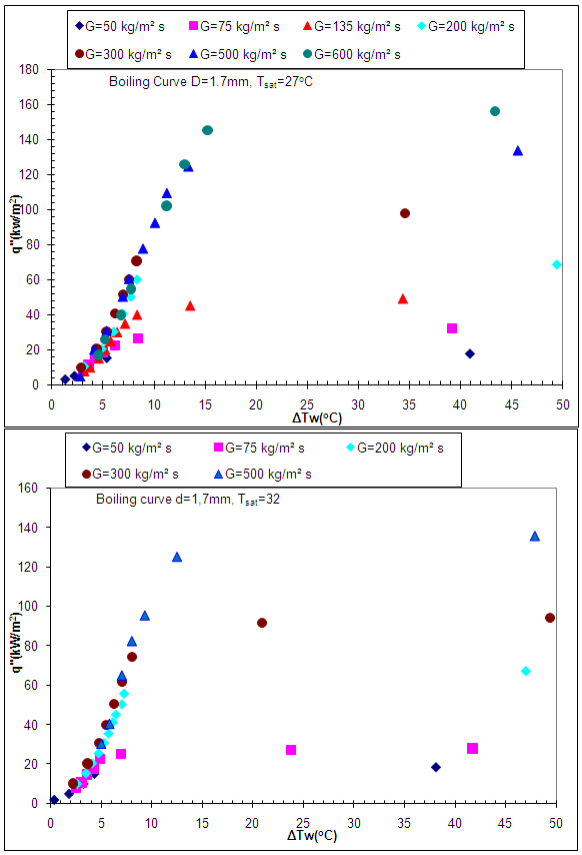

Figure 7.1 Boiling curves at T_{sat}=27 °C and T_{sat}=32 °C

7.2.2 The local heat transfer coefficient

The local heat transfer coefficients at different mass fluxes and saturation temperatures are shown in Figure 7.2, Figure 7.3 and Figure 7.4. These diagrams show the heat transfer coefficients at five different axial locations along the test tube. The following observations can be made from the results shown:

- Firstly, the heat transfer coefficient increases monotonically with heat flux in all the diagrams.
- Secondly, even the heat transfer coefficients at x≈0 are strongly dependent on the heat flux, indicating that sub cooled boiling is of importance in most of the cases. Similar trends were also observed by Lazarek and Black (1982; Lin et al. (2001; Bertsch et al. (2008).
- Thirdly, the heat transfer coefficient increases with vapour quality for low vapour qualities, levels out i.e. does not change, decreases slowly for a range of vapour qualities to finally decrease rapidly for vapour qualities above some specific value. The rapid decrease is not found in all tests as the vapour quality never reaches the critical value in the test section.

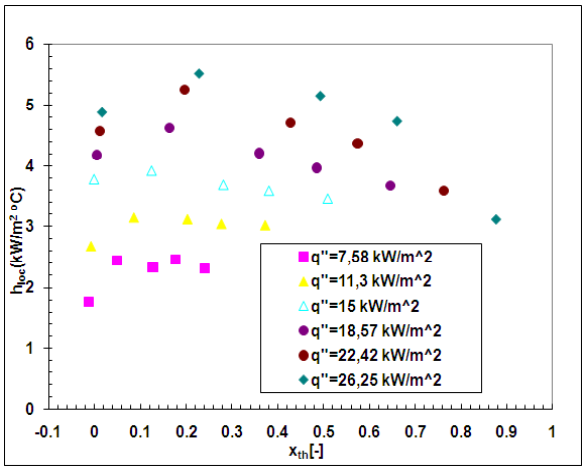

Figure 7.2 Local heat transfer coefficient at G=75 kg/m^2 s, T_{sat}=27 °C

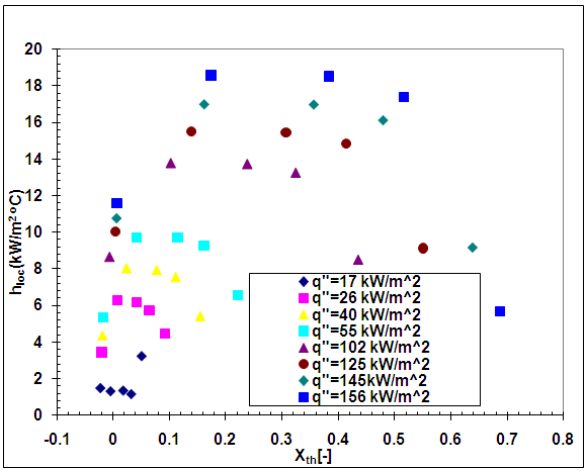

Figure 7.3 Local heat transfer coefficient at G=600 kg/m^2 s, T_{sat}=27 ºC

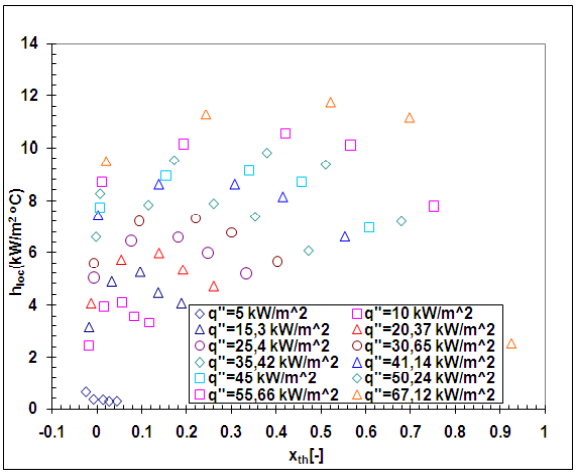

Figure 7.4 Local heat transfer coefficient at G=200 kg/m^2 s, T_{sat}=32 ºC

The effect of mass flux on the local heat transfer coefficient can be seen in Figure 7.5. It may be observed that for a given heat flux the heat transfer coefficient is not affected by the variation of mass flux up to a certain range of vapour quality. For the case of low heat and mass flux i.e. G=75 kg/m^2 s, q"=7.6 kW/m^2 and G=135 kg/m^2 s, q"=7.7 kW/m^2 the heat transfer coefficient is independent on mass flux and vapour quality. For medium heat and mass fluxes the heat transfer coefficient shows the same trend except that heat transfer coefficient starts decreasing above a certain vapour quality. Also at mass fluxes of 500 kg/m^2 s

and 600 kg/m² s and heat flux of 125 kW/m², the heat transfer coefficient is independent on mass flux and not changing with vapour quality up to a vapour quality of about 0.4 to 0.5.

The effect of system pressure on the local heat transfer coefficient is depicted in Figure 7.6. It can be seen that increasing system pressure slightly enhances the heat transfer coefficient. In general, the fact that the heat transfer coefficient is dependent on heat flux and sensitive to system pressure and is independent on mass flux and on vapour quality up to a certain range, shows a strong similarity with what would be expected for nucleate boiling. However, based on previous visualization tests using the same test facility by Owhaib et al. (2006); Martin-Callizo et al. (2010), it was observed that the nucleation of bubbles did not occur anywhere except at the very beginning of the test section. The similarity is rather a result of the close relation between the nucleate boiling and the thin film evaporation. This may, however, not explain the similarity in the part of the test section where annular flow is expected i.e. for x_{th} > 0.2-0.4. Similar trends in flow boiling heat transfer were also observed by Huo et al. (2004) and Martín-Callizo et al. (2007).

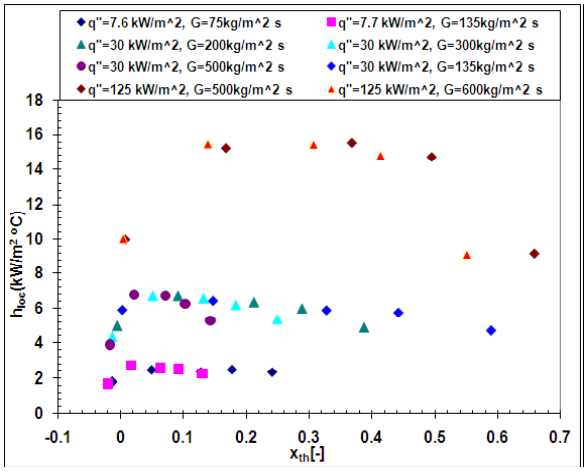

Figure 7.5 Effect of mass flux on the local heat transfer coefficient at T_{sat}=27 ˚C

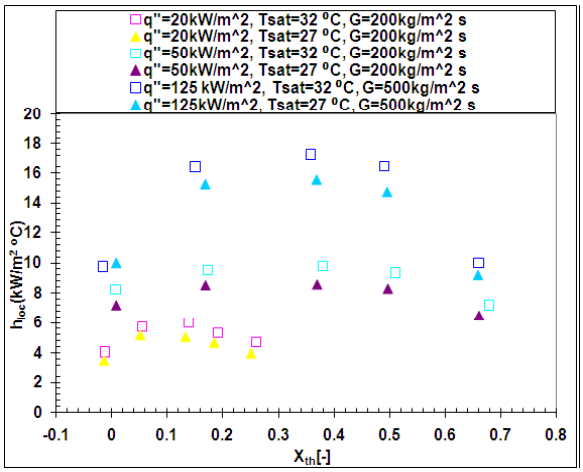

Figure 7.6 Effect of system pressure on local heat transfer coefficient

7.2.3 The average heat transfer coefficient

The average heat transfer coefficients are plotted versus mass flux in Figure 7.7. It is seen that the heat transfer coefficient is, within the accuracy of the measurements, independent of mass flux and is only a function of heat flux, as can be expected based on the trends for the local heat transfer coefficients described above. The independence of heat transfer coefficient on mass flux also suggests the low impact of convective heat transfer mechanism. Similar observations were made by Huo et al. (2004; Owhaib et al. (2004a).

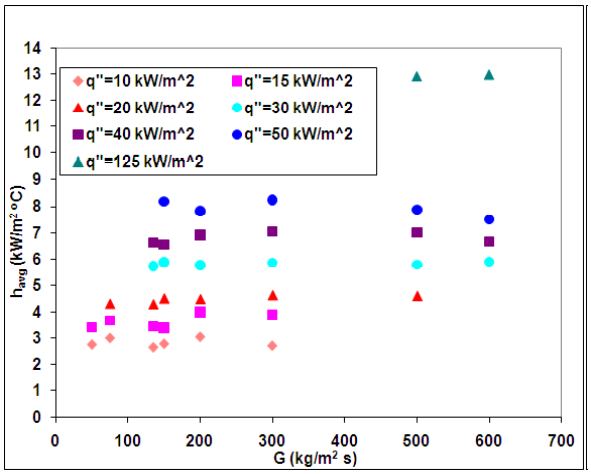

Figure 7.7 Average heat transfer coefficient at T_{sat}=27 ˚C

7.2.4 Heat transfer and wall temperature profile close to the dryout condition

A continuous outer wall temperature profile for a mass flux of G=300 kg/m^2 s and T_{sat}=32 ^{o}C is shown in Figure 7.8. The local heat transfer coefficients and the standard deviations in the wall temperatures for the same case are shown in Figure 7.9. It can be seen that fluctuations in wall temperature shown by last thermocouple start to appear at a heat flux of q"=74kW/m^2 which can be observed by the slight increase in the corresponding standard deviation of the wall temperature. It is conjectured that the fluctuations in wall temperatures appear due to appearance of dryout patches at the heater surface. Similar phenomena of wall temperature fluctuations and increase in standard deviation was also observed by Cavallini et al. (2007). They also performed similar experiments for condensation and did not observe the fluctuations in wall temperature and hence concluded that the observed fluctuations were due to some physical phenomena.

When the heat flux is increased after the incipience of dryout, the dryout portion of the surface may get intermittently dried out and rewetted again by the incoming waves, or expand giving rise to complete dryout condition. If the rewetting of dry spots does not occur, complete dryout is reached. However, this was not allowed to happen in these tests. As shown in Figure 7.8, the heat flux was increased slowly from 91kW/m^2, where the first sign of dryout was noted at the last thermocouple position, to 94kW/m^2 under a period of more than one hour. Similar plots can also be shown for all the other mass fluxes. As expected, the dryout conditions first started from the exit of the tube and propagated upstream as the heat flux was increased.

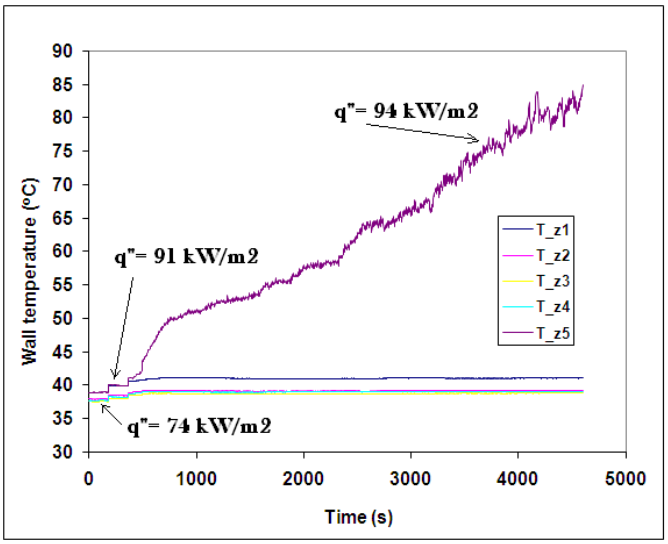

Figure 7.8 Continuous recording of outer wall temperatures at high heat fluxes, G=300 kg/m^2 s, T_{sat}=32 °C

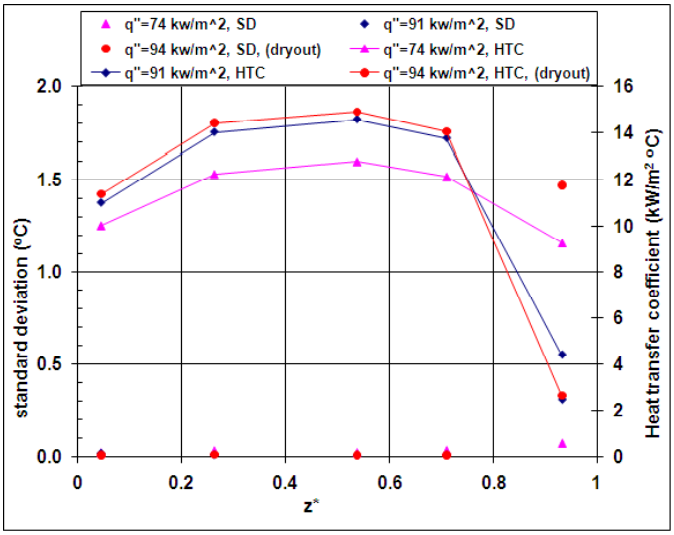

Figure 7.9 Standard deviation (SD) of wall temperatures and heat transfer coefficients (HTC) close to dryout conditions, G=300 kg/m^2 s, T_{sat}=32 °C

7.2.5 Comparison with correlations

The average and local heat transfer coefficients were compared with some well known correlations taken from the literature and a summary of the results is shown in Table 7-1. The comparison of average heat transfer coefficient with some correlations is also viewed in Figure 7.10. The correlations selected are either for pool boiling or for flow boiling based on nucleate boiling as dominant heat transfer mechanism. In general, the average heat transfer coefficient is predicted well by these correlations which will be expected based on the trends found in experimental results.

Table 7-1 Assessment of existing prediction methods for boiling heat transfer

Correlation	**MAD (%)**	**% of data within ± 30%**
Cooper (1984)	17	98
Gorenflo (1992)	12	91
Lazarek and Black (1982)	14	91
Tran et al. (1996)	8	96
Owhaib (2007)	15	90
Kew and Cornwell (1997)	15	89
Liu and Winterton (1991)	33	78
Gungor and Winterton (1986)	51	63 (within ± 50%)
Chaddock and Brunemann (1967)	34	46
Kandlikar and Balasubramanian (2004)	46	23
Zhang et al. (2004)	23	77

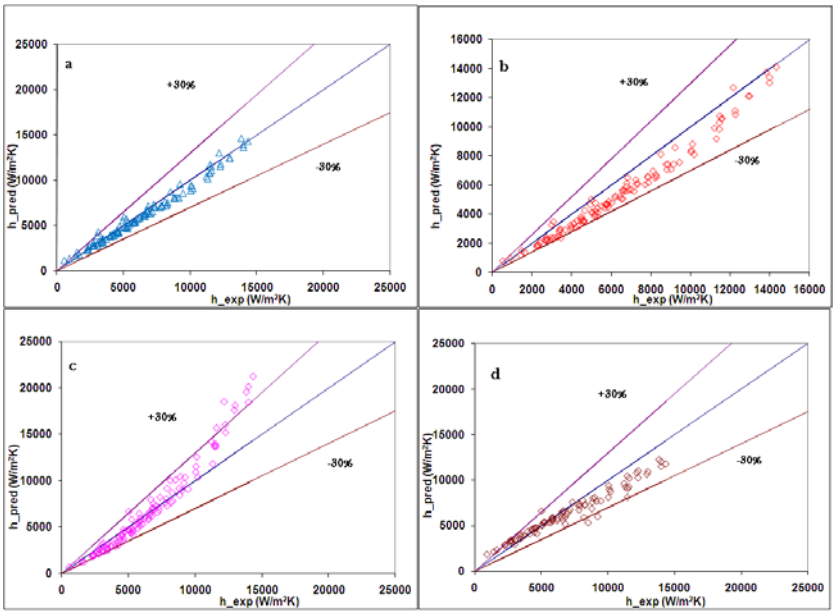

Figure 7.10 Comparison of average heat transfer coefficient with (a) Tran et al. (1996) correlation (b) Cooper (1984) correlation (c) Lazarek & Black correlation (1982) (d) Owhaib (2007) correlation

The local heat transfer coefficients were in better agreement with the Liu and Winterton (1991) correlation developed for conventional channels and Zhang et al. (2004) correlation developed for micro scale channels. However, the data close to dryout condition was not predicted well by these two correlations. The comparisons with two macro scale correlations can be viewed in Figure 7.11 and with two micro scale correlations in Figure 7.12.

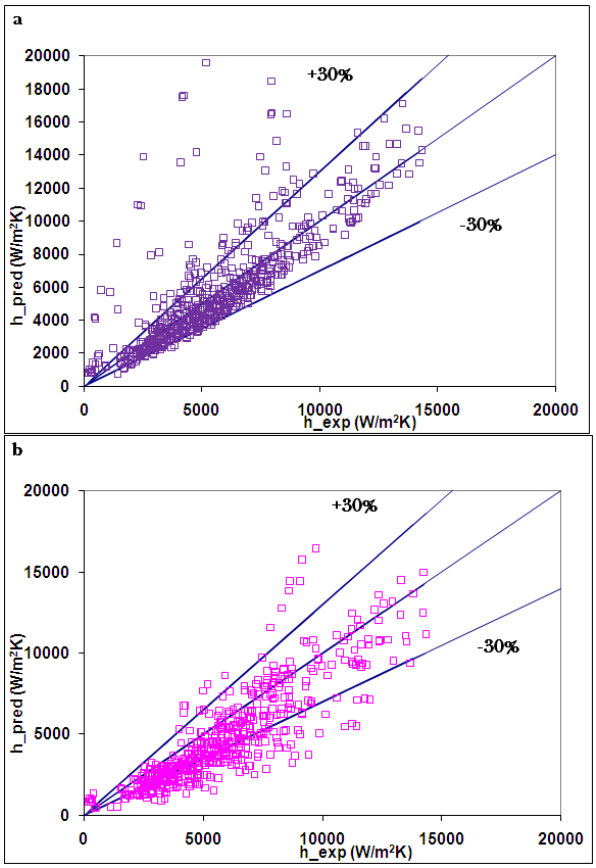

Figure 7.11 Comparison of local heat transfer coefficient with macro scale correlations (a) Liu & Winterton (1991) correlation (b) Chaddock & Brunemann (1967) correlation

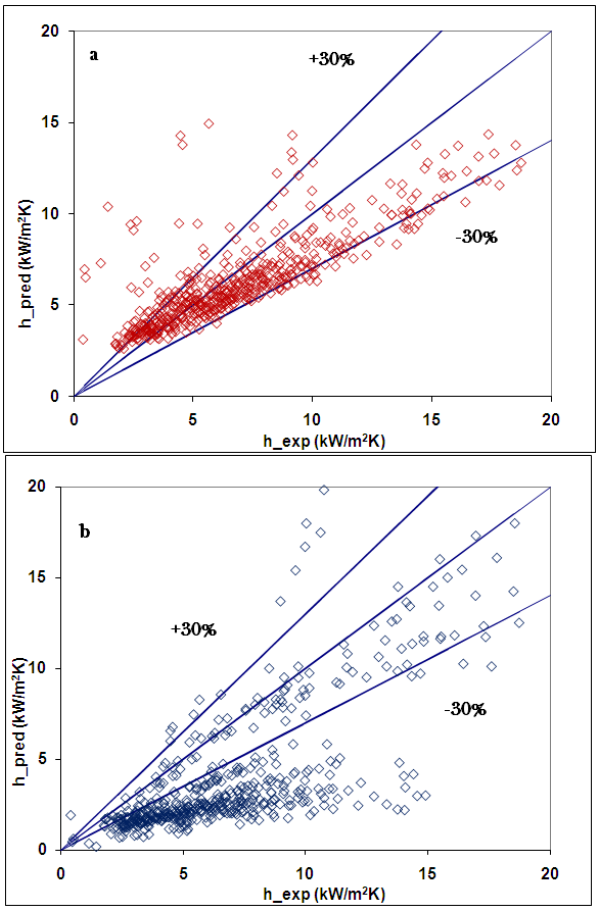

Figure 7.12 Comparison of local heat transfer coefficient with micro scale correlations (a) Zhang et al. (2004) correlation (b) Kandlikar & Balasubramanian (2004) correlation

7.2.6 Summary of results with steel tube

The heat transfer coefficient increases with heat flux and system pressure while mass flux and vapour quality have negligible effect up to dryout incipience. Beyond dryout incipience, the heat transfer coefficient decreases with vapour quality. The experimental flow boiling heat transfer data is compared to correlations developed for macro and microchannels and for pool boiling. Correlations developed for pool boiling show a good agreement with experimental data.

7.3 Heat Transfer in Glass Tube (Paper #4)

The experiments in the quartz test tube were carried out using R134a and R245fa as working fluids. The main objective with using two refrigerants was to study the effect of two refrigerants on the heat transfer coefficient and assess the capability of the existing correlations in predicting the experimental data with fluids having different thermo-physical properties. As can be seen in Table 7-2, the thermo-physical properties R134a and R245fa are quite different.

Table 7-2 Comparison of thermo-physical properties of R245fa and R134a at T_{sat}≈30 ˚C

Refrigerant	Pressure (bar)	Liquid density (kg/m³)	Vapour density (kg/m³)	Liquid viscosity (μPa-s)	Surface tension (mN/m)	Liquid specific heat (J/kgK)	Latent heat of vaporization (kJ/kg)	Liquid Prandtl number (-)	Liquid thermal conductivity (W/mK)
R134a	7.7	1187	37.60	183	7.40	1447	173	3.35	0.0789
R245fa	1.79	1325	10.16	380	13.4	1350	188	5.80	0.0883
% Difference with R134a	-78	11.6	-73	107.7	81	-6.7	8.7	73	11.9

7.3.1 Average heat transfer coefficient

Single phase results for pressure drop and average heat transfer coefficient have already been presented in section 4.5.1 and section 4.5.2 respectively where the classical single phase theory was shown to be applicable in the case of micro channels. The average flow boiling heat transfer coefficient results for the two refrigerants at T_{sat}=30 ºC are shown in Figure 7.13. Figure 7.13a shows the variation of the heat transfer coefficient as a function of exit vapor quality and the Figure 7.13b shows the variation of the heat transfer coefficient with mass flux for several heat

flux conditions. The heat transfer coefficient is observed to increase with exit vapor quality for a given mass flux and for a given exit vapor quality the higher mass flux gives a higher heat transfer coefficient. This trend with exit vapor quality is explained by the fact that for a given mass flux, a higher exit vapor quality means a higher heat flux and for a given exit vapor quality, the higher mass flux means a higher heat flux. In other words, it can be said that the heat transfer coefficient increases with heat flux which can also be seen in Figure 7.13b where for a given mass flux, the higher the heat flux, the higher is the heat transfer coefficient. The difference in heat transfer coefficient for the two refrigerants is however marginal which is surprising in view of the significant difference in thermo-physical properties of the two refrigerants.

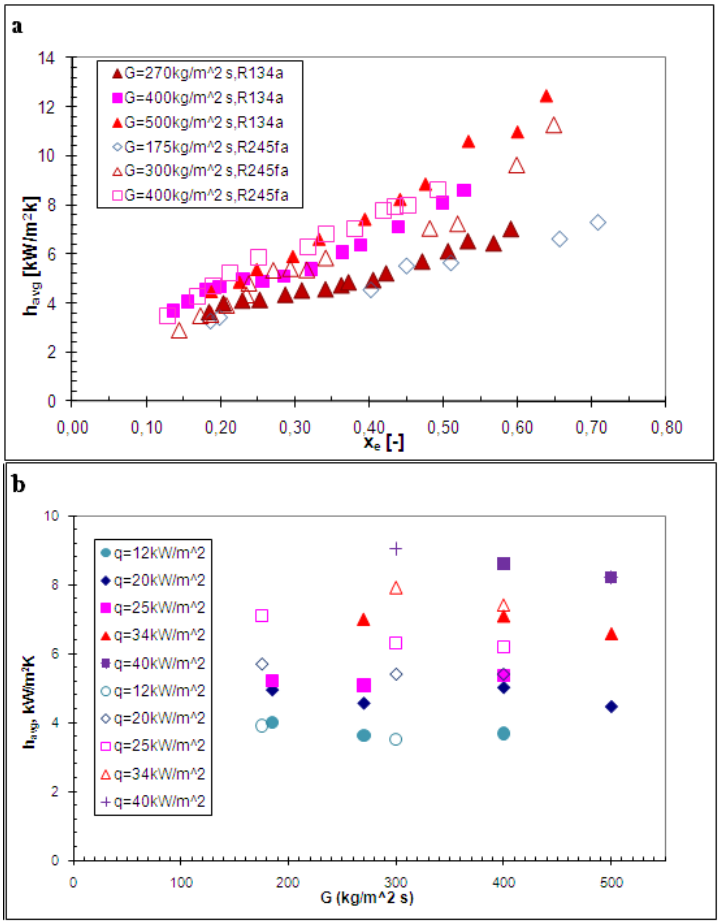

Figure 7.13 Average heat transfer coefficient for R134a and R245fa at T_{sat}=30 °C, vs. a) the outlet vapour fraction and b) the mass flux. Filled symbols are for R134a and empty symbols for R245fa

7.3.2 Comparison with correlations

The comparisons were made with the correlations suggested by Lazarek and Black (1982), Tran et al. (1996), Cooper (1984) pool boiling correlation and Owhaib (2007). The results of the comparisons with these correlations can be seen in Figure 7.14 for R134a and in Figure 7.15 for R245fa. The Lazarek and Black correlation and the Cooper pool boiling correlation give reasonable predictions in the case of R134a while in the case of R245fa all the correlations under predict the experimental data. The main reason for this discrepancy is attributed to the different thermo-physical properties of the two refrigerants.

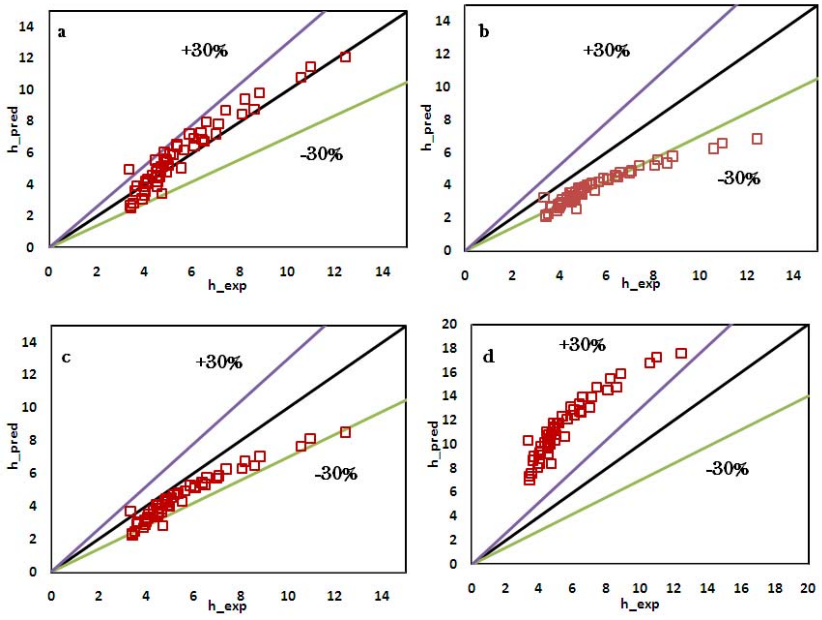

Figure 7.14 Comparison of R134a experimental data with correlations from (a) Lazarek and Black (1982) (b) Tran et al. (1996) (c) Cooper (1984) pool boiling correlation (d) Owhaib (2007) correlation

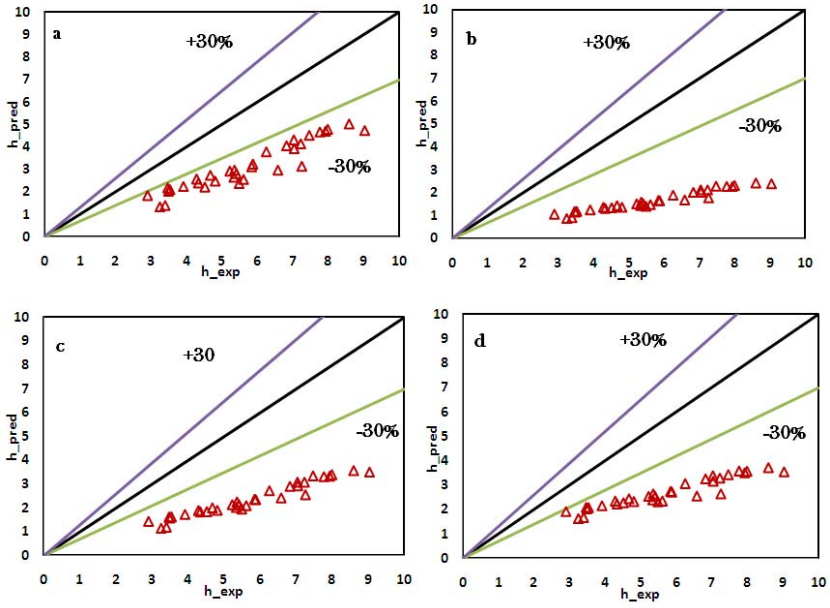

Figure 7.15 Comparison of R245fa experimental data with correlations from (a) Lazarek and Black (1982) (b) Tran et al. (1996) (c) Cooper (1984) pool boiling correlation (d) Owhaib (2007) correlation

8 Dryout During Flow Boiling

8.1 Objectives of the study

Dryout heat flux in a flow boiling system is an upper limit for a given set of operating conditions for safe and effective operation of the heat exchange system. Both incipience and complete dryout conditions become important to be known when a uniform temperature of a surface has to be maintained such as in cooling of electronics where the temperature of the electronic chip has to be maintained around 80 to 100 °C. It has been observed in many studies in the literature, as shown and discussed in section 2.4 and section 2.5, that partial dryout of the surface in microchannels occurs at comparatively low vapour qualities characterized by temperature fluctuations thereby deteriorating the heat transfer performance. Dryout incipience may therefore lead to hot spots and cause a premature failure of the device such as an electronic chip being cooled. Complete dryout on the other hand may cause a complete failure or burnout of the device.

The objectives of the dryout study were to elucidate the dryout characteristics during flow boiling of a fluid in a microchannel in order to enrich the data base with accurate data for developing design tools to predict the dryout condition in microchannels.

8.2 Experimental results of the dryout study (Paper #5)

The following sections describe the experimental findings on dryout characteristics of R134a during flow boiling in two microchannels with internal diameters of 1.70 mm and 1.22 mm.

8.2.1 Identification of dryout incipience and dryout completion condition

Dryout incipience (DI) and dryout completion (DC) were identified from boiling curves, recording of outer wall temperatures and standard deviation in corresponding wall temperatures. Boiling curves for tube diameters of 1.70 mm and 1.22 mm at T_{sat}=27 °C are shown in Figure 8.1. In this figure, the heat flux is plotted versus the temperature difference between the wall (last thermocouple position) and the saturation temperature, $\Delta T_w = T_w - T_{sat}$. Two different zones can easily be distinguished in these curves. The first zone is where the ΔT_w increases very little with an increase in heat flux while in the second zone the increment in ΔT_w is considerably larger for a small given heat flux increment. It may be observed from the boiling curves that the mass flux has a negligible effect on wall superheat in the first zone. Increment in wall superheat with increase in heat flux is small and almost all the points follow the same curve up to a certain point. The heat flux at the first shift from the boiling curve is termed dryout incipience heat flux and the corresponding vapour quality is termed as dryout incipience quality. Beyond the dryout incipience point, a small increase in heat flux gives a much larger increment in wall superheat as compared to the conditions before dryout incipience. Further increment in heat flux raises the wall temperature continuously even after waiting for long time (in most cases up to one hour during the experiments) and as the wall superheat is equal to or larger than 35 ºC (based on average wall temperature), the condition is considered to be the dryout completion and the power is cut-off.

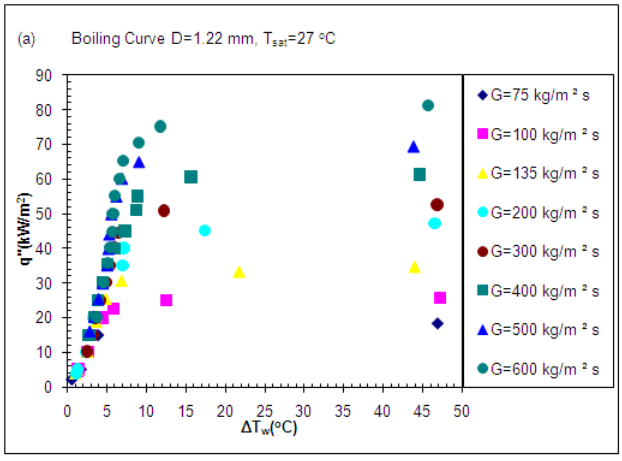

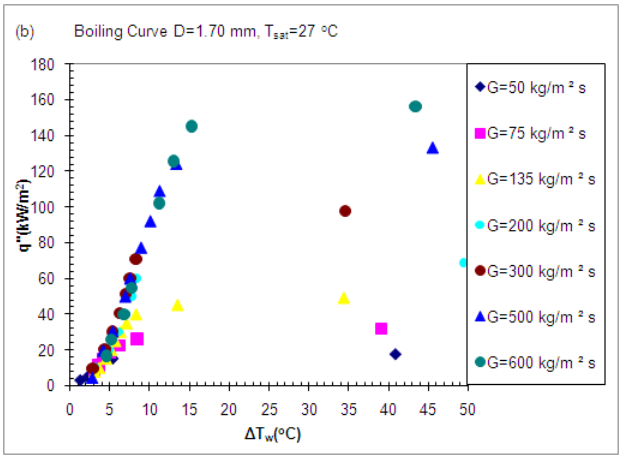

Figure 8.1 boiling curves at T_{sat}=27 ˚C for (a) tube diameter D=1.22 mm and (b) tube diameter D=1.70 mm

Another indication of dryout incipience is the fluctuations in the outer wall temperature and the associated standard deviation. A continuous recording of wall temperatures for the conditions D=1.22 mm, T_{sat}=27 °C, G=500 kg/m² s and the corresponding standard deviation in wall temperatures up to the complete dryout is shown in Figure 8.2 a and b respectively. The heat flux between 65kW/m² and 69kW/m², as seen in Figure 8.2a, was increased in very small steps after waiting for a long enough time. Similar plots for all the other cases and for both diameters can be produced. Figure 8.2a shows how the fluctuations start at the thermocouple positions at the downstream end of the test tube, at some critical heat flux, possibly as a result of dryout patches appearing on the heater surface. The same phenomenon was also observed by Owhaib et al. (2006) during visualization experiments and based on the videos it was explained to be caused by the heater surface temporarily becoming dry and temporarily flushed with a passing wave. These dryout patches are rewetted unless a certain heat flux is reached where no rewetting of the heater surface takes place and complete dryout occurs and this point is termed as dryout completion heat flux and the corresponding vapour quality is termed dryout quality. Moreover, as expected, Zhang et al. (2006) dryout conditions started close to the exit of the tube for all the mass fluxes tested and the dryout front moved upstream as the heat flux was increased. This can also be concluded by looking at the wall temperature profile where the fluctuations always start close to the exit of the tube (measurements shown by last thermocouple attached close to the exit of tube) and propagate to the upstream of the tube. The movement of the dryout front to further upstream can be observed by looking at Figure 8.2a where the temperature fluctuations start propagating from

the last thermocouple (T6) to second last thermocouple (T5) with increase in heat flux.

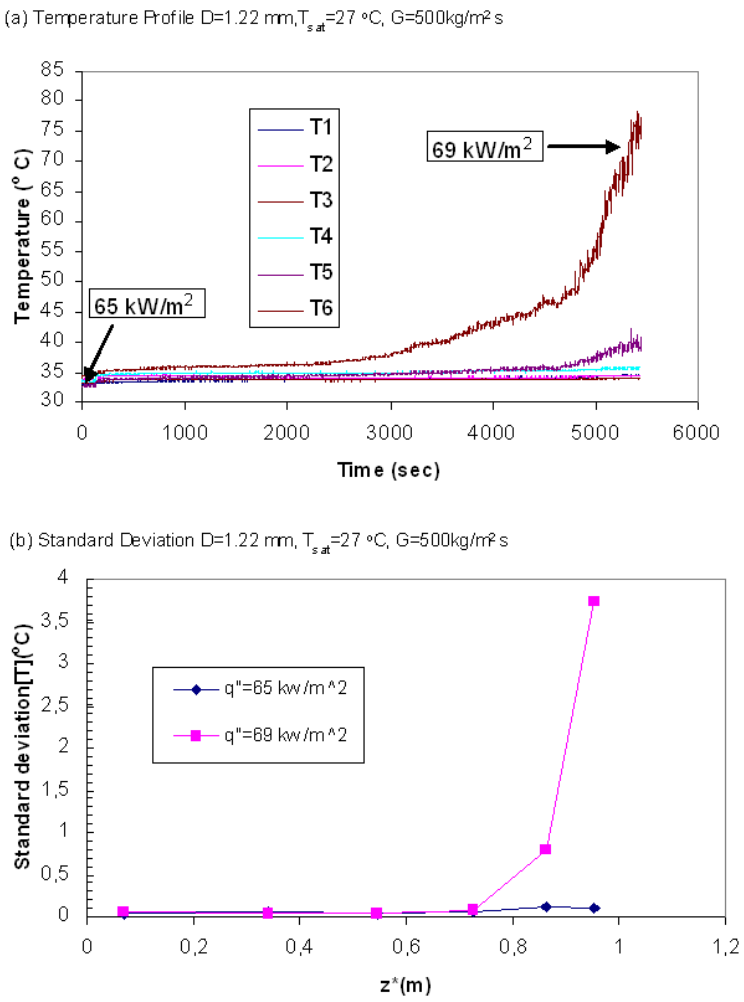

Figure 8.2 (a) A continuous temperature profile where T1 is the first thermocouple at the upstream end and T6 is the last thermocouple at the downstream end of the test section and (b) Corresponding standard deviation in temperatures of six thermocouples along the axial direction of the test section

8.2.2 Parametric effects on dryout incipience and dryout completion heat flux

8.2.2.1 Effect of mass flux

Figure 8.3 shows the effect of mass flux on DI and DC heat flux for both the tubes and at two system pressures. Results show that the DI and DC both increase with mass flux. The increment in DC heat flux with increase in mass flux is in compliance with many studies found in the literature for macro and micro scale channels. However, for DI heat flux there are not many studies available to compare. One of our previous studies Martin-Callizo et al. (2008) using the same test facility and a microchannel of 0.64 mm internal diameter showed the same trend for DI heat flux. The reason for the observed trend of increase of DI and DC heat flux is simply that an increase in mass flux at a given heat flux leads to a lower vapor fraction at any given position in the tube, and that DI and DC are highly dependent on vapor quality, as shown in the next section.

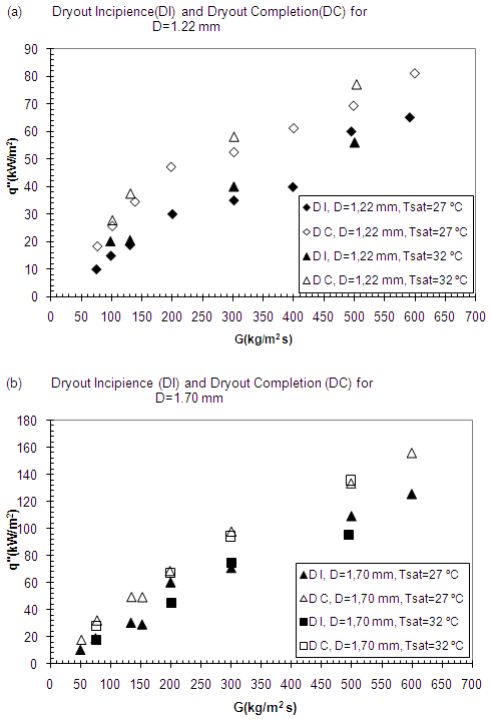

Figure 8.3 Effect of mass flux and system pressure on Dryout incipience (DI) and Dryout completion (DC) heat flux for T_{sat}=32 ˚C and T_{sat}=27 ˚C (a) D=1.22 mm (b) D=1.70 mm

8.2.2.2 Effect of vapor quality

A plot of the effect of exit vapour quality on dryout heat flux for the test tube having internal diameter of 1.22 mm is shown in Figure 8.4. For each mass flux, the figure shows two points where the first point is the dryout incipience quality and the last point is the vapor quality for complete dryout condition. A range of vapour qualities may be observed for dryout incipience to occur, for example at T_{sat}=27 ºC and G=75 to 200 kg/m² s, the dryout incipience occurs between vapour fractions of 0.48 to 0.58 while for the same saturation temperature and G=300 to 600 kg/m² s, the dryout incipience occurs in the vapour quality range of 0.38 to 0.48. For a mass flux range of 200 kg/m² s to 600 kg/m² s the vapor quality for complete dryout shifts to lower values and the heat flux for dryout completion increases with decrease in exit vapour quality. This shift to lower dryout vapour qualities for higher mass fluxes can be attributed to the liquid entrainment effect.

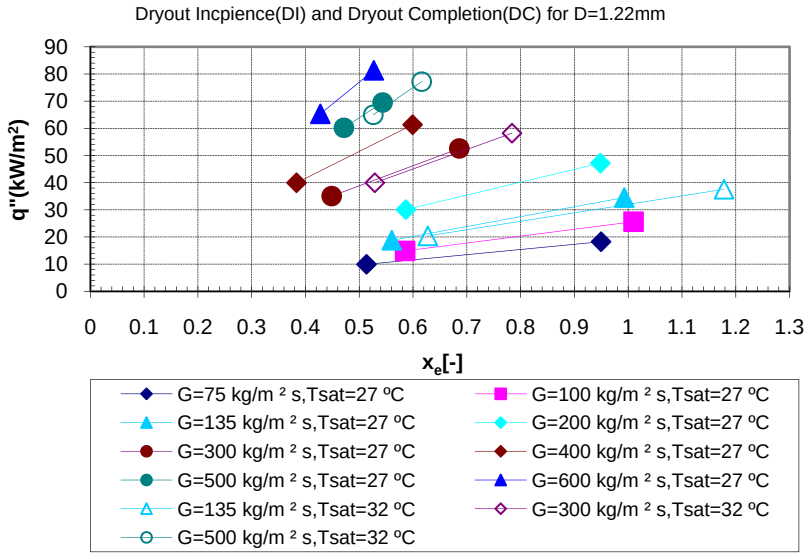

Figure 8.4 Effect of vapour quality on Dryout incipience and Dryout completion condition for D=1.22 mm at T_{sat}=32 ˚C and T_{sat}=27 ˚C

Figure 8.5 shows the plot for D=1.70 mm tube showing the effect of vapour quality on DI and DC heat flux. For this tube i.e. D=1.70 mm

the dryout incipience seems to occur at a range of vapour quality from 0.55 to 0.69 except for mass flux of 200 kg/m² s and T_{sat}=27 ºC for which dryout incipience occurs at a vapour quality of 0.85. Contrary to the small diameter tube, a pronounced decrease in dryout incipience quality for an increase in mass flux was not observed for the larger diameter tube. The heat flux at complete dryout for the larger diameter D=1.70 mm can be seen to decrease with increasing vapour quality. Unlike dryout incipience, the vapour quality for dryout completion is clearly seen to decrease with increase in mass flux which might be an effect of liquid entrainment.

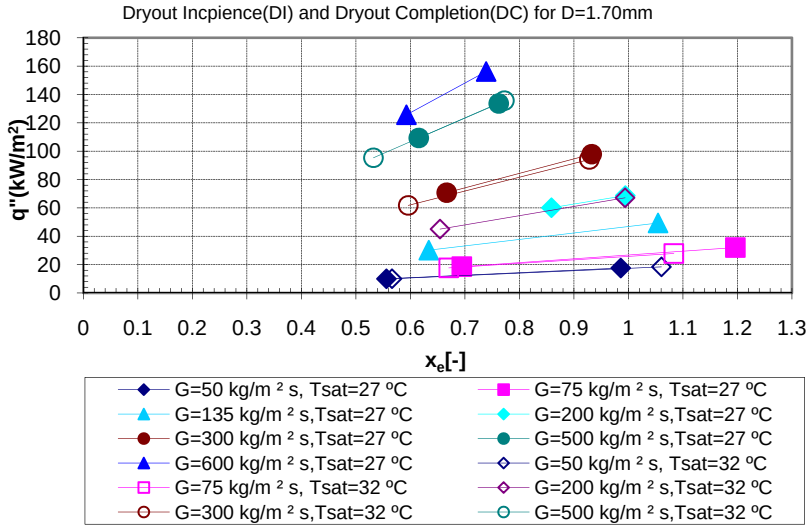

Figure 8.5 Effect of vapour quality on Dryout incipience and Dryout completion condition for D=1.70 mm at T_{sat}=32 ˚C and T_{sat}=27 ˚C

Dryout completion occurs earlier (i.e. at lower vapour qualities) for higher mass fluxes for both the test tubes. In the current study the flow regime at the condition of dryout incipience and dryout completion is believed to be annular. This was also observed by looking at the flow in the glass tubes placed at the outlet of both the test tubes. Moreover, visualization studies with the same experimental facility also show that the flow is typically annular at these vapour qualities in a microchannel. Annular flow is characterized by a vapour core flowing at the centre of the tube and a liquid film of certain thickness flowing along the tube wall and vaporization occurs at the vapour liquid interface. The increase in mass flux creates an increase in the velocity difference between the liquid and vapour phases and vapour is moving with a higher velocity, which creates increased interfacial shear stress. This increased interfacial shear

may be able to tear the liquid film and increase the droplet entrainment rate in the vapour core. Consequently liquid is flowing in the form of droplets in the vapour core at the centre of the tube and the liquid film dries out at lower vapour qualities.

8.2.2.3 Effect of channel diameter

Reduction in channel diameter enhances the relative importance of surface tension and shear forces which changes the flow patterns and associated transition between the flow patterns and consequently influences the occurrence of dryout. Figure 8.6 shows the effect of tube diameter on DI and DC heat flux. The heat flux for dryout incipience and dryout completion are both higher for larger diameter tube. At lower mass fluxes the difference in dryout heat flux is small but as mass flux increases this effect of increment in heat flux becomes more pronounced. A similar trend was also observed by Wojtan et al. (2006). Figure 8.7 shows the plot of dryout heat flux versus exit vapour quality for different mass fluxes and both tube diameters. Vapour quality at dryout incipience and dryout completion are marked by the two symbols for each case. Both are clearly seen to occur earlier (i.e. at lower vapour qualities) for 1.22 mm diameter tube as compared to 1.70 mm diameter tube. Earlier occurrence of dryout for smaller diameter tube can be explained by the fact that with reducing the diameter the shear forces get stronger thereby promoting the increased interfacial shear and liquid entrainment which causes the liquid film to dry earlier.

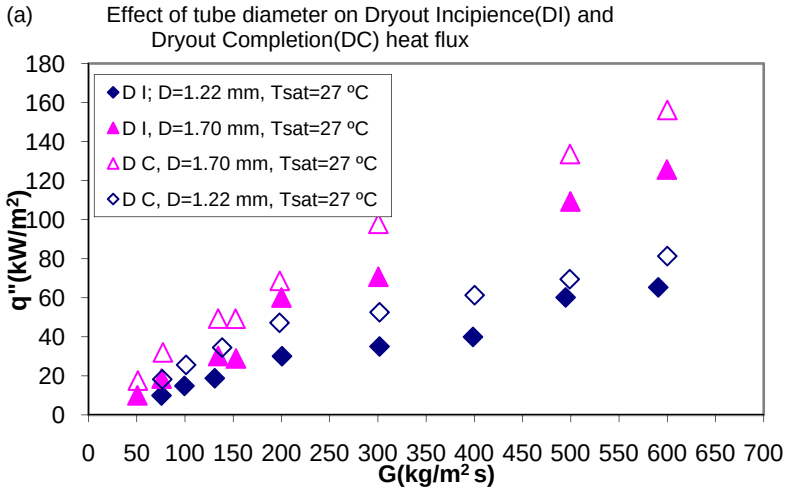

Figure 8.6 Effect of tube diameter on dryout incipience and dryout completion heat flux at T_{sat}=27 ˚C

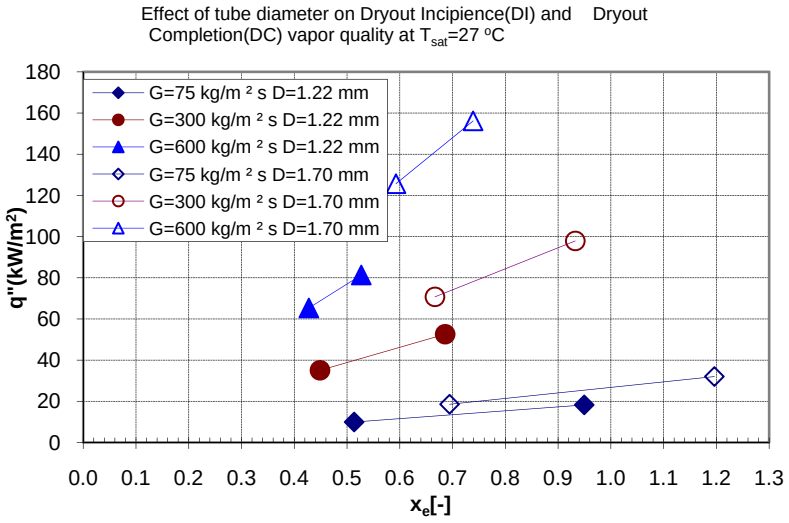

Figure 8.7 Effect of tube diameter on dryout incipience vapour quality and dryout completion vapour quality at T_{sat}= 27 ˚C

It is noted, however, that the heated length of both the channels in these experiments was the same which means that the effect of tube diameter may not be seen independently. Instead a more realistic approach will be to see the effect of the heated length to diameter (L/D) ratio. Current experimental results show that as L/D ratio increases the heat flux for dryout completion decreases which is also in agreement with many CHF studies in the literature for example Kim et al. (2000). It should also be noted that the effect of tube diameter and the effect of surface roughness on dryout cannot be distinguished from the present tests as the surface characteristics were different for the two tubes.

8.2.2.4 Effect of system pressure

Effect of system pressure on the dryout incipience and dryout completion heat flux can be seen in Figure 8.3. The effect of system pressure on dryout heat flux is marginal but for a tube diameter of 1.22 mm, the dryout completion occurs at a slightly higher heat flux for higher system pressure and the effect seems to be pronounced as the mass flux increases. For the larger tube diameter the system pressure has no clear effect on heat flux at dryout completion. System pressure effect on dryout quality is depicted in Figure 8.4 and Figure 8.5. For a tube diameter of 1.22 mm it can be seen that dryout completion is delayed to higher vapour qualities for a higher system pressure but for larger tube diameter the trend is not clear. Therefore, no clear conclusion can be made for the

effect of system pressure on dryout heat flux and vapour quality due to very narrow range of the two system pressures. It would be expected that as the density ratio (ρ_g/ρ_l) increases with pressure, thereby reducing the droplet entrainment rate in the vapour core, the dryout will be delayed to higher vapour qualities for a higher system pressure. A broader range of system pressures should be tested to see any clear effects of system pressure on dryout.

8.2.2.5 Comparison with existing macro and micro scale correlations for critical heat flux

Comparison of experimental results with predictions of several correlations taken from literature is shown in Table 8-1. The Bowring (1972) correlation developed for macrochannels gives the best predictions among all the tested macro and micro channel correlations with a MAD of 13% and 81% of the data falling within ±20% error band. 100% of the larger tube diameter data is captured within ±20% by this correlation while for D=1.22 mm the low mass flux data is captured within the prescribed error band but for G=300 kg/m^2 s and above the data is below values predicted by the correlation. The comparison with Bowring's correlation is shown in Figure 8.8. The Katto and Ohno (1984) correlation which is widely used for prediction of CHF, predicts the present experimental data with a MAD of 19%, with 67% of all the data falling within ±20%. The higher mass flux data for both the tubes is over predicted by this correlation. The comparison of the experimental data with the Katto-Ohno correlation is viewed in Figure 8.9. The Zhang et al. (2006) correlation developed for mini channels from water data, is in reasonable agreement with the current experimental data with a MAD of 18% and with 70% of data falling within the ±20% error band. The comparison with this correlation is viewed in Figure 8.10 where it can be seen that the data of the larger diameter tube is predicted to 100% within the ±20% error band, but the data points for the smaller diameter tube fall outside of the ±20% error band.

Table 8-1 Assessment of existing macro and micro scale CHF prediction methods

Correlation and reference	MAD (%)	% of data within ± 20%
Katto and Ohno (1984)	19	67
Bowring (1972)	13	81
Wojtan et al. (2006)	30	48
Martin-Callizo et al. (2008)	17	74
Zhang et al. (2006)	18	70
Qu and Mudawar (2004)	1800	0

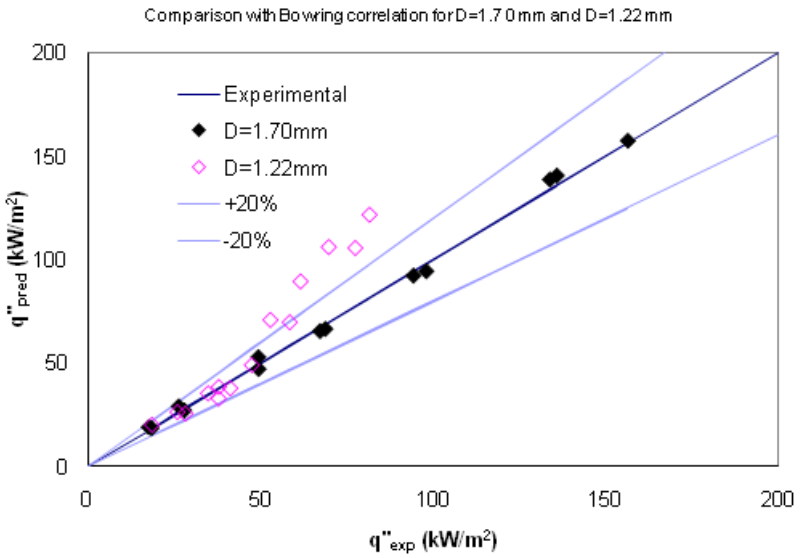

Figure 8.8 Comparison of experimental data with Bowring (1972) correlation for the critical heat flux

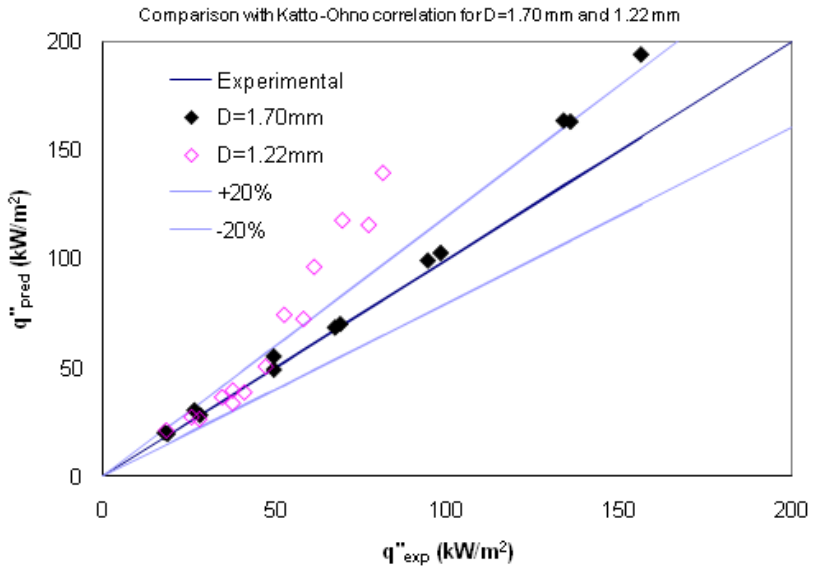

Figure 8.9 Comparison of experimental data with Katto-Ohno (1984) correlation for critical heat flux

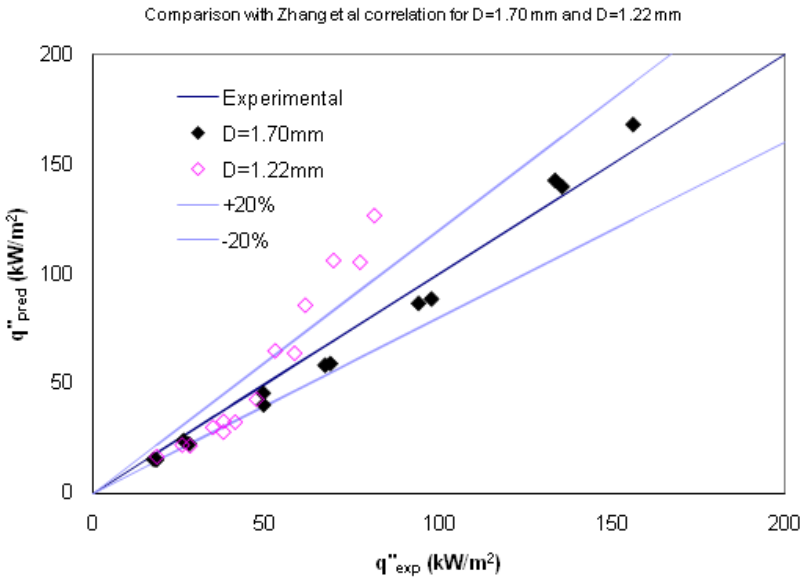

Figure 8.10 Comparison of experimental data with Zhang et al. (2006) correlation for critical heat flux

9 Two-phase Pressure Drop

9.1 Motivation and objectives of two-phase pressure drop experiments

The pressure drop during flow boiling will define the pumping power requirements in a heat exchange system. The reduction of channel dimensions is associated with increase in pressure drop. Therefore, to optimize the system, it will be required to know the pressure drop and consequently the pumping power requirements. The purpose of this study was to ascertain and analyze the pressure drop in a micro channel during flow boiling of refrigerants with different thermo-physical properties. As pointed out in the literature survey chapter, the previous two-phase pressure drop studies have mostly been carried out for air-water and for adiabatic systems which lack the actual dynamic behaviour of the pressure drop expected due to the diabatic evaporation process in a micro channel. The objectives of the two-phase pressure drop study are thus as summarised below:

- To understand the basic phenomena involved in two-phase flow and pressure drop in micro channels.
- To study the effects of operating parameters on two-phase flow in micro channels using different fluids.
- To study the effects of thermo-physical properties on two-phase pressure drop by using fluids having different properties.
- To augment the existing database of two-phase flow and pressure drop in micro channels with reliable and accurate experimental data.
- To assess the prediction capability of existing two-phase pressure drop models and correlations developed for macro and micro scale channels.

9.2 Experimental results of two-phase pressure drop (Paper # 6)

Single phase pressure drop tests were first performed to validate the instrumentation and experimental set up. The single phase results have already been presented in section 4.5.1 and in paper # 6 attached with this thesis. The details of experimental set up, data reduction and calculation procedures can also be seen in paper # 6. The parametric effects on two-phase pressure drop for the two refrigerants R134a and R245fa and the assessment results of comparison with macro and micro scale correlations are shown in the sections below. The detailed results can also be viewed in the paper mentioned before.

9.2.1 Effect of vapor quality

The variation of experimental frictional pressure drop with outlet vapour quality for R134a and R245fa is shown in Figure 9.1 and Figure 9.2 respectively. For both the refrigerants the frictional pressure drop varies almost linearly with outlet vapour fraction for a given mass flux. As expected, for a given outlet vapour quality condition, the pressure drop increases with the mass flux.

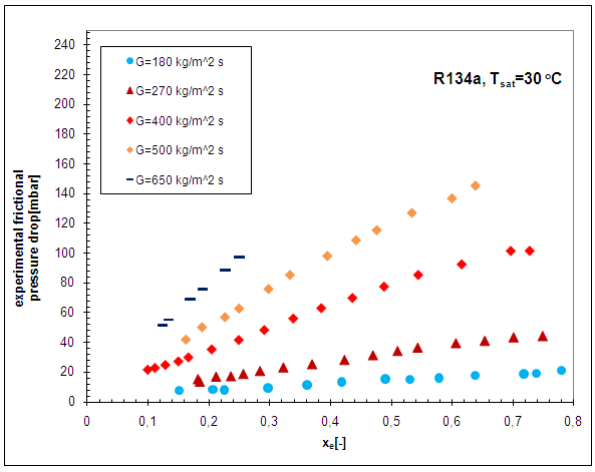

Figure 9.1 Experimental frictional pressure drop plotted versus exit vapour quality for R134a, T_{sat}=30 ˚C

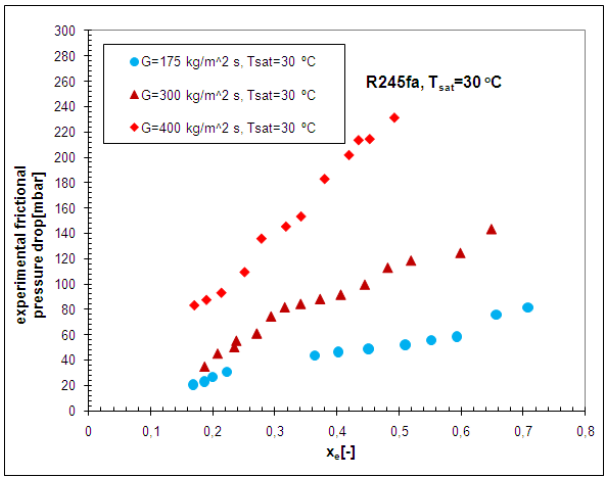

Figure 9.2 Experimental frictional pressure drop plotted versus exit vapour quality for R245fa, T_{sat}=30 ˚C

9.2.2 Effect of system pressure

Increased system pressure will mean a lower liquid to vapor density ratio resulting in a lower two-phase frictional pressure drop for a higher pressure. This trend is clearly seen for R134a at two different system pressures corresponding to saturation temperatures of 25 ˚C and 30 ˚C as shown in Figure 9.3. However, for R245fa a clear effect of system pressure was not observed as seen in Figure 9.4. The tests for R245fa were conducted at three different system pressures corresponding to saturation temperatures of 30 ˚C, 35 ˚C and 40 ˚C.

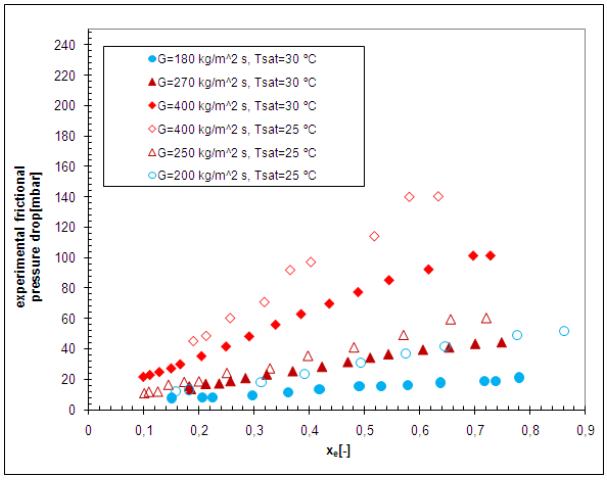

Figure 9.3 Effect of system pressure on experimental two-phase frictional pressure drop for R134a

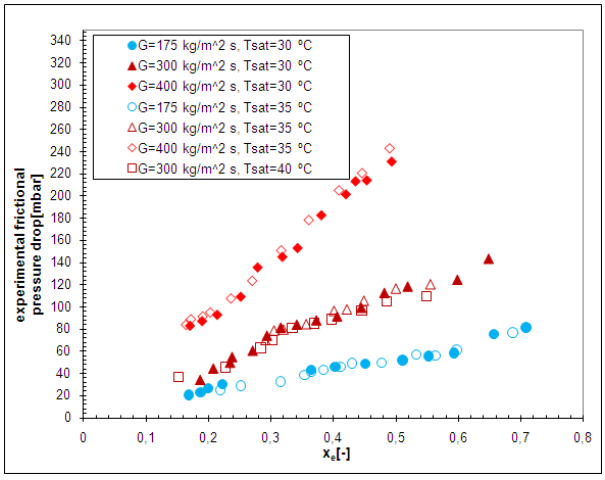

Figure 9.4 Effect of system pressure on experimental two-phase frictional pressure drop for R245fa

9.2.3 Effect of refrigerant

The thermo-physical properties of R134a and R245fa are quite different as shown in Table 7-2. The properties are a major consideration when selecting a refrigerant for a specific application since the heat transfer and pressure drop are dependent on these properties. The comparison of experimental frictional pressure drop during flow boiling of the refrigerants R134a and R245fa is depicted in Figure 9.5. As expected, the pressure drop of R245fa is significantly higher than that of R134a for the same saturation temperature. Liquid viscosity is higher and vapor density is lower for R245a than R134a at the same saturation temperature which results in a higher penalty in terms of pressure drop.

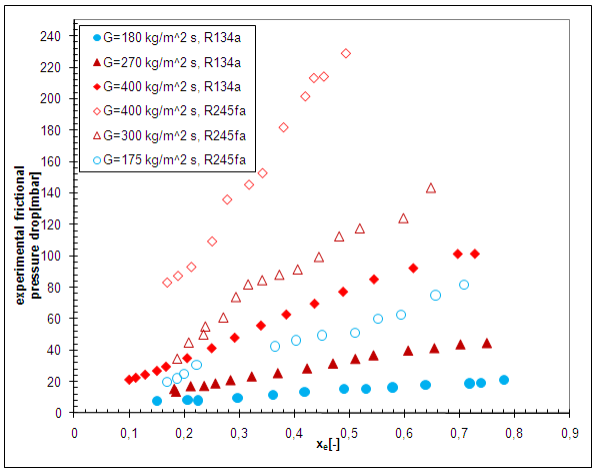

Figure 9.5 Comparison of two-phase frictional pressure drop of R134a and R245fa, T_{sat}=30 ˚C

9.2.4 Comparison with existing prediction methods

A number of models and correlations for two-phase frictional pressure drop were considered for comparison with experimental results. The following sections discuss the comparison to macro scale models and micro scale models for two-phase frictional pressure drop.

9.2.4.1 Comparison with macro scale models

Under this category, two frequently used models are the homogeneous model and the separated flow model (Lockhart and Martinelli (1949) model being the most popular one). Many of the other models and correlations are modified forms of these two models.

The experimental data was compared to the homogeneous model using several definitions of viscosity. The results for both the refrigerants with this model can be viewed in Table 9-1. The predictions with homogeneous model are not satisfactory for either of the refrigerants with any of the viscosity definitions. Certainly, the assumption in the homogeneous model that the liquid and the vapour move with the same velocity is not valid in micro scale two-phase flow, where the two-phases are expected to move with different velocities.

Table 9-1 Assessment of homogeneous model employing different definitions of homogeneous viscosity

Viscosity definition	MAD (%)		% of data within ±20%	
	R134a	R245fa	R134a	R245fa
McAdams et al. (1942)	35	27	10	27
Cicchitti et al. (1960)	21	70	58	16
Dukler et al. (1964)	39	35	7	13
Beattie and Whalley (1981)	29	52	27	25

The comparisons with other macro scale models are listed in Table 9-2. Muller-Steinhagen and Heck correlation works best among all the tested correlations. The homogeneous model with Cicchitti et al. viscosity definition is second best for R134a after Muller-Steinhagen and Heck correlation.

The Lockhart-Martinelli model uses a two-phase multiplier expressed in terms of the Martinelli parameter X and the Chisholm parameter C. The value of the parameter C is selected on the basis of whether the liquid and vapour phases are in laminar or turbulent conditions. For the current experimental conditions the C parameter as suggested by Lockart-Martinelli will fall in the range 12 to 20 for most of the data points. The experimental value of the parameter C on the other hand gives a value between 2 to 5 as seen in Figure 9.6 and if this value is used in evaluating the two-phase multiplier, the predictions with the Lockhart-Martinelli correlation should be close to the experimental results.

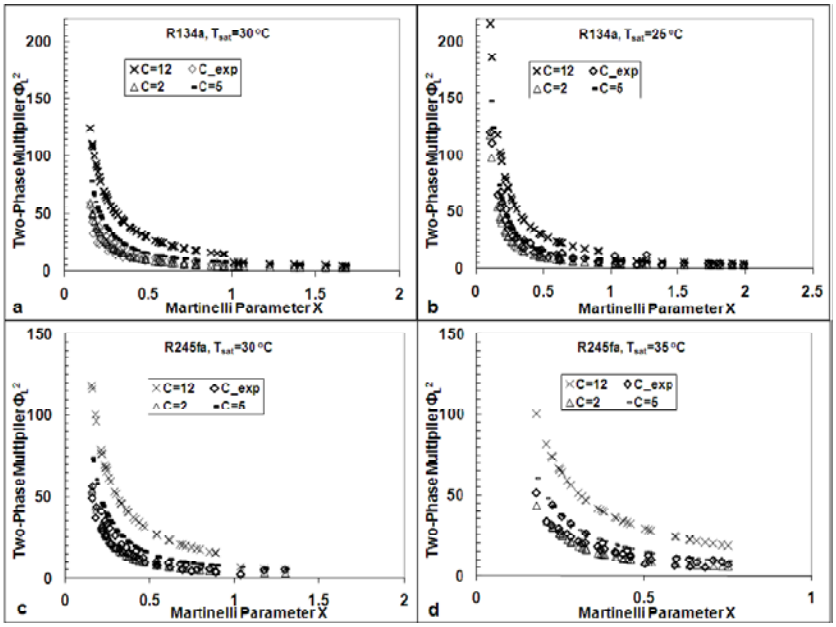

Figure 9.6 Martinelli parameter versus two-phase multiplier for (a) R134a T_{sat}=30 °C (b) R134a T_{sat}=25 °C (c) R245fa T_{sat}=30 °C (d) R245fa T_{sat}=35 °C

Table 9-2 Assessment of macro scale two-phase frictional pressure drop correlations and models

Correlation	MAD (%)		% of data within ± 20%	
	R134a	R245fa	R134a	R245fa
Homogeneous (Cicchitti et al. (1960) definition of viscosity)	21	70	58	16
Lockhart and Martinelli (1949)	52	64	27	5
Müller-Steinhagen and Heck (1986)	18	32	65	46
Friedel (1979)	56	148	33	0
Grönnerud (1979)	26	90	43	9

9.2.4.2 Comparison with micro scale correlations

A comparison of the experimental results with predictions obtained from micro scale correlations is shown in Table 9-3. Experimental results for both refrigerants show a reasonable agreement with Mishima and Hibiki (1996) and Tran et al. (2000) correlations. Both the correlations take into account the effect of tube diameter while in addition Tran et al. (2000) correlation includes the effects of surface tension and buoyancy forces by incorporating the confinement number in the correlation. Interestingly, the value of the parameter C calculated by the Mishima and Hibiki (1996) correlation is 4.6 which is close to the experimentally found C value of 2 to 5.

Table 9-3 Assessment of micro scale two-phase frictional pressure drop correlations and models

Correlation	MAD (%)		% of data within ± 20%	
	R134a	R245fa	R134a	R245fa
Mishima and Hibiki (1996)	20	16	57	65
Tran et al. (2000)	17	26	71	62
Zhang and Webb (2001)	47	520	27	0
Lee and Mudawar (2005)	115	57	4	17

10 Conclusions and Future Recommendations

An extensive survey of prior studies on micro channels, presented in chapter 2 indicated several discrepancies existing among the available data. A serious need was felt to conduct a comprehensive study of phase change phenomena in microchannels to understand the fundamental mechanisms involved in the process. Therefore, an experimental study was conducted in stainless steel and fused silica tubes to systematically investigate and analyse the flow boiling characteristics of micro channels. The heat transfer and pressure drop experiments were supported by a visualization study employing quartz tubes with two different diameters. The most important results of this study are summarized below and some recommendations are given based on the results obtained from the current study.

10.1 Results from flow boiling visualization study

High speed camera was employed for visualization of the flow boiling in vertical and horizontal quartz tubes. Unlike most adiabatic visualization studies found in the literature or other studies where visualization of the process is performed at the exit of the actual evaporator (not the heated length), the current experiments are unique in the sense that the actual micro evaporator (heated section of the tube) was visualized during the tests. The results show that the confinement effects are apparently present in micro channels. A flow pattern unique to micro channels, called elongated bubble flow pattern which is formed due to restricted channel dimensions, was also observed. The bubbly flow zone exists for very short length after the nucleation point. The bubble departure diameter decreases with mass flux which is in agreement with our previous flow visualization study carried out for a 1.33 mm inner diameter tube Owhaib (2007) and it also increases with heat flux. A comparison with the same visualization study by Owhaib et al. (2007) for a larger diameter tube of 1.33 mm shows that bubble frequency is higher for the smaller diameter (0.781 mm) tube (current study). The mean length and velocity

of elongated bubbles increased with vapour quality and mass flux, as expected. Flow patterns were recorded and presented as charts in the terms of different parameters such as superficial gas and liquid velocity or in terms of Reynolds number and vapour quality. The effect of saturation temperature revealed that the annular flow transition lines shifted to higher superficial gas velocities for a higher saturation temperature. It was observed that the annular flow is reached earlier (i.e. at low vapour fractions) in smaller diameter tubes as compared to conventional sized channels. Increase in mass flux shifts the annular flow regime further towards lower vapour fractions. A comparison to an earlier study of flow patterns in a 1.33 mm diameter tube by Martin-Callizo et al. (2010) revealed that the bubbly to slug flow transition line is shifted to lower vapour qualities which might be an effect of increased confinement effects as the diameter is reduced.

10.2 Results from the flow boiling heat transfer study

Heat transfer experiments for R134a and R245fa were performed in stainless steel and quartz tubes and in general, the results show that the heat transfer coefficients under most conditions increase with heat flux. The heat transfer results for steel tube show that the heat transfer coefficient increases monotonically with heat flux. With respect to local vapour quality, the local heat transfer coefficient increases with vapour quality for low vapour qualities, levels out i.e. does not change, decreases slowly for a range of vapour qualities to finally decrease rapidly for vapour qualities above some specific value. For higher system pressure, the heat transfer coefficient was higher. The effect of mass flux was negligible in these tests. The study for the quartz tube was supported with simultaneous visualization of the flow boiling of R134a.

A comparison of experimental results with existing correlations was also performed. Pool boiling correlations and flow boiling correlations based on nucleate boiling dominated effects are partially successful in predicting the R134a experimental data but in the case of R245fa, none of the correlations is able to predict the experimental data satisfactorily which shows that the correlations are not able to take into account the thermophysical properties of the fluids. For the design purposes, the micro scale correlations by Tran et al. (1996; Zhang et al. (2004) and macro scale correlation by Liu and Winterton (1991) can be recommended based on the results of the current study.

10.3 Results from the dryout study

Dryout experiments were carried out in stainless steel tubes with inner diameters of 1.70 mm and 1.22 mm. Dryout condition was identified by

recording the fluctuations in the outer wall temperature and the corresponding standard deviation in temperature within the dryout zone. Dryout conditions always started at close to the exit of the test tube and propagated towards upstream as the heat flux was increased. The heat flux for dryout incipience as well as for complete dryout increased with increase in mass flux. The dryout for the smaller tube occurred at comparatively lower vapor qualities. The increase in mass flux also shifted the dryout towards lower vapor qualities. One of the reasons of this shift to lower vapor qualities is believed to be liquid entrainment due to increased vapor shear. The experimental dryout data were compared with some well known CHF correlations. Reasonable agreement with the experimental data was observed with some macro as well as micro scale correlations. The macro scale correlations by Bowring (1972) and Katto and Ohno (1984) and the micro scale correlation by Zhang et al. (2006) can be recommended for the design purposes based on the results of the current study.

10.4 Results from the two-phase pressure drop study

Diabatic two-phase pressure drop results were obtained for a quartz tube with an internal diameter of 0.781 mm using two refrigerants with significantly different thermo-physical properties. The test section was unique in the sense that the holes for the pressure taps were drilled just at the inlet and outlet of the heated section. This eliminated the need to compensate for two-phase flow in a large part at the exit of the test tube and thereby eliminated the associated error otherwise introduced due to this unwanted two-phase flow part. The two-phase frictional pressure drop increases with exit vapour quality and mass flux for both the refrigerants. Increase in system pressure decreases the pressure drop for R134a but the effect of system pressure on R245fa is negligible which is not according to the generally available trends in the literature. Finally, the macro scale and micro scale correlations from the literature were selected for the comparison with experimental data. The experimental data of R134a were in a reasonable agreement with the macro scale correlation by Müller-Steinhagen and Heck (1986) but in the case of R245fa none of the macro scale correlations worked satisfactorily. The micro scale correlation by Mishima and Hibiki (1996) was in agreement with R134a data. The micro scale correlation by Tran et al. (2000) predicted both the R134a and the R245fa data reasonably well.

10.5 Future recommendations

Use of micro channels is usually associated with increased heat transfer and pressure drop. Increased pressure drop is, however, undesired due to large pumping requirements which will increase the cost and decrease the efficiency of overall heat exchange system. Increased pressure drop can be avoided by using multiple parallel tubes. However, this will also influence heat transfer. Therefore, it will be of interest to conduct an optimization study based on which a choice of optimum heat transfer and pressure drop could be made by choosing a suitable channel size and required number of parallel channels.

Experiments with parallel channels are suggested especially focusing on the issue of fluid mal-distribution at the inlet, which, based on the studies in literature, has been found a major issue in the area of micro channels.

High speed visualization experiments are suggested with enhanced magnification to investigate if any nucleation occurs in thin liquid film present between vapour bubble and the channel wall. This will help in understanding if the nucleate boiling dominates even in elongated bubble and slug flows as reported in some studies.

The current study and other studies in literature indicate that intermittent dryout is observed at comparatively lower vapour qualities which is not desirable. Studies focusing on developing different methods to delay the intermittent dryout will be essential in order to fully exploit the micro channel based compact heat exchangers.

Finally it can be said that choosing the appropriate models and correlations is fundamental for the evaluation of heat transfer and pressure drop in order to design the compact heat exchangers. This comprehensive, flow pattern based study of micro channel flow boiling will assist in understanding the basic phenomena involved in phase change during fluid flow in microchannels and in developing accurate models and correlations for compact and efficient micro evaporators for a number of applications.

Nomenclature

Roman

A	Heat transfer area (m^2)
A_c	Cross-sectional area (m^2)
Cp	Specific heat (kJ/kg-K)
D	Diameter (m)
DI	Dryout incipience
DC	Dryout completion
f	Friction factor (-)
G	Mass flux (kg/m^2-s)
h_{fg}	Latent heat of vaporization (kJ/kg)
I	Current (A)
J	superficial velocity (m/s)
k	Thermal conductivity (W/mK)
L	Length (m)
MAD	Mean absolute deviation ($1/N\ \Sigma\lvert X_{pred} - X_{exp}\rvert$)
$\dot{m}$	Refrigerant mass flow rate (kg/s)
P	Pressure (bar)
q	Power (W)
q''	heat flux (kW/m^2)

T	Temperature (°C)
t	Time (s)
V	Voltage (V)
x	Vapour quality (-)
z	Axial location (m)
z*	Normalized length (z/z_{hs})

Greek

α	Heat transfer coefficient (W/m^2-C)
Δ	Difference (-)
ΔP	Pressure drop (kPa)
ΔT	Temperature difference (°C)
ρ	Density (kg/m^3)
μ	Dynamic viscosity (Ns/m^2)
σ	Surface tension (N/m)

Subscript

ele	Electrical
exp	Experimental
eff	Effective
f	Fluid
g	Gas
h	Hydraulic

hs	Heated section
i	Inner
in	Inlet
lo	Liquid only
l	Liquid
o	Outer
out	Outlet
pred	Predicted
sat	Saturation
t	Tube
th	Thermal
tot	Total
tp	Two phase
v	Vapour
w	wall

Dimensionless Numbers

Bo	Boiling number, $(q''/(Gh_{fg})$
Nu	Nusselt number, $(\alpha D/k)$
Pr	Prandtl number, $(\mu Cp/k)$
Re	Reynolds number, (GD/μ)
We	Weber number, $(G^2D/(\sigma\rho)$

List of figures

List of Tables

Bibliography

Arcanjo, A. A., Tibiriçá, C. B. and Ribatski, G. (2010). "Evaluation of Flow Patterns and Elongated Bubble Characteristics During the Flow Boiling of Halocarbon Refrigerants in a Micro-Scale Channel." *Experimental Thermal and Fluid Science* **34**(6): 766-775.

Baker, O. (1954). "Simultaneous Flow of Oil and Gas." *Oil and Gas Journal* **53**: 185.

Bao, Z. Y., Fletcher, D. F. and Haynes, B. S. (2000). "Flow Boiling Heat Transfer of Freon R11 and Hcfc123 in Narrow Passages." *International Journal of Heat and Mass Transfer* **43**(18): 3347-3358.

Beattie, D. R. H. and Whalley, P. B. (1981). "A Simple Two-Phase Frictional Pressure Drop Calculation Method." *international Journal of Multiphase Flow* **8**: 83-87.

Bergles, A. E. (1962). Forced Convection Surface-Boiling Heat Transfer and Burn out in Tubes of Small Diameter. *Mechanical Engineering Department*, *Massachusetts Institute of Technolotgy*. Doctoral Thesis.

Bergles, A. E. and Dormer, T. J. (1969). "Subcooled Boiling Pressure Drop with Water at Low Pressure." *International Journal of Heat and Mass Transfer* **12**(4): 459-470.

Bertsch, S. S., Groll, E. A. and Garimella, S. V. (2008). "Refrigerant Flow Boiling Heat Transfer in Parallel Microchannels as a Function of Local Vapor Quality." *International Journal of Heat and Mass Transfer* **51**(19-20): 4775-4787.

Bertsch, S. S., Groll, E. A. and Garimella, S. V. (2009). "Effects of Heat Flux, Mass Flux, Vapor Quality, and Saturation Temperature on Flow Boiling Heat Transfer in Microchannels." *International Journal of Multiphase Flow* **35**(2): 142-154.

Bowers, M. B. and Mudawar, I. (1994). "High Flux Boiling in Low Flow Rate, Low Pressure Drop Mini-Channel and Micro-Channel Heat Sinks." *International Journal of Heat and Mass Transfer* **37**(2): 321-332.

Bowring, R. W. (1972). A Simple but Accurate Round Tube Uniform Heat Flux Correlation over the Perssure Range 0.7-17 Mn/M^2. *Report AEEW-R789*. *Winfrith, UK*.

Brauner, N. and Maron, D. M. (1992). "Identification of the Range of 'Small Diameters' Conduits, Regarding Two-Phase Flow Pattern Transitions." *International Communications in Heat and Mass Transfer* **19**(1): 29-39.

Cavallini, A., Bortolin, S., Del Col, D., Matkovic, M. and Rossetto, L. (2007). "Experiments on Dry-out During Flow Boiling in a Round Minichannel." *Microgravity Science and Technology* **19**(3): 57-59.

Cavallini, A., Del Col, D., Doretti, L., Matkovic, M., Rossetto, L. and Zilio, C. (2005). "Two-Phase Frictional Pressure Gradient of R236ea, R134a and R410a inside Multi-Port Mini-Channels." *Experimental Thermal and Fluid Science* **29**(7): 861-870.

Celata, G. P., Cumo, M. and Mariani, A. (1995). "High Heat Flux Burn-out in Subcooled Flow Boiling." *Journal of Thermal Science* **4**(3): 151-161.

Chaddock, J. B. and Brunemann, H. (1967). Forced Convection of Refrigerants in Horizontal Tubes. *School of Engineering, Duke University***:** HL-113.

Chen, I. Y., Chen, Y.-M., Liaw, J.-S. and Wang, C.-C. (2007). "Two-Phase Frictional Pressure Drop in Small Rectangular Channels." *Experimental Thermal and Fluid Science* **32**(1): 60-66.

Chen, L., Tian, Y. S. and Karayiannis, T. G. (2005). Vertical Upward Flow Patterns in Small Diameter Tubes. *6th World Conference on Experimental Heat Transfer, Fluid Mechanics and Thermodynamics*, Matsushima, Miyagi, Japan.

Chen, T. and Garimella, S. V. (2007). "Flow Boiling Heat Transfer to a Dielectric Coolant in a Microchannel Heat Sink." *IEEE Transactions on Components and Packaging Technologies* **30**(1): 24-31.

Chih-Jung, K., Kosar, A., Peles, Y., Virost, S., Mishra, C. and Jensen, M. K. (2006). "Bubble Dynamics During Boiling in Enhanced Surface Microchannels." *Journal of Microelectromechanical Systems* **15**(6): 1514-1527.

Chiou, J. P. (1980). "The Advancement of Compact Heat Exchanger Theory Considering the Effects of Longitudinal Heat Conduction and Flow Non-Uniformity." *Symposium on Compact Heat Exchangers, ASME HTD* **10** 101-121.

Chung, P. M. Y. and Kawaji, M. (2004). "The Effect of Channel Diameter on Adiabatic Two-Phase Flow Characteristics in Microchannels." *International Journal of Multiphase Flow* **30**(7-8): 735-761.

Churchill, S. W. and Chu, H. H. S. (1975). "Correlating Equations for Laminar and Turbulent Free Convection from a Horizontal Cylinder." *International Journal of Heat and Mass Transfer* **18**(9): 1049-1053.

Cicchitti, A., Lombardi, C., Silvestri, M., Soldaini, G. and Zavattarelli, R. (1960). "Two-Phase Cooling Experiments- Pressure Drop, Heat Transfer and Burnout Measurements." *Energ. Nucl* **7**(6): 407-425.

Coleman, J. W. and Garimella, S. (1999). "Characterization of Two-Phase Flow Patterns in Small Diameter Round and Rectangular

Tubes." *International Journal of Heat and Mass Transfer* **42**(15): 2869-2881.

Collier, J. G. and Thome, J. R. (1994). Convective Boiling and Condensation, *Oxford Science Publications*. 3rd Edition.

Cooper, M. G. (1984). Saturation Nucleate Pool Boiling - a Simple Correlation. *Institution of Chemical Engineers Symposium Series*. 86**:** 785-793.

Cornwell, K. and Kew, P. A. (1992). Boiling in Small Parallel Channels *Proceedings of CEC Conference on Energy Efficiency in Process Technology*, Athens, Paper E22, Elsevier Applied Science, 624-638.

Damianides, D. A. and Westwater, J. W. (1988). Two-Phase Flow Patterns in Compact Heat Exchanger and in Small Tubes. *Second UK National Heat Transfer Conference. Glasgow, UK.* 2**:** 1257-1268.

Dukler, A. E., Wicks, M. and Cleveland, R. G. (1964). "Pressure Drop and Hold-up in Two-Phase Flow Part a- a Comparison of Existing Correlations and Part B- an Approach through Similarity Analysis." *AIChe J* **10**(1): 38-51.

Dutkowski, K. (2009). "Two-Phase Pressure Drop of Air-Water in Minichannels." *International Journal of Heat and Mass Transfer* **52**(21-22): 5185-5192.

Felcar, H. O. M., Ribatski, G. and Saiz-Jabardo, J. M. (2007). A Gas–Liquid Flow Pattern Predictive Method for Macro and Mini Scale Round Channels. *in Proceedings of the 10th UK National Heat Transfer Conference*, Edinburgh, UK.

Friedel, L. (1979). Improved Friction Pressure Drop Correlations for Horizontal and Vertical Two-Phase Pipe Flow. *The European Two-Phase Flow Group Meeting. Ispra, Iraly*. Paper E2.

Fritz, W. (1935). "Maximum Volume of Vapor Bubbles." *Physik Zeittschr* **36**: 379-384.

Fu, X., Qi, S. L., Zhang, P. and Wang, R. Z. (2008). "Visualization of Flow Boiling of Liquid Nitrogen in a Vertical Mini-Tube." *International Journal of Multiphase Flow* **34**(4): 333-351.

Fukano, T. and Kariyasaki, A. (1993). "Characteristics of Gas-Liquid Two-Phase Flow in a Capillary Tube." *Nuclear Engineering and Design* **141**(1-2): 59-68.

Gaertner, R. F. and Westwater, J. W. (1960). "Population of Active Sites in Nucleate Boiling Heat Transfer." *Chemical Engineering Progress* **46**: 39.

Garimella, S., Killion, J. D. and Coleman, J. W. (2002). "An Experimentally Validated Model for Two-Phase Pressure Drop in the Intermittent Flow Regime for Circular Microchannels." *Journal of Fluids Engineering* **124**: 205-214.

Gorenflo, D. (1992). "Pool Boiling." *VDI Heat Atlas English Version* Ha1-Ha25.

Grönnerud, R. (1979). "Investigation of Liquid Hold-up, Flow-Resistance and Heat Transfer in Circulation Type Evaporators, Part Iv: Two-Phase Flow Resistance in Boiling Refrigerants." *Annexe 1972-I, Bull. de l'Inst. du froid.*

Gungor, K. E. and Winterton, R. H. S. (1986). "A General Correlation for Flow Boiling in Tubes and Annuli." *International Journal of Heat and Mass Transfer* **29**(3): 351-358.

Han, Y. and Shikazono, N. (2009). "Measurement of the Liquid Film Thickness in Micro Tube Slug Flow." *International Journal of Heat and Fluid Flow* **30**(5): 842-853.

Harirchian, T. and Garimella, S. V. (2008). "Microchannel Size Effects on Local Flow Boiling Heat Transfer to a Dielectric Fluid." *International Journal of Heat and Mass Transfer* **51**(15-16): 3724-3735.

Harirchian, T. and Garimella, S. V. (2010). "A Comprehensive Flow Regime Map for Microchannel Flow Boiling with Quantitative Transition Criteria." *International Journal of Heat and Mass Transfer* **53**(13-14): 2694-2702.

Hetsroni, G., Mosyak, A., Segal, Z. and Pogrebnyak, E. (2003). "Two-Phase Flow Patterns in Parallel Micro-Channels." *International Journal of Multiphase Flow* **29**(3): 341-360.

Holman, J. P. (1992). Heat Transfer, *McGraw-Hill.*

Hrnjak, P. and Tu, X. (2007). "Single Phase Pressure Drop in Microchannels." *International Journal of Heat and Fluid Flow* **28**(1): 2-14.

Hsieh, F. C., Li, K. W., Lie, Y. M., Chen, C. A. and Lin, T. F. (2008). "Saturated Flow Boiling Heat Transfer of R-407c and Associated Bubble Characteristics in a Narrow Annular Duct." *International Journal of Heat and Mass Transfer* **51**(15-16): 3763-3775.

Huh, C., Choi, C. and Kim, M. (2007). "Elongated Bubble Behavior During Flow Boiling in a Microchannel." *Journal of Mechanical Science and Technology* **21**(11): 1819-1827.

Huh, C. and Kim, M. H. (2007). "Pressure Drop, Boiling Heat Transfer and Flow Patterns During Flow Boiling in a Single Microchannel." *Heat Transfer Engineering* **28**(8): 730-737.

Huo, X., Chen, L., Tian, Y. S. and Karayiannis, T. G. (2004). "Flow Boiling and Flow Regimes in Small Diameter Tubes." *Applied Thermal Engineering* **24**(8-9): 1225-1239.

Ide, H., Kariyasaki, A. and Fukano, T. (2007). "Fundamental Data on the Gas-Liquid Two-Phase Flow in Minichannels." *International Journal of Thermal Sciences* **46**(6): 519-530.

Inasaka, F. and Nariai, H. (1992). "Critical Heat Flux of Subcooled Flow Boiling for Water in Uniformly Heated Straight Tubes." *Fusion Engineering and Design* **19**(4): 329-337.

Incropera, F. P. and Dewitt, D. P. (2006). Fundamentals of Heat and Mass Transfer, *Wiley Publishers.*

Intel (2010). Http://Www.Intel.Com/Technology/Architecture-Silicon/2billion.Htm?Iid=Tech_Micro+2b.

Itoh, M., Fujita, T., Nishiwaki, N. and Hirata, M. (1970). "A New Method of Correlating Heat-Transfer Coefficients for Natural Convection in Horizontal Cylindrical Annuli." *International Journal of Heat and Mass Transfer* **13**(8): 1364-1368.

Ivey, H. J. (1967). "Relationships between Bubble Frequency, Departure Diameter and Rise Velocity in Nucleate Boiling." *International Journal of Heat and Mass Transfer* **10**(8): 1023-1040.

Jung, D. S. and Radermacher, R. (1991). "Prediction of Heat Transfer Coefficients of Various Refrigerants During Evaporation." *ASHRAE Trans.* **97**(2): 48-53.

Kandlikar, S. G. and Balasubramanian, P. (2004). "An Extension of the Flow Boiling Correlation to Transition, Laminar, and Deep Laminar Flows in Minichannels and Microchannels." *Heat Transfer Engineering* **25**(3): 86 - 93.

Kandlikar, S. G. and Grande, W. J. (2003). "Evolution of Microchannel Flow Passages--Thermohydraulic Performance and Fabrication Technology." *Heat Transfer Engineering* **24**(1): 3 - 17.

Kast, W. and Klan, H. (1992). "Heat Transfer by Free Convection in Enclosed Fluid Layers." *VDI Heat Atlas English Version* Fc1-Fc3.

Katto, Y. (1980). "General Features of Chf of Forced Convection Boiling in Uniformly Heated Vertical Tubes with Zero Inlet Subcooling." *International Journal of Heat and Mass Transfer* **23**(4): 493-504.

Katto, Y. and Ohno, H. (1984). "An Improved Version of the Generalized Correlation of Critical Heat Flux for the Forced Convective Boiling in Uniformly Heated Vertical Tubes." *International Journal of Heat and Mass Transfer* **27**(9): 1641-1648.

Kawahara, A., Chung, P. M. Y. and Kawaji, M. (2002). "Investigation of Two-Phase Flow Pattern, Void Fraction and Pressure Drop in a Microchannel." *International Journal of Multiphase Flow* **28**(9): 1411-1435.

Kew, P. A. and Cornwell, K. (1997). "Correlations for the Prediction of Boiling Heat Transfer in Small-Diameter Channels." *Applied Thermal Engineering* **17**(8-10): 705-715.

Kim, H. C., Baek, W.-P. and Chang, S. H. (2000). "Critical Heat Flux of Water in Vertical Round Tubes at Low Pressure and Low Flow Conditions." *Nuclear Engineering and Design* **199**(1-2): 49-73.

Kosar, A., Kuo, C.-J. and Peles, Y. (2005). "Boiling Heat Transfer in Rectangular Microchannels with Reentrant Cavities." *International Journal of Heat and Mass Transfer* **48**(23-24): 4867-4886.

Kosar, A. and Peles, Y. (2007). "Critical Heat Flux of R-123 in Silicon-Based Microchannels." *Journal of Heat Transfer* **129**(7): 844-851.

Kuan, W. K. and Kandlikar, S. G. (2006). Experimental Study on Saturated Flow Boiling Critical Heat Flux in Microchannels. *Fourth International Conference on Nanochannels, Microchannels and Minichannels, ICNMM2006*. *Limerick, Ireland*.

Kureta, M., Kobayashi, T., Mishima, K. and Nishihara, H. (1998). "Pressure Drop and Heat Transfer for Flow-Boiling of Water in Small-Diameter Tubes." *JSME International Journal, Series B: Fluids and Thermal Engineering* **41**(4): 871-879.

Kurihara, H. M. and Myers, J. E. (1960). "Fundamental Factors Affecting Boiling." *Journal of American Institute of Chemical Engneers* **6**: 83.

Kuznetsov, V. V. and Shamirzaev, A. S. (2007). "Boiling Heat Transfer for Freon R21 in Rectangular Minichannel." *Heat Transfer Engineering* **28**(8): 738 - 745.

Lazarek, G. M. and Black, S. H. (1982). "Evaporative Heat Transfer, Pressure Drop and Critical Heat Flux in a Small Vertical Tube with R-113." *International Journal of Heat and Mass Transfer* **25**(7): 945-960.

Lee, C. Y. and Lee, S. Y. (2008). "Pressure Drop of Two-Phase Plug Flow in Round Mini-Channels: Influence of Surface Wettability." *Experimental Thermal and Fluid Science* **32**(8): 1716-1722.

Lee, H. J. and Lee, S. Y. (2001). "Heat Transfer Correlation for Boiling Flows in Small Rectangular Horizontal Channels with Low Aspect Ratios." *International Journal of Multiphase Flow* **27**(12): 2043-2062.

Lee, J. and Mudawar, I. (2005). "Two-Phase Flow in High-Heat-Flux Micro-Channel Heat Sink for Refrigeration Cooling Applications: Part I--Pressure Drop Characteristics." *International Journal of Heat and Mass Transfer* **48**(5): 928-940.

Lee, J. H. and Lee, Y. S. (2001). "Pressure Drop Correlations for Two-Phase Flow within Horizontal Rectangular Channels with Small Heights." *International Journal of Multiphase Flow* **27**(5): 783-796.

Lee, P.-S. and Garimella, S. V. (2008). "Saturated Flow Boiling Heat Transfer and Pressure Drop in Silicon Microchannel Arrays." *International Journal of Heat and Mass Transfer* **51**(3-4): 789-806.

Lee, P. C., Tseng, F. G. and Pan, C. (2004). "Bubble Dynamics in Microchannels. Part I: Single Microchannel." *International Journal of Heat and Mass Transfer* **47**(25): 5575-5589.

Lelea, D., Nishio, S. and Takano, K. (2004). "The Experimental Research on Microtube Heat Transfer and Fluid Flow of Distilled Water." *International Journal of Heat and Mass Transfer* **47**(12-13): 2817-2830.

Lie, Y. M. and Lin, T. F. (2005). "Saturated Flow Boiling Heat Transfer and Associated Bubble Characteristics of R-134a in a Narrow

Annular Duct." *International Journal of Heat and Mass Transfer* **48**(25-26): 5602-5615.

Lie, Y. M. and Lin, T. F. (2006). "Subcooled Flow Boiling Heat Transfer and Associated Bubble Characteristics of R-134a in a Narrow Annular Duct." *International Journal of Heat and Mass Transfer* **49**(13-14): 2077-2089.

Lie, Y. M., Su, F. Q., Lai, R. L. and Lin, T. F. (2008). "Experimental Study of Evaporation Pressure Drop Characteristics of Refrigerants R-134a and R-407c in Horizontal Small Tubes." *International Journal of Heat and Mass Transfer* **51**(1-2): 294-301.

Lin, S., Kew, P. A. and Cornwell, K. (2001). "Two-Phase Heat Transfer to a Refrigerant in a 1 Mm Diameter Tube." *International Journal of Refrigeration* **24**(1): 51-56.

Lin, S., Kwok, C. C. K., Li, R. Y., Chen, Z. H. and Chen, Z. Y. (1991). "Local Frictional Pressure Drop During Vaporization of R-12 through Capillary Tubes." *International Journal of Multiphase Flow* **17**(1): 95-102.

Liu, Z. and Winterton, R. H. S. (1988). "Wet Wall Flow Boiling Correlation with Explicit Nucleate Term." *Multiphase Transport and Particulate Phenomena* **1**: 419-432.

Liu, Z. and Winterton, R. H. S. (1991). "A General Correlation for Saturated and Subcooled Flow Boiling in Tubes and Annuli, Based on a Nucleate Pool Boiling Equation." *International Journal of Heat and Mass Transfer* **34**(11): 2759-2766.

Lockhart, R. C. and Martinelli, R. W. (1949). "Proposed Correlation of Data for Isothermal Two-Phase, Two-Component Flow in Pipes " *Chemical Engineering Progress* **45**(1): 39-48.

Lockhart, R. W. and Martinelli, R. C. (1949). "Proposed Correlation of Data for Isothermal Two-Phase, Two-Component Flow in Pipes." *Chemical Engineering Progress* **45**(1): 39-48.

Madrid, F., Caney, N. and Marty, P. (2007). "Study of a Vertical Boiling Flow in Rectangular Mini-Channels." *Heat Transfer Engineering* **28**(8): 753-760.

Mandhane, J. M., Gregory, G. A. and Aziz, K. (1974). "A Flow Pattern Map for Gas--Liquid Flow in Horizontal Pipes." *International Journal of Multiphase Flow* **1**(4): 537-553.

Maranzana, G., Perry, I. and Maillet, D. (2004). "Mini- and Micro-Channels: Influence of Axial Conduction in the Walls." *International Journal of Heat and Mass Transfer* **47**(17-18): 3993-4004.

Martin-Callizo, C. (2010). Flow Boiling Heat Transfer in Single Vertical Channels of Small Diameter. *Division of Applied Thermodynakics and Refrigeration, Department of Energy Technology*, *Royal Institute of Technology, Stockholm, Sweden.*. Doctoral Thesis**:** 52.

Martin-Callizo, C., Ali, R. and Palm, B. (2008). Dryout Incipience and Critical Heat Flux in Saturated Flow Boiling of Refrigerants in a

Vertical Uniformly Heated Microchannel. *Sixth ASME International Conference on Nanochannels Microchannels and Minichannels, ICNMM2008*. *Darmstadt, Germany*.

Martín-Callizo, C., Ali, R. and Palm, B. (2007). New Experimental Results on Flow Boiling of R-134a in a Vertical Microchannel. *Proceedings of the10th UK National Heat Transfer Conference*, Edinburgh, UK.

Martin-Callizo, C., Palm, B., Owhaib, W. and Ali, R. (2010). "Flow Boiling Visualization of R-134a in a Vertical Channel of Small Diameter." *Journal of Heat Transfer* **132**(3): 031503-8.

Mauro, A. W., Thome, J. R., Toto, D. and Vanoli, G. P. (2010). "Saturated Critical Heat Flux in a Multi-Microchannel Heat Sink Fed by a Split Flow System." *Experimental Thermal and Fluid Science* **34**(1): 81-92.

McAdams, W. H., Woods, W. K. and Bryan R. L. (1942). "Vaporization inside Horizontal Tubes-Ii-Benzene-Oil Mixtures." *ASME Transactions* **64**: 193.

Megahed, A. and Hassan, I. (2009). "Two-Phase Pressure Drop and Flow Visualization of Fc-72 in a Silicon Microchannel Heat Sink." *International Journal of Heat and Fluid Flow* **30**(6): 1171-1182.

Mehendale, S. S., Jacobi, A. M. and Shah, R. K. (2000). "Fluid Flow and Heat Transfer at Micro- and Meso-Scales with Application to Heat Exchanger Design." *Applied Mechanics Reviews* **53**(7): 175-193.

Mishima, K. and Hibiki, T. (1996). "Some Characteristics of Air-Water Two-Phase Flow in Small Diameter Vertical Tubes." *International Journal of Multiphase Flow* **22**(4): 703-712.

Mishima, K. and Ishii, M. (1984). "Flow Regime Transition Criteria for Upward Two-Phase Flow in Vertical Tubes." *International Journal of Heat and Mass Transfer* **27**(5): 723-737.

Mishima, K. and Nishihara, H. (1985). "The Effect of Flow Direction and Magnitude on Chf for Low Pressure Water in Thin Rectangular Channels." *Nuclear Engineering and Design* **86**(2): 165-181.

Moffat, R. J. (1988). "Describing the Uncertainties in Experimental Results." *Experimental Thermal and Fluid Science* **1**(1): 3-17.

Moore, G. E. (1965). "Cramming More Components onto Integrated Circuits." *Electronics* **38**(8): 114-117.

Moore, G. E. (2003). No Exponential Is Forever: But "Forever"Can Be Delayed! *in Proceedings of IEEE2003 International Solid-State Circuits Conference*, Boston, Massachusetts.

Muller-Steinhagen, H. and Heck, K. (1986). "A Simple Friction Pressure Drop Correlation for Two-Phase Flow in Pipes." *Chemical Engineering Progress* **20**: 297-308.

Müller-Steinhagen, H. and Heck, K. (1986). "A Simple Friction Pressure Drop Correlation for Two Phase Flow in Pipes." *Chemical Engineering Progress* **20**: 297-308.

Nino, V. G., Hrnjak, P. S. and Newell, T. A. (2003). "Two-Phase Flow Visualization of R134a in a Multiport Microchannel Tube." *Heat Transfer Engineering* **24**(1): 41 - 52.

Nishikawa, K. and Yamagata, K. (1960). "On the Correlation of Nucleate Boiling Heat Transfer." *International Journal of Heat and Mass Transfer* **1**(2-3): 219-235.

Oh, C. H. and Englert, S. B. (1993). "Critical Heat Flux for Low Flow Boiling in Vertical Uniformly Heated Thin Rectangular Channels." *International Journal of Heat and Mass Transfer* **36**(2): 325-335.

Oh, H. K., Katsuta, M. and Shibata, K. (1998). Heat Transfer Characterisitics of R134a in a Capillary Tube Heat Exchanger. *11th International Heat Transfer Conference. Kyongju, Korea.* 6**:** 473-478.

Ong, C. L. and Thome, J. R. (2009). "Flow Boiling Heat Transfer of R134a, R236fa and R245fa in a Horizontal 1.030 mm Circular Channel." *Experimental Thermal and Fluid Science* **33**(4): 651-663.

Owhaib, W. (2007). Experimental Heat Transfer, Pressure Drop and Flow Visualization of R134a in Vertical Mini/Micro Tubes. *Department of Energy Technology*, *Royal Institute of Technology*. Doctoral Thesis**:** 68.

Owhaib, W. (2007). Experimental Heat Transfer, Pressure Drop and Flow Visualization of R134a in Vertical Mini/Micro Tubes. *Department of Energy Technology. Stockholm, Sweden*, *Royal Institute of Technology, KTH*. Doctoral Thesis.

Owhaib, W., Martín-Callizo, C. and Palm, B. (2004a). "Evaporative Heat Transfer in Vertical Circular Microchannels." *Applied Thermal Engineering* **24**(8-9): 1241-1253.

Owhaib, W. and Palm, B. (2004b). "Experimental Investigation of Single-Phase Convective Heat Transfer in Circular Microchannels." *Experimental Thermal and Fluid Science* **28**(2-3): 105-110.

Owhaib, W. and Palm, B. (2004c). Experimental Investigation of Convective Single-Phase Heat Transfer and Pressure Drop in Circular Microchannels. *IIR Inter. Comference, Zero Leakage.Minimum Charge*, Stockholm, Sweden.

Owhaib, W., Palm, B. and Martin-Callizo, C. (2007). "A Visualization Study of Bubble Behavior in Saturated Flow Boiling through a Vertical Mini-Tube." *Heat Transfer Engineering* **28**(10): 852 - 860.

Owhaib, W., Palm, B. and Martín-Callizo, C. (2006). "Flow Boiling Visualization in a Vertical Circular Minichannel at High Vapor Quality." *Experimental Thermal and Fluid Science* **30**(8): 755-763.

Palm, B. (1991). Enhancement of Boiling Heat Transfer by Aid of Perforated Metal Foils. *Division of Applied Thermodynakics and Ref-*

rigeration, Department of Energy Technology Royal Institute of Technology, Stockholm, Sweden,. Doctoral Thesis, 134-136.

Palm, B. (2001). "Heat Transfer in Microchannels." *Microscale Thermophysical Engineering* **5**(3): 155-175.

Park, J. E. and Thome, J. R. (2010). "Critical Heat Flux in Multi-Microchannel Copper Elements with Low Pressure Refrigerants." *International Journal of Heat and Mass Transfer* **53**(1-3): 110-122.

Pehlivan, K., Hassan, I. and Vaillancourt, M. (2006). "Experimental Study on Two-Phase Flow and Pressure Drop in Millimeter-Size Channels." *Applied Thermal Engineering* **26**(14-15): 1506-1514.

Pierre, B. (1969). "Värmeövergång Vid Kokande Köldmedier I Horizontalla Rör." *Kylteknisk Tidskrift* **28**(5): 3-12.

Qu, W. and Mudawar, I. (2003). "Measurement and Prediction of Pressure Drop in Two-Phase Micro-Channel Heat Sinks." *International Journal of Heat and Mass Transfer* **46**(15): 2737-2753.

Qu, W. and Mudawar, I. (2004). "Measurement and Correlation of Critical Heat Flux in Two-Phase Micro-Channel Heat Sinks." *International Journal of Heat and Mass Transfer* **47**(10-11): 2045-2059.

Quan, X., Cheng, P. and Wu, H. (2008). "An Experimental Investigation on Pressure Drop of Steam Condensing in Silicon Microchannels." *International Journal of Heat and Mass Transfer* **51**(21-22): 5454-5458.

Ravigururajan, T. S. (1998). "Impact of Channel Geometry on Two-Phase Flow Heat Transfer Characteristics of Refrigerants in Microchannel Heat Exchangers." *Journal of Heat Transfer* **120**(2): 485-491.

Revellin, R., Agostini, B., Ursenbacher, T. and Thome, J. R. (2008). "Experimental Investigation of Velocity and Length of Elongated Bubbles for Flow of R-134a in a 0.5 mm Microchannel." *Experimental Thermal and Fluid Science* **32**(3): 870-881.

Revellin, R., Dupont, V., Ursenbacher, T., Thome, J. R. and Zun, I. (2006). "Characterization of Diabatic Two-Phase Flows in Microchannels: Flow Parameter Results for R-134a in a 0.5 mm Channel." *International Journal of Multiphase Flow* **32**(7): 755-774.

Revellin, R. and Thome, J. R. (2007). "Adiabatic Two-Phase Frictional Pressure Drops in Microchannels." *Experimental Thermal and Fluid Science* **31**(7): 673-685.

Revellin, R. and Thome, J. R. (2007). "Experimental Investigation of R-134a and R-245fa Two-Phase Flow in Microchannels for Different Flow Conditions." *International Journal of Heat and Fluid Flow* **28**(1): 63-71.

Revellin, R. and Thome, J. R. (2007). "A New Type of Diabatic Flow Pattern Map for Boiling Heat Transfer in Microchannels." *Journal of Micromechanics and Microengineering* **17**: 788-796.

Roach, G. M., Abdel-Khalik, S. I., Ghiaasiaan, S. M., Dowling, M. F. and Jeter, S. M. (1999). "Low-Flow Critical Heat Flux in Heated Microchannels." *Nuclear Science and Engineering* **131**: 411-425.

Roday, A. P. and Jensen, M. K. (2009). "Study of the Critical Heat Flux Condition with Water and R-123 During Flow Boiling in Microtubes. Part I: Experimental Results and Discussion of Parametric Effects." *International Journal of Heat and Mass Transfer* **52**(13-14): 3235-3249.

Saisorn, S. and Wongwises, S. (2008). "Flow Pattern, Void Fraction and Pressure Drop of Two-Phase Air-Water Flow in a Horizontal Circular Micro-Channel." *Experimental Thermal and Fluid Science* **32**(3): 748-760.

Saisorn, S. and Wongwises, S. (2010). "The Effects of Channel Diameter on Flow Pattern, Void Fraction and Pressure Drop of Two-Phase Air-Water Flow in Circular Micro-Channels." *Experimental Thermal and Fluid Science* **34**(4): 454-462.

Saitoh, S., Daiguji, H. and Hihara, E. (2005). "Effect of Tube Diameter on Boiling Heat Transfer of R-134a in Horizontal Small-Diameter Tubes." *International Journal of Heat and Mass Transfer* **48**(23-24): 4973-4984.

Salim, A., Colin, C., Grah, A. and Dreyer, M. E. (2010). "Laminar Bubbly Flow in an Open Capillary Channel in Microgravity." *International Journal of Multiphase Flow* **36**(9): 707-719.

Serizawa, A., Feng, Z. and Kawara, Z. (2002). "Two-Phase Flow in Microchannels." *Experimental Thermal and Fluid Science* **26**(6-7): 703-714.

Shah, M. M. (1987). "Improved General Correlation for Critical Heat Flux During Upflow in Uniformly Heated Vertical Tubes." *International Journal of Heat and Fluid Flow* **8**(4): 326-335.

Sobierska, E., Kulenovic, R., Mertz, R. and Groll, M. (2006). "Experimental Results of Flow Boiling of Water in a Vertical Microchannel." *Experimental Thermal and Fluid Science* **31**(2): 111-119.

Steinke, M. E. and Kandlikar, S. G. (2004). "An Experimental Investigation of Flow Boiling Characteristics of Water in Parallel Microchannels." *Journal of Heat Transfer* **126**(4): 518-526.

Stephan, K. and Abdelsalam, M. (1980). "Heat-Transfer Correlations for Natural Convection Boiling." *International Journal of Heat and Mass Transfer* **23**(1): 73-87.

Sumith, B., Kaminaga, F. and Matsumura, K. (2003). "Saturated Flow Boiling of Water in a Vertical Small Diameter Tube." *Experimental Thermal and Fluid Science* **27**(7): 789-801.

Suo, M. (1963). Two-Phase Flow in Capillary Tubes. *Department of Mechanical Engineering. Massachusetts Institute of Technology*. Doctoral Thesis.

Suo, M. and Griffith, P. (1964). "Two-Phase Flow in Capillar Tubes." *ASME Journal of basic engineering* **86**(3): 576-582.

Taitel, Y. (1990). Flow Pattern Transition in Two Phase Flow. *9th International Heat Transfer Conference*, Jerusalem, Israel.

Taitel, Y., Bornea, D. and Dukler, A. E. (1980). "Modelling Flow Pattern Transitions for Steady Upward Gas-Liquid Flow in Vertical Tubes." *AIChE Journal* **26**(3): 345-354.

Taitel, Y. and Dukler, A. E. (1976). "A Model for Predicting Flow Regime Transitions in Horizontal and near Horizontal Gas-Liquid Flow." *AIChE Journal* **22**(1): 47-55.

Taylor, B. N. and Kuyatt, C. E. (1994). Guidelines for Evaluating and Expressing the Uncertainty of Nist Measurement Results. *NIST Technical Note 1297, 1994 Edition*, *United States Department of Commerce, National Institute of Standards and Technology (NIST).*

Thome, J. R., Dupont, V. and Jacobi, A. M. (2004). "Heat Transfer Model for Evaporation in Microchannels. Part I: Presentation of the Model." *International Journal of Heat and Mass Transfer* **47**(14-16): 3375-3385.

Tibiriçá, C. B. and Ribatski, G. (2010). "Flow Boiling Heat Transfer of R134a and R245fa in a 2.3 mm Tube." *International Journal of Heat and Mass Transfer* **53**(11-12): 2459-2468.

Tran, T. N., Chyu, M. C., Wambsganss, M. W. and France, D. M. (2000). "Two-Phase Pressure Drop of Refrigerants During Flow Boiling in Small Channels: An Experimental Investigation and Correlation Development." *International Journal of Multiphase Flow* **26**(11): 1739-1754.

Tran, T. N., Wambsganss, M. W. and France, D. M. (1996). "Small Circular- and Rectangular-Channel Boiling with Two Refrigerants." *International Journal of Multiphase Flow* **22**(3): 485-498.

Triplett, K. A., Ghiaasiaan, S. M., Abdel-Khalik, S. I. and Sadowski, D. L. (1999). "Gas-Liquid Two-Phase Flow in Microchannels Part I: Two-Phase Flow Patterns." *International Journal of Multiphase Flow* **25**(3): 377-394.

Tuckerman, D. B. and Pease, R. F. (1981). "High Performance Heat Sinking for Vlsi." *Electronic Device Letters* **2**: 126-129.

Wambsganss, M. W., France, D. M., Jendrzejczyk, J. A. and Tran, T. N. (1993). "Boiling Heat Transfer in a Horizontal Small-Diameter Tube." *Journal of Heat Transfer* **115**(4): 963-972.

Warrier, G. R., Dhir, V. K. and Momoda, L. A. (2002). "Heat Transfer and Pressure Drop in Narrow Rectangular Channels." *Experimental Thermal and Fluid Science* **26**(1): 53-64.

Watel, B. (2003). "Review of Saturated Flow Boiling in Small Passages of Compact Heat-Exchangers." *International Journal of Thermal Sciences* **42**(2): 107-140.

Wen, D. S. and Kenning, D. B. R. (2004). "Two-Phase Pressure Drop of Water During Flow Boiling in a Vertical Narrow Channel." *Experimental Thermal and Fluid Science* **28**(2-3): 131-138.

Whalley, P. B. (1987). Boiling, Condensation and Gas-Liquid Flow. *Clarendon Press-Oxford*.

Wojtan, L., Revellin, R. and Thome, J. R. (2006). "Investigation of Saturated Critical Heat Flux in a Single, Uniformly Heated Microchannel." *Experimental Thermal and Fluid Science* **30**(8): 765-774.

Xu, J. L., Cheng, P. and Zhao, T. S. (1999). "Gas-Liquid Two-Phase Flow Regimes in Rectangular Channels with Mini/Micro Gaps." *International Journal of Multiphase Flow* **25**(3): 411-432.

Yang, C.-Y. and Shieh, C.-C. (2001). "Flow Pattern of Air-Water and Two-Phase R-134a in Small Circular Tubes." *International Journal of Multiphase Flow* **27**(7): 1163-1177.

Yen, T.-H., Kasagi, N. and Suzuki, Y. (2003). "Forced Convective Boiling Heat Transfer in Microtubes at Low Mass and Heat Fluxes." *International Journal of Multiphase Flow* **29**(12): 1771-1792.

Yen, T.-H., Shoji, M., Takemura, F., Suzuki, Y. and Kasagi, N. (2006). "Visualization of Convective Boiling Heat Transfer in Single Microchannels with Different Shaped Cross-Sections." *International Journal of Heat and Mass Transfer* **49**(21-22): 3884-3894.

Yu, W., France, D. M., Wambsganss, M. W. and Hull, J. R. (2002). "Two-Phase Pressure Drop, Boiling Heat Transfer, and Critical Heat Flux to Water in a Small-Diameter Horizontal Tube." *International Journal of Multiphase Flow* **28**(6): 927-941.

Zhang, M. and Webb, R. L. (2001). "Correlation of Two-Phase Friction for Refrigerants in Small-Diameter Tubes." *Experimental Thermal and Fluid Science* **25**(3-4): 131-139.

Zhang, W., Hibiki, T. and Mishima, K. (2004). "Correlation for Flow Boiling Heat Transfer in Mini-Channels." *International Journal of Heat and Mass Transfer* **47**(26): 5749-5763.

Zhang, W., Hibiki, T., Mishima, K. and Mi, Y. (2006). "Correlation of Critical Heat Flux for Flow Boiling of Water in Mini-Channels." *International Journal of Heat and Mass Transfer* **49**(5-6): 1058-1072.

Zuber, N. (1963). "Nucleate Boiling. The Region of Isolated Bubbles and the Similarity with Natural Convection." *International Journal of Heat and Mass Transfer* **6**(1): 53-78.